MAGNETOHYDRODYNAMIC FLOW IN POROUS MEDIA OVER A STRETCHING SURFACE IN A ROTATING SYSTEM WITH HEAT AND MASS TRANSFER

KANG'ETHE GITERERE

DOCTOR OF PHILOSOPHY

(Applied Mathematics)

JOMO KENYATTA UNIVERSITY OF AGRICULTURE AND TECHNOLOGY

2011

Magnetohydrodynamic Flow in Porous Media over A Stretching Surface in a Rotating System with Heat and Mass Transfer

Kang'ethe Giterere

A thesis submitted in fulfillment for the Degree of Doctor of Philosophy in Applied Mathematics in the Jomo Kenyatta University of Agriculture and Technology

2011

DECLARATION

This thesis is my original work and has not been presented for a degree in any other University.

Signature: …… Date: ……

Kang'ethe Giterere

This thesis has been submitted for examination with our approval as University Supervisors.

Signature: …… Date: ……

Prof. Mathew N. Kinyanjui

JKUAT, Kenya

Signature: …… Date: ……

Prof. S. M. Uppal

JKUAT, Kenya

DEDICATION

This thesis is dedicated to my wife Felista, my children, and to the late brother Engineer D.M. Giterere for their encouragement and support towards my education.

ACKNOWLEDGEMENT

I wish to specially thank my supervisors, Professor Mathew Kinyanjui, and Professor S. M. Uppal for their guidance, advice and inspiration throughout my postgraduate programs at the Jomo Kenyatta University of Agriculture and Technology (JKUAT). I give thanks to the members of Pure and Applied Mathematics (PAM) department for their assistance and guidance during my studies: and specially to thank Dr. Johana Sigey, Dr. David Theuri, Dr. E. Mwenda and Mr. Roy Kiogora for their dedicated input in making this thesis a success.

I would like to thank my Wife and Children for their prayers, love and support. And special thanks to my brother, the late Engineer D. M. Giterere for funding my secondary school education and for all his pronounced good wishes about the future of my academic life. His home library, full of engineering books, motivated me to have a positive outlook towards Applied Mathematics.

I wish to register my appreciation and gratitude to the Jomo Kenyatta University of Agriculture and Technology (JKUAT) for supporting me financially during the period study, at the Masters and PhD levels respectively.

TABLE OF CONTENTS

LIST OF TABLES

LIST OF FIGURES

NOMENCLATURE

Roman Symbol	Quantity
A	Aspect ratio.
A_s	Control surface, [m^{-2}].
B	Magnetic field strength vector, [Wbm^{-2}].
B_o	Magnetic flux density along the z-axis, [Wbm^{-2}].
g	Acceleration due to gravity vector, [ms^{-2}].
H	Magnetic field intensity vector in Amperes per metre, [Am^{-1}].
H	Dimensional distance between vertical sheets, [m].
J	Current density, [Am^{-2}].
C_w	Dimensional concentration at the stretching sheet, [Kgm^{-3}].
C_∞	Dimensional freestream concentration of species, [Kgm^{-3}].
C_U	Dimensional concentration of species at the upper sheet, [Kgm^{-3}].
c_s	Concentration susceptibility, [$kmolm^3$].
D	Electric flux density, [Cm^{-2}].
e	Unit electric charge, [C].
E	Electric field, [V].
e_e	Charge density, [Cm^{-3}].
m	Hall parameter.
M	Magnetic parameter.
Sr	Soret number.

Xi	Permeability parameter.
Gr_θ	Local temperature Grashof number.
Gr_m	Local mass Grashof number.
Df	Dufour number.
Sc	Schmidt number.
Re	Reynold's number.
Ro	Rotation parameter.
Xi	Permeability parameter.
h	Specific enthalpy, [$JKg^{-1}K^{-1}$].
q_w	Local surface heat flux, [Wm^2].
Q_o	Heat generation constant, [Wm^3].
P	Pressure force, [Nm^{-2}].
P^*	Dimensionless pressure force.
k_f	Fluid thermal diffusion ratio, [m^2s^1].
N	Radiation parameter.
k_T	Thermal conductivity of porous medium, [$Wm^{-1}K^{-1}$].
Nu	The local Nusselt number.
$\mathbf{q}$	Velocity vector, [ms^{-1}].
$\mathbf{i}, \mathbf{j}, \mathbf{k}$	Unit vectors in the x, y and z directions respectively.
T_m	Mean fluid temperature, [K].

u, v, w	Components of velocity vector $\mathbf{q}$, [ms^{-1}]
u^*, v^*, w^*	Dimensionless velocity components.
x^*, y^*, z^*	Dimensionless Cartesian co-ordinates.
x, y, z	Dimensional Cartesian co-ordinates.
F_i	Body force tensor, [N].
U_i	Velocity tensor, [ms^{-1}].
x_j	Space tensor, [m].
T	Absolute free temperature of the fluid, [K].
T_∞	Absolute temperature of the upper sheet, [K].
T_w	Absolute temperature of the stretching sheet, [K].
T^*	Dimensionless temperature.
c	Stretching rate constant, [s^{-1}].
C_p	Specific heat at constant pressure, [$Jkg^{-1}K^{-1}$].
C_k	Forchheimer Constant, [m].
s_1	Rate of stretching of the sheet, [s^{-1}].
K_p	Darcy permeability, [m^2].
k^*	Mean absorption coefficient of the fluid, [m^{-1}].
D	Displacement current density, [Cm^{-2}].
D_M	Molecular diffusion coefficient, [m^2s^{-1}].
D_T	Thermal diffusion coefficient, [$kgm^{-1}s^{-1}K^{-1}$].
$\mathbf{F}_e$	Electromagnetic force, [$kgms^{-2}$].

Pr	Prandtl number.
Ha	Hartmann number.
Ec	Eckert Number.
w_o	Suction velocity, [ms^{-1}].
V	Volume of the porous medium, [m^3].
V_f	Volume occupied by the fluid, [m^3].
C_f	Local skin friction coefficient.
V_s	Control volume, [m^3].
q_r	Radiative heat flux, [Wm^{-2}].
Q_o	Volumetric heat generation parameter, [Wm^{-3}].
Q	Dimensionless heat source parameter.

Greek Symbol	Quantity
β	Volumetric coefficient of thermal expansion, [K^{-1}].
β^*	Coefficient of thermal expansion due to concentration gradient, [K^{-1}].
ϵ^+	Porosity.
ϵ	Emissivity of black body.
u_f	Pore velocity, [ms^{-1}].
ρ	Fluid density, [kgm^{-3}].
μ	Coefficient of viscosity, [$kgm^{-1}s^{-1}$].
σ^*	Stefan-Boltzmann constant, [Wm^-2K^-4].
ϕ	Viscous dissipation function, [s^{-1}].
Ω	Angular velocity, [s^{-1}].
σ	Electrical conductivity, [$\Omega^{-1}m^{-1}$].
σ_{ij}	Total stress tensor, [Nm^{-2}].
τ_{ij}	Viscous stress tensor, [Nm^{-2}].
τ_x	Viscous stress due to primary velocity profiles, [Nm^{-2}].
τ_y	Viscous stress due to secondary velocity profiles, [Nm^{-2}].
C_{fx}	The local skin friction coefficient due the primary velocity profiles.
C_{fy}	The local skin friction coefficient due to secondary velocity profiles.
δ_{ij}	Kronecker delta.

ν	Kinematic viscosity, [$m^2 s^{-1}$].
μ_e	Magnetic permeability, [Hm^{-1}].
λ	Ratio of kinematic viscosity to Darcy permeability constant, [m^2].
τ_e	Electron collision time, [t].
ω_e	Electron frequency, [s^{-1}].
ℓ	Specific internal energy, [$JKg^{-1}K^{-1}$].
∇	Gradient operator $\left(\mathbf{i}\frac{\partial}{\partial x} + \mathbf{j}\frac{\partial}{\partial y} + \mathbf{k}\frac{\partial}{\partial z}\right)$.

LIST OF ABBREVIATIONS

FD	Finite Difference
HOT	Higher Order Terms
MHD	Magnetohydrodynamics
PDE's	Partial Differential Equations

ABSTRACT

The unsteady laminar boundary layer hydromagnetic flow of an incompressible, viscous, and electrically conducting Newtonian fluid over a stretching sheet embedded in a porous medium in a rotating system has been investigated. The fluid is subjected to a transverse magnetic field that cuts perpendicularly across the flow in the positive direction of the z-axis. The flow takes place between two parallel flat sheets that are made of an electrically non-conducting material. The stretching sheet has a permeable surface, while the surface of the other sheet is impermeable. Each of the sheets has an isothermal surface, and both sheets are kept at different temperatures of T_W and T_∞ such that the temperature differences within the flow are sufficiently small. The small magnitude of the temperature difference allows expression of the Taylor series expansion about the freestream temperature T_∞ as a linear function of temperature at any interior point within the flow region. The unsteady boundary layer flow over a permeable sheet that stretches with a linear velocity has been investigated. The effect of varying various parameters on the velocity, temperature and concentration profiles has been discussed. These parameters include the Reynolds number Re, Prandtl number Pr, Eckert Number Ec, Magnetic parameter M, the Suction parameter w_o, Joule heating parameter N, Radiation parameter R, Permeability constant Xi, Rotational parameter Ro, local temperature Grashof number Gr_θ, the local mass Grashof number Gr_c, Schmidt number Sc, Soret number Sr and time t. The coupled non-linear partial differential equations governing the flow field have been solved numerically using the finite difference method. The results that are obtained are then presented on graphs and the observations are discussed. Later the method of Least Squares

is used to study the effect of changing some of these parameters on the skin-friction coefficients, rate of mass transfer and local wall heat flux. A change in the parameters is observed to either increase, decrease or to have no effect on the velocity, temperature, and concentration profiles respectively. The results that are obtained are presented in tables and then discussed. A change in the various parameters is observed to alter the velocity profiles, the concentration profiles, the temperature profiles, the rate of skin friction, the rates of heat and mass transfer on the surface of the stretching sheet.

CHAPTER ONE

1.0 INTRODUCTION

The production of sheeting material, which includes both metal and polymer sheets, arises in a number of industrial manufacturing processes. The fluid dynamics due to a stretching surface have important applications in many engineering processes. For instance, a number of technical processes concerning polymers involve the cooling of continuous strips (or filaments) extruded from a die by drawing them through a stagnant fluid with controlled cooling system. In the process of drawing these strips their surfaces are sometimes stretched and the quality of the final product depends on the rate of heat transfer and mass transfer on the stretching surface, Magapatra and Gupta (2004). Therefore rates of cooling and mass transfer have to be controlled effectively in order to attain the expected quality of the final product. In recent years considerable interest has been given to the theory of rotating fluids due to its applications in cosmic and geophysical sciences. In the last few years many studies on boundary layer flows of viscous fluids due to a uniformly stretching sheet have been done. For instance such studies have been carried out by Nazal *et al.* (2004), Kumari *et al.* (2006), Hayat *et al.* (2009), and many others. A linearly stretching sheet has been considered in this study because of the simplicity of modeling linear stretching.

Heat transfer on a continuously moving surface has many applications in industrial manufacturing processes. The flow of fluids through porous media in a rotating system is of interest for instance to the petroleum engineer, who is concerned with the

movement of oil and gas through the reservoir; and to the hydrologist who is interested in the study of migration of underground water. Study of flows through porous media in a rotating system also finds applications in geothermal energy systems, oil and gas recovery, and in the spread of pollutants in groundwater. Research on flows through porous media has lately been applied in the manufacture of industrial machinery and computer disk drives, Herrero *et al.* (1994). In the field of energy conservation, attention has been focused on the use of saturated porous materials for insulation in storage tanks so as to control the rate of heat transfer. Insulating underground water pipes prevents the water in the pipes from freezing during winter. In this chapter the main terms used in this study have been defined and the literature review on MHD rotating flow in porous media over a stretching surface with heat and mass transfer has been cited. The chapter ends by stating the objectives and the applications of this study.

1.1. Magnetohydrodynamic (MHD) Flow

Magnetohydrodynamics (MHD) is the science of the motion of electrically conducting fluids under magnetic fields. MHD studies the dynamics of the interaction of electrically conducting fluids and the electromagnetic field. The fluids can be ionized gases (commonly called plasmas) or liquid metals. The flow of an electrically conducting fluid under a magnetic field in general gives rise to induced electric currents. The magnetic field exerts mechanical forces on the induced electric currents. The induced electric currents flow in the direction perpendicular to both the magnetic field and the direction

of motion of the fluid. However the induced currents also generate their own magnetic field, which in turn affects the original magnetic field.

1.2. Velocity Boundary Layer

Velocity boundary layer arises as a result of the velocity difference between the fluid particles adjacent to a solid surface and those in the freestream. The fluid particles adjacent to the solid surface acquire the velocity of that surface, hence the assumption of the no-slip condition. The latter is a physical requirement that the fluid and solid have equal velocities at their interface. Thus the flow velocity of a fluid is retarded by a fixed solid surface, and a finite, slow-moving boundary layer is formed. For a viscous fluid, velocity boundary layer thickness is defined as the perpendicular distance, measured away from the solid surface, where the velocity of the fluid becomes 0.99 of the freestream velocity. As the fluid moves past the surface of the object, collisions of the fluid molecules within the fluid with those molecules touching the object's surface reduce the kinetic energy of the molecules that are further away from the solid-fluid interface. Thus a relatively thin layer of fluid is formed near the solid-fluid interface in which there is a rapid change of velocity from zero to the freestream value. This is the layer referred to as the velocity boundary layer.

1.3. Thermal Boundary Layer

When temperature difference exists between the solid-fluid interface and the fluid in the freestream, a thermal boundary layer is formed. The fluid particles in contact with the

solid-fluid interface acquire the temperature of the interface. If the temperature of the interface is higher than that of the ambient fluid, the kinetic energy of the molecules of the adjacent fluid particles increases. These particles in turn exchange the acquired kinetic energy with those fluid particles in the adjacent fluid layers further away from the interface. This process continues in the adjacent fluid layers and temperature gradients develop in the fluid.

1.4. Concentration Boundary Layer

Concentration is a measure of how much of a given species is dissolved in another substance per unit volume. Concentration boundary layer manifests itself when species concentration difference exists between the solid-fluid interface and the freestream region of the fluid. The region in which the species concentration gradient exists is known as the concentration boundary layer. The species transfer takes place through the process of diffusion and convection, and is governed by the properties of the concentration boundary layer.

1.5. Radiation Heat Transfer

Heat transfer through radiation takes place in form of electromagnetic waves mainly in the infrared region. Radiation emitted by a body is due to thermal agitation of its molecules. Radiation heat transfer can be described in reference to the so-called ’black body’. A black body is defined as a hypothetical body that completely absorbs all wavelengths of thermal radiation incident on it. It is approximated by a hole in a box

filled with highly absorptive material. The emission spectrum of such a black body was first fully described by Max Planck in 1918. All black bodies heated to a given temperature emit thermal radiation. Radiation energy per unit time from a blackbody is proportional to the fourth power of the absolute temperature and can be expressed with Stefan-Boltzmann Law as $q_r = \sigma^* T^4 A.$ For objects other than ideal black bodies ('gray bodies') the Stefan-Boltzmann Law can be expressed as $q_r = \epsilon\sigma^* A T^4$ where $\sigma^* = 5.6703 \times 10^8 (W/m^2 K^4)$ is the Stefan-Boltzmann constant and ϵ is emissivity of a black body.

For the gray body the incident radiation (also called irradiation) is partly reflected, absorbed or transmitted. The emissivity coefficient lies in the range $0 < \epsilon < 1$ depending on the type of material and the temperature of the surface. The fluid is considered to be a gray body and the Rosseland approximation is used to describe the radiative heat flux in the energy equation, Rohsenow, *et al.* (1998). In this study, the respective radiative heat flux in the x and y directions is considered negligible in comparison with that along the z-axis direction. By using the Rosseland approximation, radiation energy per unit time is

$$q_r = -\frac{4\sigma^*}{3k^*}\frac{\partial T^4}{\partial z} \tag{1.1}$$

where k^* is the mean absorption coefficient.

The assumption in this study is that the temperature differences within the flow are assumed to be sufficiently small so that the term T^4 in equation (1.1) can be expressed as a linear function of the temperature T, using a truncated Taylor series about the freestream temperature T_∞. The orders of T and T_∞ are assumed to be more or less equal

so that any product of the two respective temperatures whose order is higher than 4 is neglected. Thus

$$f(T) = T^4 = {T_\infty}^4 + (T - T_\infty) f'(T_\infty) + \frac{(T - T_\infty)^2}{2!} f''(T_\infty) + \cdots$$

$$\Rightarrow f(T) = T_\infty^4 + 4TT_\infty^3 - 4T_\infty^4 + 6T_\infty^2 (T^3 - 3T^2 T_\infty - 3TT_\infty^2 - T_\infty^3) + \cdots$$

$$\Rightarrow f(T) \cong 4TT_\infty^3 - 3T_\infty^4 \tag{1.2}$$

Substituting the partial derivative with respect to T of equation (1.2) in equation (1.1), the rate of change of radiative heat flux in the z-axis direction becomes

$$\frac{\partial q_r}{\partial z} = -\frac{4\sigma^*}{3k^*} \frac{\partial}{\partial z} \left(4TT_\infty^3 - 3T_\infty^4\right) = -\frac{16\sigma^* T_\infty^3}{3k^*} \frac{\partial^2 T}{\partial z^2} \tag{1.3}$$

1.6. Flow in Rotating Co-ordinate System

A rotating co-ordinate system is one whose axes as seen in an inertial coordinate system are rotating. When fluid flows within such a system, the fluid flow is said to take place in a rotating system. Coriolis effect is the apparent deflection of moving objects from a straight path when they are viewed from a rotating frame of reference. The effect is an inertial force described by the 19th-century French engineer-mathematician Gustave-Gaspard Coriolis in 1835. Coriolis showed that if the ordinary Newtonian laws of motion of bodies are to be used in a rotating frame of reference, an inertial force acting to the right of the direction of body motion for counterclockwise rotation of the reference frame, or to the left for clockwise rotation, must be included in the equations of motion.

1.7. Joule Heating

Joule heating, also known as ohmic heating or resistive heating, is the process by which the passage of an electric current through a conductor releases heat. Joule heating was first studied by James Prescott Joule in 1841. When an electric current passes through an electrolyte, it causes Joule heating. The increase in the kinetic or vibrational energy of the ions manifests itself as heat, and the heat causes a rise in the temperature of the fluid. The rise in the temperature of the fluid translates to non-uniform properties of the fluid, such as change in density and conductivity of the fluid. Changes in the applied electric potential field and the flow field are among some of the factors that alter the properties of the fluid.

1.8. Porous Medium

A porous medium is a solid permeated by an interconnected network of pores filled with a fluid (liquid or gas). The pore network is usually assumed to be continuous so as to form two interpenetrating continua, such as in a sponge. Many natural substances such as rocks, soils, bones; and man-made materials such as cement slabs, foam and ceramics are some examples of porous media. Porosity is a measure of the void spaces in a material, and is the fraction of the volume of voids over the total volume of the material; its value ranges between 0 and 1, or as a percentage between 0 and 100. The bulk material includes the sum of volumes of the solid and the void. The void may be occupied by air, water, or hydrocarbons. Hydrodynamic permeability measures the

ability of fluids to flow through porous media. Variation in the temperature may give rise to change in both the viscosity and the permeability of a porous medium.

1.9. Significance of Boundary layer

The velocity boundary layer is associated with the presence of the velocity gradients and shear stress. Thermal boundary layer is associated with the temperature gradients and heat transfer. Concentration boundary layer is associated with the concentration gradients and species transfer. Fluid flowing through porous media may cause the formation of the velocity, concentration and temperature boundary layers respectively. The three layers can affect each other. The respective distances over which the velocity, the temperature and the concentration change from zero to their freestream values are often different for the three types of boundary layers. The physical significance of the boundary layer is that it is the region that determines the magnitude of the surface friction, convective heat and convective mass transfer in a fluid.

1.10. LITERATURE REVIEW

The study of heat transfer in boundary layer flows has many engineering applications such as in the design of thrust bearings and radial diffusers, in transpiration cooling, in drag reduction and in thermal recovery of oil. In the past many authors have studied a wide variety of flow situations. Some of these studies can be found in the works of Magyari and Keller (1999, 2000), Liao and Pop (2004), and Nazar *et al.* (2004). Most of these studies have dealt with steady-state flows. However the flow and thermal fields

may be naturally unsteady due to either impulsive stretching of the surface, sudden change in the surface temperature, or changes in the fluid stream. Most of the studies undertaken are experimental, numerical, analytical, or any combination of these. For instance Dawood *et al.* (2006) investigated numerically steady free convection flow through a porous medium around a rectangular isothermal body. This study showed that the Nusselt number Nu is a strong function of the modified Rayleigh number, the isothermal body size and boundary conditions.

Sattar and Maleque, (2005) considered the effects of variable fluid properties, namely the density, viscosity and thermal conductivity to the flow due to a porous rotating disk. This study showed that for fixed values of the suction parameter and Prandtl number, the momentum boundary layer increased considerably. Emmanuel (2007) extended the work of Sattar and Maleque (2005) by including the effects of a magnetic field on flow due to a rotating disk in an electrically conducting fluid with a temperature dependent density, viscosity and thermal conductivity. Singh *et al.* (2007) studied two dimensional free convection and mass transfer flow of an incompressible, viscous and electrically conducting fluid past a continuously moving infinite vertical porous plate in the presence of a heat source, thermal diffusion, large suction and uniform magnetic field applied normal to the flow.

Sakiadis (1961 a, b) pioneered the study of boundary layer flow over a continuous solid surface moving with constant velocity. Since then boundary layer flow over a stretching

surface has drawn the attention of many other researchers such as Griffin and Thorne (1967), Crane (1970), Gupta and Gupta (1977), Fox *et al.* (1966), Dutta *et al.* (1985), and Chen and Char (1988). Aboeldahab (2001) and Salem (2004) investigated the effects of magnetic field, convective and radiative heat transfer on flow over a stretching surface with heat and mass transfer. Hinze (1959) studied turbulent fluid motion in an irregular condition of flow; and showed that various quantities exhibited a random variation with time and space coordinates.

There is extensive literature on flow through porous media that is governed by the generalized Darcy's law. For instance Yamamoto and Iwamura (1976) investigated boundary layer flow of a Newtonian fluid through a highly porous medium. Later Raptis *et al.* (1981) used these equations to study the influence of free convective flow and mass transfer on flow through a porous medium. Raptis and Perdikis (1985) investigated oscillatory flow of a Newtonian fluid through a porous medium.

Ahmed *et al.* (2010) carried out an analytical study of a two dimensional unsteady MHD free convective flow past a vertical porous plate immersed in a porous medium with Hall currents, thermal diffusion and heat source. The influence of certain flow parameters on velocity, temperature, species concentration, and shearing stress at the plate were investigated. This study concluded that the concentration at the surface of the plate increases under the Soret effect; and the Soret effect causes the main-flow shear stress to

rise and the crossflow shear stress to fall. A decrease in the Soret effect leads to an increase in the main flow and crossflow velocities.

Soundalgekar and Patil (1982) studied the effects of suction, free oscillations and free convection currents on the flow of a Newtonian fluid. Erickson *et al.* (1966) extended this problem to a case in which the transverse velocity at the moving surface is non-zero, with heat and mass transfer in the boundary layer being taken into account. Danberg and Fansler (1976) investigated the non-similar solution for the flow in the boundary layer past a wall that is stretched with a velocity proportional to the distance along the wall, the free-stream velocity being constant. Gupta and Gupta (1977) analyzed the heat and mass transfer corresponding to the similarity solution for the boundary layer over a stretching sheet subjected to suction/blowing.

Since the pioneering study by Crane (1970) who presented an exact analytical solution for the steady two-dimensional stretching of a surface in a quiescent fluid, many authors have considered various aspects of this problem and obtained similar solutions. Bathaiah and Venkataramana (1986) investigated the effect of buoyancy force on the parallel flows bounded above by a rigid permeable plate which may be moving or stationary, and below, by a permeable bed. To discuss the solution, the flow region was divided into two zones: one zone made up of laminar flow and governed by the Navier-Stokes equations, and the other zone was governed by the Darcy's law. The study observed, in part, that in

the first zone the velocity decreases with the increase in magnetic parameter, and in the other zone velocity increases in the case of Poiseuille flow.

Jagadeeswara *et al.* (1987) studied viscous fluid flow past a hot vertical porous plate. The flow parameters in this study were analyzed under the assumptions that the suction velocity was constant and the wall temperature was spanwise cosinusoidal. The solutions for the velocity, the temperature, skin friction and rate of heat transfer were obtained using perturbation method. The study observed that both the velocity and the skin friction decrease as the Magnetic parameter increases. The values of all flow quantities in the magnetic case were less than the values in the non-magnetic case. The study also found that the velocity and the skin friction increased with increasing suction. Chaturvedi (2003) investigated MHD flow past an infinite porous plate with variable suction.

Kinyanjui, *et al.* (1998) studied the MHD Stokes problem for a vertical infinite plate in a dissipative rotating fluid with Hall currents. Kinyanjui, *et al.* (2001) presented work on MHD free convection heat and mass transfer of a heat generating fluid past an impulsively started infinite porous plate with Hall currents and radiation absorption. Subhas *et al.* (2001) analyzed the effect of magnetic field on the visco-elastic fluid flow and heat transfer over a non-isothermal stretching sheet with internal heat generation. The solutions for heat transfer characteristics were evaluated numerically for different parameters such as Prandtl number, magnetic field, suction and visco-elasticity. The

study concluded that visco-elasticity decreased the temperature profiles in the flow field for small values of the Prandtl number; and that the temperature profiles decreased with increase in the strength of the magnetic field.

Tania and Samad (2010) studied the effects of radiation, heat generation and viscous dissipation on MHD free convection flow along a stretching sheet. The study found that larger values of buoyancy parameter can be used to control the temperature and concentration boundary layers; and that suction stabilizes the boundary layer growth. The boundary layers were found to be highly influenced by the Prandtl number. The study also concluded that magnetic field can be used to control the flow characteristics and has significant effect on heat and mass transfer. In the study, increasing radiation reduced the momentum boundary layer and the thermal boundary layer thicknesses. The presence of a heavier species (large Sc) decreased the fluid velocity, heat transfer and the concentration in the boundary layer. Large values of heat source parameter Q had a significant effect on the velocity and temperature distributions whereas such large values reduced the concentration distribution in the boundary layer. Eckert number was found to have a significant effect on the boundary layer growth.

Ram (1991) analyzed the effects of Hall currents on the combined thermal and mass diffusion effects through a porous medium in a rotating system bounded by a vertical plate when a strong magnetic field is imposed in a plane that makes various angles with

the normal to the plate. The works of Tania and Samad (2010), and Ram (1991) are main motivating factor behind this study.

Various aspects of the problem of flow over a stretching surface have been studied under varied conditions. Most studies on fluid flows over stretching or non-stretching surfaces have only focused on free convective flows occurring due to the temperature difference between the surface and the ambient fluid. Heat transfer due to the effects of radiation is rarely taken into account. The ambient fluid cannot always be pure and there are situations where it is mixed, naturally or industrially, with some foreign species. For example air may be mixed with water, benzene or ammonia. The concentration difference of such species would alter its rate of diffusion from the surface to the ambient fluid or vice versa. Thus for considerable concentration differences, free convection occurs not only due to temperature difference but also due to concentration difference or the combination of these two. The aim of this work is therefore to study MHD flow and analyze the combined effects of various parameters on the velocity, the concentration, the temperature, the rates of heat transfer and species transfer in the boundary layer region adjacent to the stretching sheet.

1.11. Hypothesis

MHD flow over a linearly stretching permeable surface embedded in porous medium in a rotating system does not affect heat and mass transfer characteristics of the system.

1.12. Problem statement

In the studies cited above, the combined effects of stretching and thermal radiation, Joule heating, viscous dissipation, concentration and temperature gradients to the MHD flow in a rotating system have not been investigated in one combined study and such is the motivation behind this work. This study is on MHD flow over a linearly stretching permeable surface embedded in porous media in a rotating system with heat and mass transfer.

1.13. General Research Objectives

1. To study MHD heat and mass transfer characteristics near a linearly stretching permeable surface embedded in a porous medium in a rotating system.
2. To determine the effects of various parameters that affect fluid flow over a stretching surface in porous medium.

1.13.1. Specific Research Objectives

1. To investigate the effects of Magnetic parameter M, Soret number Sr, Permeability parameter Xi, Grashof number Gr_θ and modified Grashof number Gr_c on the velocity, the temperature and the concentration distributions.
2. To investigate the effects of time t on the velocity, the temperature and the concentration distributions within the boundary layer.
3. To investigate the effects of Dufour number Df, Reynolds number Re, Radiation parameter N and Eckert number Ec on the velocity, the temperature and the concentration distributions.

4. To investigate the effects of Injection parameter w_o on the flow field variables.
5. To investigate the effects of Schmidt number Sc and Rotation parameter Ro on the flow field variables.
6. To investigate the effects of heat source/sink on the rate of heat transfer, rate of mass transfer and the shearing stress on the stretching sheet.

1.14. Applications

The study of MHD flow through porous media is of fundamental importance in a wide range of disciplines, including natural sciences and technology. For instance it finds applications in engineering and hydrogeology in dealing with 'seepage' problems in rock mass, sand beds and subterranean aquifers. In civil and agricultural engineering, knowledge of flows through porous media is applied in the efficient layout of drainage systems for irrigation, and in the recovery of swampy areas. In geotechnical engineering and soil physics, studies of flows through porous media are used in predicting the water movement in clays and other surface-active soils. The chemical engineers and ceramic engineers may make use of the filtration and seepage properties of the porous materials used. In nuclear science, MHD flows have applications in regulating fluid flow through reactors so as to maintain a uniform temperature throughout the bed of the reactors. In textile technology determining the rate of fluid flow through fibres has applications in dyeing. Biologists are interested in water movement through plant roots and out of the cells of living systems. Fluid flows involving rotation are encountered in various natural phenomena and finds applications in areas such as oceanography, meteorology and

aeronautics. Porous materials find applications in filtering harmful particles in a contaminated fluid. Fluid dynamics due to a stretching surface many industrial applications such as polymer technology, metallurgy, production of sheeting materials, cooling of metallic plates, aerodynamic extrusion of plastic sheets, control of the boundary layer along a liquid film in condensation processes, paper production, glass blowing, and metal spinning and drawing of plastic films. It is also necessary to understand the boundary layer manifestation along material handling conveyors. The Earth has its own magnetic field; therefore all activities taking place on earth involve an interaction with magnetic field.

The general equations governing MHD flow over a stretching surface embedded in a porous medium, which include the equation of conservation of mass, the equation of momentum, the equation of conservation of energy, the equation of species concentration and the Maxwell's equations are given in the next chapter.

CHAPTER TWO

2.0 GOVERNING EQUATIONS AND METHODOLOGY

In this chapter the equations governing the MHD flow of an electrically conducting fluid in a porous medium in a rotating system are given. The chapter starts by stating some of the approximations to be made when studying this type of flow. Thereafter, the basic electromagnetic equations that govern the flow of an electrically conducting fluid between two parallel sheets are given. This is followed by a discussion of the laws governing flow in porous media in a rotating system. The equations of the conservation of momentum, the equation of energy, and the equation of concentration are derived. This is followed by non-dimensionalizing process of the equations governing the flow. The finite difference method used to approximate the solution to the governing equations is then discussed. Finally the results are discussed at the end of the chapter.

2.1. Approximations and Assumptions

1. The velocity of the fluid is too small compared with that of light i.e. $\frac{q^2}{c^2} \ll 1$. This means that the velocity scale in this study is non-relativistic.
2. The fluid flow is restricted to a laminar domain.
3. Electrical conductivity, thermal conductivity, viscosity, Darcy permeability, and diffusion coefficient are constant.
4. The density is a linear function of the temperature and species concentration so that the usual Boussinesq's approximation is applicable in the boundary- layer flow.

5. There is no chemical reaction between the fluid and the diffusing species.
6. The force $\rho e_e \mathbf{E}$ due to electric field is negligible compared with the force $\mathbf{J} \times \mathbf{B}$ due to magnetic field.
7. The induced magnetic field, the external electric field and the electric field due to the polarization of charges are negligible.
8. The porous medium is isotropic, homogeneous and non-magnetic, therefore there is no magnetic induction.
9. The fluid and the porous medium are in local thermodynamic equilibrium.
10. The velocity components, the temperature, and the concentration are functions of variables x, z and t.

1.0 There is no slip flow at the walls.

2.2. Electromagnetic equations

2.2.1. Maxwell's equations

Maxwell's equations give the relations between the interacting electric and magnetic fields. Maxwell's equations consist of four fundamental electromagnetic equations for time-varying magnetic field, and the equations are given as

$$\nabla \times \mathbf{E} = -\frac{\partial \mathbf{B}}{\partial t} \tag{2.1}$$

$$\nabla \times \mathbf{H} = \mathbf{J} + \frac{\partial \mathbf{D}}{\partial t} \tag{2.2}$$

$$\nabla \cdot \mathbf{D} = e_e \tag{2.3}$$

$$\nabla \cdot \mathbf{B} = 0 \tag{2.4}$$

Equation (2.1) is known as Faraday's law, named after Michael Faraday, who, in 1831, discovered experimentally that a current is induced in a conducting loop when magnetic flux linking the loop changes. It is an experimental law and can be considered as a postulate. The equation expresses the postulate for electromagnetic induction, which simply means that the electric field intensity in a region of time-varying magnetic flux density is non-conservative and cannot be expressed as a gradient or scalar potential. Equation (2.2) is Ampere's law, named after the Ampere Andre-Marie, who showed that wires carrying electric currents attract and repel each other magnetically.

From Maxwell's electromagnetic equations, the solenoidal relation $\nabla \cdot \mathbf{B} = 0$ yields $\frac{\partial \mathbf{B}}{\partial z} = 0$. When the magnetic Reynolds number is small, induced magnetic field is negligible in comparison with the applied magnetic field, so that

$B_x = B_y = 0$ and $B_z = B_0$ (a constant).

If (J_x, J_y, J_z) are components of electric current density **J**, the equation of conservation of electric charge $\nabla \cdot \mathbf{J} = 0$ yields

$$J_z = constant \tag{2.5}$$

Since the sheet is non-conducting, $J_z = 0$ at the sheet and hence zero everywhere in the flow. Neglecting polarization effect, the electric field $\mathbf{E}$ is given as $\mathbf{E} = 0$.

So

$$\mathbf{J} = (J_x, J_y, 0)\,, \mathbf{B} = (0, 0, B_0)\,, \mathbf{q} = (u, v, w_o) \tag{2.6}$$

The generalized Ohm's law, neglecting Hall effect, is expressed as

$$\mathbf{J} = \sigma\,(\mathbf{E} + \mathbf{q} \times \mathbf{B}) \tag{2.7}$$

Magnetic field is considered to be divergenceless, that is, there are not magnetic flux sources and sinks within the field, and therefore$\nabla \cdot \mathbf{B} = 0$. The mathematical expression of equation of continuity in the case of conservation of electric charge is

$$\nabla \cdot \mathbf{J} = -\frac{\partial e_e}{\partial t} \tag{2.8}$$

The term $\mathbf{q} \times \mathbf{B}$ in equation (2.7) yields

$$\mathbf{q} \times \mathbf{B} = \begin{vmatrix} \mathbf{i} & \mathbf{j} & \mathbf{k} \\ u & v & w_o \\ 0 & 0 & B_0 \end{vmatrix} = vB_0\mathbf{i} - uB_0\mathbf{j} \tag{2.9}$$

Thus from equations (2.7) and (2.9), the x and y-axis components of the current density respectively become

$$J_x = \sigma v B_0, \qquad\qquad J_y = -\sigma u B_0 \tag{2.10}$$

The Lorentz force $\mathbf{J} \times \mathbf{B}$ is given as

$$\mathbf{J} \times \mathbf{B} = \begin{vmatrix} \mathbf{i} & \mathbf{j} & \mathbf{k} \\ \sigma v B_0 & -\sigma u B_0 & 0 \\ 0 & 0 & B_0 \end{vmatrix} = -\sigma u B_0^2\mathbf{i} - \sigma v B_0^2\mathbf{j} \tag{2.11}$$

Heat generated due to electrical resistance of the fluid to the flow of induced electric current is

$$\frac{\mathbf{J}^2}{\sigma} = \sigma v^2 B_0^2 + \sigma u^2 B_0^2 = \sigma B_0^2 \left(u^2 + v^2\right) \tag{2.12}$$

Taking both Joule heating and radiative heat flux into consideration the equation of energy becomes

$$\rho C_P \frac{DT}{Dt} = k\nabla^2 T + \mu \left[\left(\frac{\partial u}{\partial z}\right)^2 + \left(\frac{\partial v}{\partial z}\right)^2 \right] + \sigma B_0^2 \left(u^2 + v^2\right) - \frac{16\sigma^* T_\infty^3}{3k^*} \frac{\partial^2 T}{\partial z^2} \tag{2.13}$$

2.2.2. Forces on an electric charge

When a unit electric charge e moves with velocity $\mathbf{q}$ in a region comprising of an electric field $\mathbf{E}$ and a magnetic field $\mathbf{B}$, it experiences two types of forces: the electric force $e\mathbf{E}$, and magnetic force $e(\mathbf{q} \times \mathbf{B})$. The total electromagnetic force F_e on e is given by Lorentz's equation as the sum of these two forces, Bhag and Huseyin (2005). The electromagnetic force is therefore expressed as

$$\mathbf{F}_e = e(\mathbf{E} + \mathbf{q} \times \mathbf{B}) \tag{2.14}$$

The force $\mathbf{F}_e$ is known as Lorentz force and is a force that acts on the fluid particles. Experiments show that this force acts in a direction perpendicular to both $\mathbf{J}$ and $\mathbf{B}$ and is proportional to their respective magnitudes. The generalized Ohm's law can be written as

$$\mathbf{J} = \sigma\,(\mathbf{E} + \mathbf{q} \times \mathbf{B}) + e_e\mathbf{q} \tag{2.15}$$

The last term in equation (2.15) refers to current displacement current, which can be ignored since it is negligibly small at fluid velocity $\mathbf{q}$.

2.3. The Coriolis effect

The Coriolis effect is the apparent deflection of moving objects from a straight path when they are viewed from a rotating frame of reference. The Coriolis effect is caused by the Coriolis force, which appears in the equation of motion in a rotating frame of reference, Persson (1998). The whole system rotates with constant angular velocity of Ω about the z-axis. The vector formula for the magnitude and direction of the Coriolis acceleration is

$$2\Omega \times \mathbf{q} = \begin{vmatrix} \mathbf{i} & \mathbf{j} & \mathbf{k} \\ 0 & 0 & 2\Omega \\ u & v & w_o \end{vmatrix} = -2\Omega v\mathbf{i} + 2\Omega u\mathbf{j} \tag{2.16}$$

2.4. Darcy's Law

Darcy's law states that the area-averaged velocity through a column of porous material between two points is directly proportional to the pressure gradient $\frac{dP}{dx}$ and inversely proportional to both the fluid viscosity μ and the distance between the two points. Thus

$$u = -\frac{K_p}{\mu}\left(\frac{dP}{dx}\right) \tag{2.17}$$

Each individual porous structure has a complex geometry. It has been common practice to smooth out the local complexity of the actual phenomena by concentrating on the overall aspects of mass and momentum conservation principles, Nakayama (1995). In macroscopic view, flow through porous column is unidirectional, though each fluid particle inside a porous structure experiences a complex three-dimensional motion. The pressure P is the intrinsic average pressure measured by a pressure gauge inside the fluid. The permeability K_p is an empirical constant that depends on the microstructure of the solid medium, and is independent of the properties of the saturated fluid. The velocity u is known as Darcian velocity, and is less than the actual pore velocity u_f. Both velocities are related by the expression

$$u = \frac{u_f}{\epsilon^+} \tag{2.18}$$

Equation (2.18) is called the Dupuit-Forchheimer relation, and ϵ^+ is permeability, that is, the fraction of the total volume that is occupied by the fluid. So

$$\epsilon^{+} = \frac{V_f}{V} \tag{2.19}$$

The values of K_p are usually very small: in a brick K_p varies from 10^{-15} to 10^{-13}; in a cigarette $K_p = 10^{-9}$, and in sand K_p varies from 10^{-11} to $10^{-10} m^2$.

2.5. The Equation of continuity

The mass conservation equation is also called the equation of continuity. It is derived from the law of conservation of mass. The law of conservation of mass assumes that mass can neither be created nor destroyed and that on a steady flow process, the stored mass in a control volume does not change. A steady flow process is one where the flow rate does not change over time. This implies that inflow into the control volume equals outflow. For a steady fluid flow, the tensor form of the equation of continuity is

$$\frac{\partial \rho}{\partial t} + \frac{\partial}{\partial x_i}(\rho u_i) = 0 \tag{2.20}$$

where i = 1, 2, 3 along x, y and z directions respectively. Since the fluid in consideration is assumed to be incompressible, the equation of continuity takes the following form:

$$\frac{\partial u_i}{\partial x_i} = 0 \tag{2.21}$$

2.6. Conservation of momentum

The law of the conservation of momentum states that the rate of change of momentum in the control volume is equal to the sum of the net momentum flux into the control volume and any external forces acting on the control volume. This implies that the total momentum of a closed system of objects is constant.

The general momentum equation in tensor form is

$$\rho(\frac{\partial u_i}{\partial t} + u_j \frac{\partial u_i}{\partial x_j}) = \rho F_i + \frac{\partial \sigma_{ij}}{\partial x_j} \tag{2.22}$$

where $i = 1, 2, 3$ and $j = 1, 2, 3$ are the summation variables along x, y and z axes respectively. The term ρF_i represents body forces acting on the fluid. In this study the two body forces considered are the gravitational force and the electromagnetic force. The other two terms $\rho \frac{\partial u_i}{\partial t}$ and $\rho u_j \frac{\partial u_i}{\partial x_j}$ in equation (2.22) represent the local acceleration and the convective acceleration respectively.

In the equation of the conservation of momentum (2.22), the body forces and surface forces balance with the rate of change of momentum. Body forces act on the entire control volume. The most common body force is that due to gravity. Surface forces act on only one particular surface of the control volume at a time, and arise due to pressure or viscous stresses. All gases are Newtonian, as are most common liquids such as water, hydrocarbons, and oils. Water is a medium viscosity Newtonian fluid. Motor oil and Maple Syrup are high viscosity Newtonian fluids. A Newtonian fluid is one in which the viscous stress is linearly proportional to the rate of deformation. Fluids that do not follow the Newtonian behaviour law include toothpaste, blood and paints; and are referred to as non-Newtonian fluids.

For a three-dimensional flow in a gravitational field, Darcy's law (2.17) may be generalized to the following equation:

$$-\nabla P + \rho \mathbf{g} = \frac{\mu}{K_p}\mathbf{q} \tag{2.23}$$

This is purely a momentum equation striking a balance between viscous forces and the pressure gradient in the porous medium. However this relation does not apply to flows in porous media at high velocity. Darcy's law is based purely on the balance of viscous forces and pressure gradient. Forchheimer (1901) modified Darcy's law to the following equation:

$$-\frac{dP}{dx} = \frac{\mu}{K_p}u + \frac{C_k}{K_p^{1/2}}\rho u^2 \tag{2.24}$$

Equation (2.24) is known as *Forchheimer-extended Darcy's law*, where C_k represents the Forchheimer constant, which is usually determined experimentally for different porous media. The linear Darcy term describing the distributed body force exerted by the fibers in the porous medium is retained, as discussed by Wu *et al.* (2005); but the non-linear Forchheimer term is neglected in this study. The physical variables governing the flow are functions of x, z and t.

For the case of highly porous media, the wall frictional effect becomes appreciable, and extends deep into the bulk of the flow, jumping over the microstructure. To model such boundary frictional effects, Brinkman (1947) modified Darcy's law and made it appear as

$$-\frac{dP}{dx} = \frac{\mu}{K_p}u - \mu_B\frac{d^2u}{dy^2} \tag{2.25}$$

where μ_B is taken to be equal to μ for the first approximation. For large values of K_p, equation (2.25) reduces to the momentum equation for a viscous fluid flow where the flow does not occur in a porous medium.

The following equation is a combination of Forchheimer and Brinkman modifications in form of a law known as *Brinkman-Forchheimer-extended Darcy's law*:

$$-\nabla P + \rho \mathbf{g} + \mu_B \nabla^2 \mathbf{q} - \frac{\mu}{K_p}\mathbf{q} - \frac{C_k}{K_p^{1/2}}\rho \mid \mathbf{q} \mid \mid \mathbf{q} \mid = 0 \tag{2.26}$$

If the convective inertia terms are included in the Brinkman-Forchheimer-extended Darcy model as given by (2.26), the general macroscopic momentum equation for the fluid-saturated porous media is

$$\rho \frac{\partial \mathbf{q}}{\partial t} + \rho \left(\mathbf{q} \cdot \nabla\right) \mathbf{q} = -\nabla P + \rho \mathbf{g} + \mu_B \nabla^2 \mathbf{q} - \frac{\mu}{K_p}\mathbf{q} - \frac{C_k}{K_p^{1/2}}\rho \mid \mathbf{q} \mid\mid \mathbf{q} \mid \tag{2.27}$$

The macroscopic inertia terms on the left hand side of equation (2.27) are referred to as *convective inertia*, while the last three terms on the right hand side are called *Brinkman term (or boundary friction term), Darcy term (or porous viscous term)* and *Forchheimer term (or porous inertia term)*, respectively. As permeability K_p increases, the last two terms on the right hand side vanish, and equation (2.27) becomes the Navier-Stokes equation. For subsonic flows and in free convection, the buoyancy force terms may be added to the right-hand side of equation (2.26) to obtain

$$\begin{aligned} \rho \frac{\partial \mathbf{q}}{\partial t} + \rho \left(\mathbf{q} \cdot \nabla\right) \mathbf{q} \quad = \quad & -\nabla P + \rho \mathbf{g} + \mu_B \nabla^2 \mathbf{q} - \frac{\mu}{K_p}\mathbf{q} - \frac{C_k}{K_p^{1/2}}\rho \mid \mathbf{q} \mid\mid \mathbf{q} \mid \\ & -\rho \mathbf{g} \beta (T - T_w) - \rho \mathbf{g} \beta^* (C - C_w) \end{aligned} \tag{2.28}$$

Equations (2.27) and (2.28) represent the macroscopic momentum equations for flow in porous media.

2.7. The Equation of Species Concentration

The equation of species concentration is based on the law of conservation of mass. This equation is used when the porous medium is saturated with fluid and obeys Darcy's law. Convection is one of the major modes of heat transfer and mass transfer. Convective heat and mass transfer take place through both diffusion - the random Brownian motion of individual particles in the fluid - and advection, in which dissolved substances or heat are carried along with bulk fluid flow. In advection the species spread out from the path expected to be followed by the advection alone. The equation of species concentration is given as

$$\begin{aligned}\frac{\partial C}{\partial t} &= D_{MX}\frac{\partial^2 C}{\partial x^2} + D_{MY}\frac{\partial^2 C}{\partial y^2} + D_{MZ}\frac{\partial^2 C}{\partial z^2} + \frac{D_{TX}k_T}{c_s C_p}\frac{\partial^2 T}{\partial x^2} + \frac{D_{TY}k_T}{c_s C_p}\frac{\partial^2 T}{\partial y^2} \\ &+ \frac{D_{TZ}k_T}{c_s C_p}\frac{\partial^2 T}{\partial z^2} - u\frac{\partial C}{\partial x} - v\frac{\partial C}{\partial y} - w\frac{\partial C}{\partial z} - k_1 C\end{aligned} \tag{2.29}$$

where D_{MX}, D_{MY}, D_{MZ} are the molecular diffusion coefficients and D_{TX}, D_{TY}, D_{TZ} are the thermal diffusion coefficients in the x, y, and z-axis respectively. The last term on the right hand side of (2.29) represents change in species concentration due to chemical reaction. The species concentration is assumed to be a function of z and t, that is, $C(z,t)$. Equation (2.30) assumes that the thermal and molecular diffusion rates are equal. Since this study assumes there is no chemical reaction, equation (2.29) becomes

$$\frac{\partial C}{\partial t} = D_{MZ}\frac{\partial^2 C}{\partial z^2} + \frac{D_{MZ}k_T}{c_s C_p}\frac{\partial^2 T}{\partial z^2} - w\frac{\partial C}{\partial z} \tag{2.30}$$

2.8. Equation of Conservation of Energy

The equation of conservation of energy is derived from the First Law of Thermodynamics, which states that energy is conserved in any process involving a thermodynamic system and its surroundings. It simply states that the increase in the internal energy of dE of a system is equal to the amount of energy added by heating the system Q minus the amount lost as a result of the work done by the system on its surroundings $dW = pdv$. So $dE = dQ - dW = dQ - pdv$.

The First Law of Thermodynamics requires that

$$\rho\frac{D\ell}{Dt} + \ell\left(\frac{D\rho}{Dt} + \rho\nabla\cdot\mathbf{q}\right) = -\nabla\cdot\mathbf{Q}'' + Q''' - P\nabla\cdot\mathbf{q} + \mu\phi \tag{2.31}$$

where $\mathbf{Q}''$ and Q''' are the heat flux and internal heat generation respectively, Bejan, (1984); and $\frac{D}{Dt}$ is the material derivative or particle derivative. The two quantities in brackets on the left hand side of equation (2.31) represent material derivative of density ρ and the equation of continuity respectively. The material derivative is expressed as

$$\frac{D}{Dt} = \frac{\partial}{\partial t} + u\frac{\partial}{\partial x} + v\frac{\partial}{\partial y} + w\frac{\partial}{\partial z} \tag{2.32}$$

Using the law of conservation of mass and assuming that the fluid is incompressible, the material derivative of density and the equation of momentum are each equated to zero. The term $\mu\phi$ is the internal heating due to viscous dissipation. For an incompressible fluid flow, viscous dissipation function ϕ in three-dimensions is expressed as

$$\begin{aligned}\phi &= 2\left[\left(\frac{\partial u}{\partial x}\right)^2+\left(\frac{\partial v}{\partial y}\right)^2+\left(\frac{\partial w}{\partial z}\right)^2\right] \\ &+ \left[\left(\frac{\partial u}{\partial y}+\frac{\partial v}{\partial x}\right)^2+\left(\frac{\partial v}{\partial z}+\frac{\partial w}{\partial y}\right)^2+\left(\frac{\partial w}{\partial x}+\frac{\partial u}{\partial z}\right)^2\right] \\ &- \frac{2}{3}\left(\frac{\partial u}{\partial x}+\frac{\partial v}{\partial y}+\frac{\partial w}{\partial z}\right)^2 \end{aligned} \tag{2.33}$$

The term $\left(\frac{\partial u}{\partial x}+\frac{\partial v}{\partial y}+\frac{\partial w}{\partial z}\right)$ reduces to zero since it represents the equation of continuity. The partial derivatives of w; that is, $\frac{\partial w}{\partial x}$, $\frac{\partial w}{\partial y}$ and $\frac{\partial w}{\partial z}$ vanish since all are equal to zero. Since the sheet is moving parallel to the x-axis, the contribution of the terms $\frac{\partial u}{\partial x}$ and $\frac{\partial v}{\partial x}$ to viscous dissipation is assumed to be negligible and the terms are therefore dropped from the equation. Lastly y-axis is infinite and so the partial derivatives with respect to y are dropped from the equation. The viscous dissipation equation (2.33) thus reduces to

$$\phi = \left(\frac{\partial u}{\partial z}\right)^2+\left(\frac{\partial v}{\partial z}\right)^2 \tag{2.34}$$

In thermodynamics, enthalpy is defined as $h = \ell + \left(\frac{1}{\rho}\right)P$; hence

$$\frac{Dh}{Dt} = \frac{D\ell}{Dt} + \frac{1}{\rho}\frac{DP}{Dt} - \frac{P}{\rho^2}\frac{D\rho}{Dt} \tag{2.35}$$

The local temperature gradient value $\mathbf{Q}''$ can now be expressed using the Fourier Law of Heat Conduction as

$$\mathbf{Q}'' = -k_T \nabla T \tag{2.36}$$

where k_T is the thermal conductivity of the fluid. The negative sign signifies that heat flows from regions of high temperature to regions of low temperature. Substituting equations (2.33), (2.35) and (2.36) into equation (2.31) yields

$$\rho\frac{Dh}{Dt} = \nabla\cdot(k_T\nabla T) + Q''' + \frac{DP}{Dt} + \mu\phi - \frac{P}{\rho}\left(\frac{D\rho}{Dt} + \rho\nabla\cdot\mathbf{q}\right) \tag{2.37}$$

Since the fluid is assumed to be incompressible, the divergence of the velocity vector is equal to zero. Hence the last term in parentheses in equation (2.37) is equal to zero. Thus the First Law of Thermodynamics reduces to

$$\rho\frac{Dh}{Dt} = \nabla\cdot(k_T\nabla T) + Q''' + \frac{DP}{Dt} + \mu\phi \qquad [Bejan, (1984)] \tag{2.38}$$

Change in specific enthalpy can be written as

$$dh = Tds + \frac{1}{\rho}dP \tag{2.39}$$

where ds is the change in specific entropy. The latter can be written as

$$ds = \left(\frac{\partial s}{\partial T}\right)_P dT + \left(\frac{\partial s}{\partial P}\right)_T dP \tag{2.40}$$

Maxwell's relation is expressed as

$$\begin{aligned}\left(\frac{\partial s}{\partial P}\right)_T &= -\left[\frac{\partial\left(\frac{1}{\rho}\right)}{\partial T}\right]_P \\ &= -\frac{1}{\rho^2}\left(\frac{\partial\rho}{\partial T}\right)_P \\ &= -\frac{\beta}{\rho}\end{aligned} \tag{2.41}$$

where β is the coefficient of thermal expansion; which can be expressed as

$$\beta = -\frac{1}{\rho}\left(\frac{\partial\rho}{\partial T}\right)_P \tag{2.42}$$

The partial derivative of the specific entropy with respect to time is

$$\frac{\partial s}{\partial T} = \frac{C_p}{T} \tag{2.43}$$

Substituting equations (2.39), (2.40), (2.41) and (2.42) into equation (2.43) yields

$$dh = C_P dT + \frac{1}{\rho}(1 - \beta T)\, dP \tag{2.44}$$

Therefore the equation of energy (2.38) reduces to

$$\rho \frac{Dh}{Dt} = \rho C_P \frac{DT}{Dt} + (1 - \beta T) \frac{DP}{Dt} \tag{2.45}$$

Thus First Law of Thermodynamics in terms of absolute temperature T is

$$\rho C_P \frac{DT}{Dt} = \nabla \cdot (k_T \nabla T) + Q''' + \beta T \frac{DP}{Dt} + \mu\phi \tag{2.46}$$

For a saturated porous medium assumed to have constant thermal conductivity k_T and a negligible compressibility effect $\beta T \frac{DP}{Dt}$, taking radiation heat flux into consideration, the equation of energy (2.46) reduces to

$$\rho C_P \frac{DT}{Dt} = k_T \nabla^2 T + Q''' + \mu\phi - q_r \tag{2.47}$$

The equation of continuity for the kind of flow under consideration is given as

$$\frac{\partial w}{\partial z} = 0 \tag{2.48}$$

On integration, equation (2.48) reduces to $w = -w_o$ which represents a constant suction velocity. A negative value of w_o implies constant injection.

The next chapter investigates MHD flow over a stretching surface in porous media in a rotating system with heat and mass transfer. After studying the effects of various flow parameters on the velocity, temperature and concentration fields, the chapter concludes by investigating wall shear stress and rates of heat and mass transfer. The method of solution of the governing equations that arise is also given and the results have been discussed.

CHAPTER THREE

3.0 MHD Flow Over a Stretching Surface in Porous Media in a Rotating System with Heat and Mass Transfer

3.1. Mathematical Formulation

Consider an unsteady MHD laminar boundary layer flow of an incompressible, electrically conducting, viscous Newtonian fluid past a stretching electrically non-conducting semi-infinite sheet embedded in porous media in a rotating system with heat and mass transfer. The stretching sheet is permeable to allow for possible blowing or suction, and is continuously stretching in the x-axis direction in the plane $z = 0$ with a velocity $u = cx$. At distance H units away, a second impermeable and electrically non-conducting sheet is placed parallel to the stretching sheet. The whole system is rotated with a constant angular velocity Ω about the z-axis. The y-axis is taken to be infinite. The pressure gradient is in the positive x-axis direction, and is directed upward parallel to the direction of gravity. Due to rotation, Coriolis force is taken into consideration. The velocity vector $\mathbf{q}$ and magnetic field $\mathbf{B}$ have components (u, v, w) and (B_x, B_y, B_z) along the x, y, and z-axis respectively. The fluid flows upwards against the force of gravity due to a constant pressure gradient $\frac{\partial P}{\partial x}$ transmitted to the fluid by the stretching sheet. The permeable stretching sheet is subjected to a uniform injection of magnitude w_o.

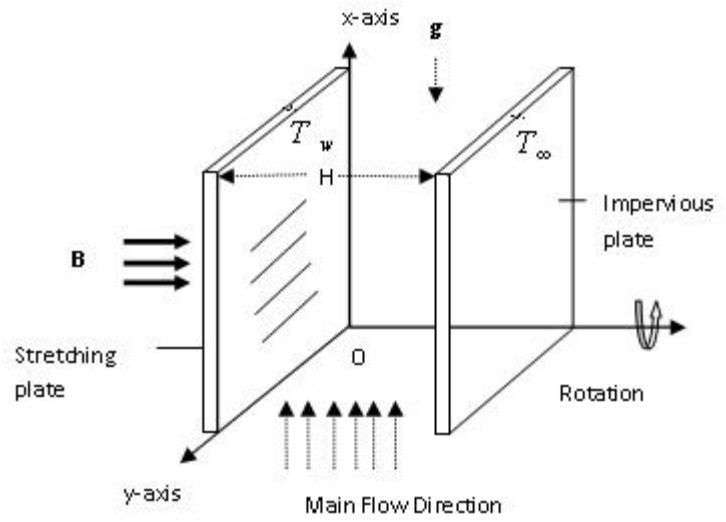

Figure 3.1 : The Flow Configuration

The surface of the stretching sheet is maintained at a uniform temperature T_w. The freestream temperature and the concentration of species are T_∞ and C_∞ respectively. The temperature T_w may either exceed the freestream temperature T_∞ or may be less than T_∞; and C_w may either exceed the ambient concentration C_∞ or may be less than C_∞. When $Tw > T_\infty$ an upward flow is established along the surface due to free convection; when $Tw < T_\infty$, there is a down flow. Additionally, a magnetic field of strength B_o is applied normal to the two plates. In this flow Boussinesq approximation is used. There is variation in the temperature and the density respectively, so the buoyancy force also contributes towards driving the fluid. The variation in density is neglected everywhere except in the buoyancy terms.

$$\rho \cong \rho_\infty + \left(\frac{\partial \rho}{\partial T}\right)_P (T - T_\infty) + \left(\frac{\partial \rho}{\partial C}\right)_P (C - C_\infty) \qquad (3.1)$$

The volumetric coefficient of thermal expansion is given as

$$\beta = -\frac{1}{\rho}\left(\frac{\partial \rho}{\partial T}\right)_P. \tag{3.2}$$

The coefficient of thermal expansion due to concentration gradient is given as

$$\beta^* = -\frac{1}{\rho}\left(\frac{\partial \rho}{\partial C}\right)_P \tag{3.3}$$

From equations (3.2) and (3.3), equation (3.1) becomes

$$\rho_\infty - \rho = \rho\beta\left(T - T_\infty\right) + \rho\beta^*\left(C - C_\infty\right) \tag{3.4}$$

Keeping the origin fixed, a force is suddenly applied to the permeable sheet along the x-axis. The force stretches the sheet and an upward pressure gradient is created. To determine the pressure gradient term, the momentum equation is evaluated at the edge of the boundary layer where $\rho \to \rho_\infty$. When the fluid is at momentum equilibrium, the pressure gradient due to stretching is balanced by the pressure gradient downward due to the variation of the fluid density. Thus

$$-\frac{\partial P}{\partial x} = \rho_\infty g \tag{3.5}$$

The body force term in the momentum equation along the x-axis direction is

$$-\nabla P - \rho g = -\frac{\partial P}{\partial x} - \rho g \tag{3.6}$$

Substituting the value of $\frac{\partial P}{\partial x}$ given in equation (3.5) into equation (3.6):

$$-\rho g + \rho_\infty g = \rho g\beta\left(T - T_\infty\right) + \rho g\beta^*\left(C - C_\infty\right) \tag{3.7}$$

Equation (3.7) represents the overall pressure gradient term in the momentum equation along the x-axis.

From equations (2.28), (2.29) and (2.13) and considering the usual boundary layer approximations, the equations of momentum, concentration, and energy in porous medium with the Darcian effects are given below.

The equation of momentum along the x-axis is

$$\frac{\partial u}{\partial t}+u\frac{\partial u}{\partial x}-w_o\frac{\partial u}{\partial z}-2\Omega v=\nu\left(\frac{\partial^2 u}{\partial x^2}+\frac{\partial^2 u}{\partial z^2}\right)-\frac{\nu}{K_p}u-\frac{\sigma u B_0^2}{\rho}+\beta g(T-T_\infty)+\beta^* g(C-C_\infty) \tag{3.8}$$

The equation of momentum along the y-axis is

$$\frac{\partial v}{\partial t}+u\frac{\partial v}{\partial x}-w_o\frac{\partial v}{\partial z}+2\Omega u=\nu\left(\frac{\partial^2 v}{\partial x^2}+\frac{\partial^2 v}{\partial z^2}\right)-\frac{\nu}{K_p}v-\frac{\sigma v B_0^2}{\rho} \tag{3.9}$$

The equation of energy is

$$\begin{aligned}\frac{\partial T}{\partial t}+u\frac{\partial T}{\partial x}-w_o\frac{\partial T}{\partial z} &= \frac{k_f}{\rho C_p}\left(\frac{\partial^2 T}{\partial x^2}+\frac{\partial^2 T}{\partial z^2}\right)+\frac{D_M k_T}{c_s C_p}\left(\frac{\partial^2 C}{\partial x^2}+\frac{\partial^2 C}{\partial z^2}\right)\\ &+ \frac{\sigma}{\rho C_p}B_0^2\left(u^2+v^2\right)\\ &+ \frac{\mu}{\rho C_p}\left[\left(\frac{\partial u}{\partial z}\right)^2+\left(\frac{\partial v}{\partial z}\right)^2\right]-\frac{16\sigma^* T_\infty^3}{3\rho C_p k^*}\frac{\partial^2 T}{\partial z^2}\end{aligned} \tag{3.10}$$

Equation of species concentration is

$$\frac{\partial C}{\partial t}=D_M\left(\frac{\partial^2 C}{\partial x^2}+\frac{\partial^2 C}{\partial z^2}\right)+\frac{D_M k_T}{T_m}\left(\frac{\partial^2 T}{\partial x^2}+\frac{\partial^2 T}{\partial z^2}\right)-u\frac{\partial C}{\partial x}+w_o\frac{\partial C}{\partial z} \tag{3.11}$$

The initial and boundary conditions of this problem are:

$$\begin{aligned}
&t\le 0 \;:\; u=0, v=0, w=0, C=0, T=0 \quad at \quad 0\le z\le H\\
&t>0 \;:\; U=U_\infty, C=C_W, T=T_W \qquad at \qquad x=0 \quad (Channel \quad entrance)\\
&t>0 \;:\; u=cx, v=0, C=C_W, T=T_W, w=w_0 \qquad at \quad z=0 \quad (Porous \quad wall)\\
&t>0 \;:\; u=0, v=0, C=C_\infty, T=T_\infty \quad at \quad z=H \quad (Impermeable \quad wall).
\end{aligned}$$

3.1.1. Non-dimesionalisation

The subject of dimensional analysis considers how to determine the required set of scales for any given problem. It is a process that starts with selecting a suitable scale against which all dimensions in a given physical model are based. Non-dimensionalization is basically aimed at ensuring that the results are applicable to other geometrically similar configurations under a similar set of flow conditions. The non-dimensionalized boundary layer equations have a solution that is bounded, where the solution values lie between 0 and 1 inclusive. The characteristic length is taken as perpendicular distance H units between the parallel sheets. The characteristic velocity is taken as the freestream velocity U_∞.

The non-dimensional parameters are defined as follows:

$$u' = \frac{u}{U_\infty}, v' = \frac{v}{U_\infty}, w_o' = \frac{w_o}{U_\infty}, t' = \frac{U_\infty t}{H}$$
$$y' = \frac{y}{H}, x' = \frac{x}{H}, z' = \frac{z}{H}, T' = \frac{T - T_\infty}{T_W - T_\infty}, C' = \frac{C - C_\infty}{C_W - C_\infty} \quad (3.12)$$

In order to transform the equations of continuity, momentum, energy, and concentration into their respective non-dimensional form, the following analysis is first carried out:

$$\frac{\partial u}{\partial t} = \frac{\partial u}{\partial u'} \cdot \frac{\partial u'}{\partial t'} \cdot \frac{\partial t'}{\partial t} = \frac{U_\infty^2}{H} \frac{\partial u'}{\partial t'} \quad (3.13)$$

$$\frac{\partial u}{\partial z} = \frac{\partial u}{\partial u'} \cdot \frac{\partial u'}{\partial z'} \cdot \frac{\partial z'}{\partial z} = \frac{U_\infty}{H} \frac{\partial u'}{\partial z'} \quad (3.14)$$

$$w \frac{\partial u}{\partial z} = w \frac{\partial u}{\partial u'} \frac{\partial u'}{\partial z'} \frac{\partial z'}{\partial z} = \frac{U_\infty^2}{H} w' \frac{\partial u'}{\partial z'} \quad (3.15)$$

$$\nu \frac{\partial^2 u}{\partial z^2} = \nu \frac{\partial}{\partial z'} \left(\frac{\partial u}{\partial u'} \cdot \frac{\partial u'}{\partial z'} \frac{\partial z'}{\partial z} \right) \frac{\partial z'}{\partial z} = \frac{\nu U_\infty}{H^2} \frac{\partial^2 u'}{\partial z'^2} \quad (3.16)$$

$$\frac{\partial v}{\partial t} = \frac{\partial v}{\partial v'} \cdot \frac{\partial v'}{\partial t'} \cdot \frac{\partial t'}{\partial t} = \frac{U_\infty^2}{H} \frac{\partial v'}{\partial t'} \tag{3.17}$$

$$w\frac{\partial v}{\partial z} = w' U_\infty \frac{\partial v}{\partial v'} \cdot \frac{\partial v'}{\partial z'} \cdot \frac{\partial z'}{\partial z} = \frac{U_\infty^2}{H} \frac{\partial v'}{\partial z'} \tag{3.18}$$

$$\nu\frac{\partial^2 v}{\partial z^2} = \nu\frac{\partial}{\partial z'}\left(\frac{\partial v}{\partial v'} \cdot \frac{\partial v'}{\partial z'}\frac{\partial z'}{\partial z}\right)\frac{\partial z'}{\partial z} = \frac{\nu U_\infty}{H^2}\frac{\partial^2 v'}{\partial z'^2} \tag{3.19}$$

$$\frac{\partial T}{\partial t} = \frac{\partial T}{\partial T'}\frac{\partial T'}{\partial t'}\frac{\partial t'}{\partial t} = \frac{(T_W - T_\infty)\, U_\infty}{H}\frac{\partial T'}{\partial t'} \tag{3.20}$$

$$w\frac{\partial T}{\partial z} = w' U_\infty \frac{\partial T}{\partial T'}\frac{\partial T'}{\partial z'}\frac{\partial z'}{\partial z} = \frac{U_\infty\,(T_W - T_\infty)}{H} w'\frac{\partial T'}{\partial z'} \tag{3.21}$$

$$\frac{k_f}{\rho C_p}\frac{\partial^2 T}{\partial z^2} = \frac{k_f}{\rho C_p}\frac{\partial}{\partial z'}\left(\frac{\partial T}{\partial T'}\frac{\partial T'}{\partial z'}\frac{\partial z'}{\partial z}\right)\frac{\partial z'}{\partial z} = \frac{k_f}{\rho C_p}\frac{(T_W - T_\infty)}{H^2}\frac{\partial^2 T'}{\partial z'^2} \tag{3.22}$$

$$\frac{\partial C}{\partial t} = \frac{\partial C}{\partial C'}\frac{\partial C'}{\partial t'}\frac{\partial t'}{\partial t} = \frac{U_\infty}{H}\,(C_W - C_\infty)\,\frac{\partial C'}{\partial t'} \tag{3.23}$$

$$w\frac{\partial C}{\partial z} = w' U_\infty \frac{\partial C}{\partial C'}\frac{\partial C'}{\partial z'}\frac{\partial z'}{\partial z} = \frac{U_\infty (C_W - C_\infty)}{H} w'\frac{\partial C'}{\partial z'} \tag{3.24}$$

$$D_M\frac{\partial^2 C}{\partial z^2} = D_M\frac{\partial}{\partial z'}\left(\frac{\partial C}{\partial C'}\frac{\partial C'}{\partial z'}\frac{\partial z'}{\partial z}\right)\frac{\partial z'}{\partial z} = D_M\frac{(C_W - C_\infty)}{H^2}\frac{\partial^2 C'}{\partial z'^2} \tag{3.25}$$

$$\frac{D_M k_T}{c_s C_p}\frac{\partial^2 C}{\partial z^2} = \frac{D_M k_T}{c_s C_p}\frac{\partial}{\partial z'}\left(\frac{\partial T}{\partial C'}\frac{\partial C'}{\partial z'}\frac{\partial z'}{\partial z}\right)\frac{\partial z'}{\partial z} = \frac{D_M k_T}{c_s C_p}\frac{(C_W - C_\infty)}{H^2}\frac{\partial^2 C'}{\partial z'^2} \tag{3.26}$$

$$\frac{D_M k_T}{T_m}\frac{\partial^2 T}{\partial z^2} = \frac{D_M k_T}{T_m}\frac{\partial}{\partial z'}\left(\frac{\partial T}{\partial T'}\frac{\partial T'}{\partial z'}\frac{\partial z'}{\partial z}\right)\frac{\partial z'}{\partial z} = \frac{D_M k_T}{T_m}\frac{(T_W - T_\infty)}{H^2}\frac{\partial^2 T'}{\partial z'^2} \tag{3.27}$$

Substituting equations (3.13) to (3.19) into equations (3.8) and (3.9) and dividing each of the resulting terms by $\frac{U_\infty^2}{H}$, the two equations of momentum respectively become:

$$\frac{\partial u^{'}}{\partial t^{'}} + u^{'}\frac{\partial u^{'}}{\partial x^{'}} - w_o\frac{\partial u^{'}}{\partial z^{'}} - 2R_o v^{'} = \frac{1}{Re}\left(\frac{\partial^2 u^{'}}{\partial x^{'2}} + \frac{\partial^2 u^{'}}{\partial z^{'2}}\right) - Xiu^{'} - Mu^{'} + Gr_\theta T^{'} + Gr_c C^{'} \tag{3.28}$$

$$\frac{\partial v^{'}}{\partial t^{'}} + u^{'}\frac{\partial v^{'}}{\partial x^{'}} - w_o\frac{\partial v^{'}}{\partial z^{'}} + 2R_o u^{'} = \frac{1}{Re}\left(\frac{\partial^2 v^{'}}{\partial x^{'2}} + \frac{\partial^2 v^{'}}{\partial z^{'2}}\right) - Xiv^{'} - Mv^{'} \tag{3.29}$$

where $M = \frac{\sigma B_o^2 H}{\rho U_\infty}$ is the Magnetic field parameter, $Re = \frac{U_\infty H}{\nu}$ is the Reynolds number, $R_o = \frac{\Omega H}{U_\infty}$ is the Rotation parameter, $Xi = \frac{\nu H}{U_0 K_p}$ is the Permeability parameter, $Gr_\theta = \frac{\beta g H(T_W - T_\infty)}{U_\infty^2}$ is the local temperature Grashof number and $Gr_c = \frac{\beta^* g H(C_W - C_\infty)}{U_\infty^2}$ is the local mass Grashof number.

Similarly substituting equations (3.20) to (3.25) into equation (3.10) and dividing each of the resulting terms by $\frac{(T_W - T_\infty)U_\infty}{H}$, equation (3.10) becomes

$$\begin{aligned}\frac{\partial T^{'}}{\partial t^{'}} + u^{'}\frac{\partial T^{'}}{\partial x^{'}} - w_o\frac{\partial T^{'}}{\partial z^{'}} &= \frac{1}{Re}\left[\frac{1}{Pr}\left(\frac{\partial^2 T^{'}}{\partial x^{'2}} + \frac{\partial^2 T^{'}}{\partial z^{'2}}\right)\right] + D_f Re\left(\frac{\partial^2 C^{'}}{\partial x^{'2}} + \frac{\partial^2 C^{'}}{\partial z^{'2}}\right) \\ &\quad + \frac{Ec}{Re}\left[\left(\frac{\partial u^{'}}{\partial z^{'}}\right)^2 + \left(\frac{\partial v^{'}}{\partial z^{'}}\right)^2\right] - \frac{4}{3NPrRe}\left(\frac{\partial^2 T^{'}}{\partial z^{'2}}\right) \\ &+ RRe\left(u^{'2} + v^{'2}\right)\end{aligned} \tag{3.30}$$

where $Pr = \frac{\mu C_p}{k_f}$ is the Prandtl number, $D_f = \frac{\rho D_M k_f (C_W - C_\infty)}{\mu c_s C_p (T_W - T_\infty)}$ is the Dufour number, $N = \frac{k^* k_f}{4\sigma^* T_\infty^3}$ is the Radiation parameter, $Ec = \frac{U_\infty^2}{C_p \Delta T}$ is the Eckert Number, $R = \frac{\sigma B_o^2 \mu}{\rho^2 C_p \Delta T}$ is the Joule heating parameter and ΔT represents the temperature difference $(T_W - T_\infty)$.

Similarly the equation of concentration (3.11) becomes

$$\frac{\partial C'}{\partial t'} + u' \frac{\partial C'}{\partial x'} - w_o \frac{\partial C'}{\partial z'} = \frac{1}{ReSc}\left(\frac{\partial^2 C'}{\partial x'^2} + \frac{\partial^2 C'}{\partial z'^2}\right) + \frac{Sr}{Re}\left(\frac{\partial^2 T'}{\partial x'^2} + \frac{\partial^2 T'}{\partial z'^2}\right) \tag{3.31}$$

where $Sc = \frac{\mu}{\rho D_M}$ is the Schmidt number, and $Sr = \frac{\rho D_M k_f (T_W - T_\infty)}{\mu T_m (C_W - C_\infty)}$ is the Soret number. The initial and boundary conditions in equation (3.12) appear as follows when transformed to their equivalent non-dimensional form:

$$\begin{aligned}
&t' \leq 0 \;:\; u' = 0, v' = 0, w' = 0, T' = 0, C' = 0 \qquad at \qquad 0 \leq z' \leq H \\
&t' > 0 \;:\; C' = 0, T' = 0 \qquad at \qquad x' = 0 \quad (At \quad Entry) \\
&t' > 0 \;:\; u' = \frac{cH}{U_\infty} x', v' = 0, C' = 1, T' = 1 \quad at \quad z' = 0 \quad (Stretching \quad sheet) \\
&t' > 0 \;:\; u' = 0, v' = 0, w' = 0, C' = 0, T' = 0 \quad at \quad z' = H \quad (Impermeable \\
&sheet).
\end{aligned} \tag{3.32}$$

The non-dimensionalized equations above contain the non-dimensional parameters discussed below.

3.1.2. Prandtl Number

The Prandtl number (Pr) is the ratio of fluid properties controlling the velocity and the temperature distributions. It is the ratio of viscous force to thermal force.

$$Pr = \frac{\mu C_p}{k_f} = \frac{\nu}{\alpha} \tag{3.33}$$

where $\alpha = \frac{k_f}{\rho C_p}$ is the thermal diffusivity and $\nu = \frac{\mu}{\rho}$. Fluids that are particularly viscous have a relatively large value of ν and correspondingly a large Prandtl number, for instance lubricating oils have large Prandtl numbers which can exceed 10^4. A fluid with a Prandtl number close to unity has thermal and momentum boundary layers of similar (nearly equal) thickness. For instance water vapour at $700K$ has a Prandtl number of 1. Fluids which are good conductors of heat have a relatively large value of α; and this

occurrence is found in liquid metals whose Prandtl numbers are correspondingly small, such as Mercury (Pr = 0.023).

3.1.3. Dufour number

The Dufour number (Df) signifies the contribution of the concentration gradients to the thermal energy flux in the flow.

$$D_f = \frac{\rho D_M k_f \left(C_W - C_\infty\right)}{\mu c_s C_p \left(T_W - T_\infty\right)} \tag{3.34}$$

3.1.4. The local temperature Grashof number

The local temperature Grashof number (Gr_θ) signifies the relative effect of the thermal buoyancy force to the viscous hydrodynamic force in the boundary layer. A positive value of Gr_θ corresponds to cooling of the stretching sheet (or heating the fluid in contact with the sheet) while a negative value corresponds to heating the sheet (or cooling the fluid).

$$Gr_\theta = \frac{\beta g H \left(T_W - T_\infty\right)}{U_\infty^2} \tag{3.35}$$

3.1.5. The local mass Grashof number

The local mass (or solutal) Grashof number (Gr_m) defines the ratio of the species buoyancy force to the viscous hydrodynamic force.

$$Gr_c = \frac{\beta^* g H \left(C_W - C_\infty\right)}{U_\infty^2} \tag{3.36}$$

3.1.6. Schmidt number

The Schmidt number (Sc) is a dimensionless number that is a measure of the relative effectiveness of momentum and mass transport by diffusion in the velocity and the

concentration boundary layers, respectively, Incropera and DeWitt (2002). The Schmidt number embodies the ratio of the momentum to the mass diffusivity. The Schmidt number therefore quantifies the relative effectiveness of momentum and mass transport by diffusion in the hydrodynamic (velocity) and the concentration (species) boundary layers. It physically relates the relative thickness of the hydrodynamic layer and mass transfer boundary layer.

$$Sc = \frac{\nu}{D_M} \tag{3.37}$$

3.1.7. Soret number

The Soret number (Sr) defines the effect of the temperature gradients inducing significant mass diffusion effects.

$$Sr = \frac{\rho D_M k_f (T_W - T_\infty)}{\mu T_m (C_W - C_\infty)} \tag{3.38}$$

3.1.8. Eckert number

The Eckert number (Ec) expresses the relationship between the kinetic energy in the flow and the enthalpy. It represents the conversion of kinetic energy into internal energy by work that is done against the viscous fluid stresses. A positive Eckert number implies cooling of the stretching sheet (or loss of heat from the sheet to the fluid).

$$Ec = \frac{U_\infty^2}{C_p \Delta t} \tag{3.39}$$

3.1.9. Nusselt number

The Nusselt number (Nu) is the ratio of the convective heat transfer to the conductive heat transfer. For instance if Nu =1, then the rates of heat transfer by convection and by

conduction are equal. Similarly if Nu =10, then rate of convective heat transfer is 10 times the rate of heat transfer if the fluid was stagnant. Nusselt number is thus equal to the dimensionless temperature gradient at the surface and provides a measure of the convention heat transfer occurring at the surface.

$$Nu = -\left(\frac{\partial T'}{\partial z'}\right)_{z'=0} \tag{3.40}$$

3.1.10.Sherwood number

Sherwood number (Sh) is equal to the dimensionless concentration gradient at the surface, and provides a measure of the convection mass transfer occurring at the surface. Sherwood number is to the concentration boundary layer what the Nusselt number is to the thermal boundary layer.

$$Sh = -\left(\frac{\partial C'}{\partial z'}\right)_{z'=0} \tag{3.41}$$

3.2. METHODOLOGY

Equations (3.28), (3.29), (3.30) and (3.31) that govern MHD flow in porous media over a stretching surface with heat and mass transfers are coupled and highly non-linear. Getting an exact analytical solution to them is not possible. The equations are solved using the finite difference method that applies Crank-Nicholson algorithm. The latter is second order accurate. A given level of accuracy can be obtained with a coarser grid, translating to less computation cost. The finite difference method replaces each PDE with a discrete approximation for space and time domains. In this context the term 'discrete' means that the numerical solution is known only at a finite number of points in

the physical flow domain. The number of points can be selected by the user of the numerical method. In general, increasing the number of points not only increases the resolution but also the accuracy of the numerical solution, Hoffman, *et al.* (1992).

3.2.1. Definition of the mesh

The flow domain is confined by the x, z and t axes. The x-axis values range from X_{min} to X_{max}, z-axis values range from Z_{min} to Z_{max}. So $l = X_{max} - X_{min}$ and $h = Z_{max} - Z_{min}$. The t-axis has values of t that range from 0 to t. The interval $[X_{min}, X_{max}]$ is divided into $(M + 1)$ intervals at different x values indexed by i = 0, 1, . . . , M. The interval $[Z_{min}, Z_{max}]$ is divided into $(N + 1)$ equally spaced intervals along the z-axis, and the values are indexed by j=0, 1,. . . ,N. Similarly the interval [0, t] is divided into $(K + 1)$ equally spaced intervals at different t values indexed by k = 0, 1, . . . ,K. The length of each interval is h units in the x-axis direction, m units in the z-axis direction, and n units in the t-axis direction. (*See the solution grid 3.2*) shown. The aim is to get an approximation to the values of U, V, C and T at the various grid points in the discretised domain. For instance $U_{i,j,k}$ and $C_{i,j,k}$ denote the approximation for the primary velocity and the concentration values respectively at the grid point (i, j, k). A general point along the x-axis is denoted by $x = X_{min} + ih$, and a general point along the z-axis is denoted by $z = Z_{min} + ih, t = nk$ respectively.

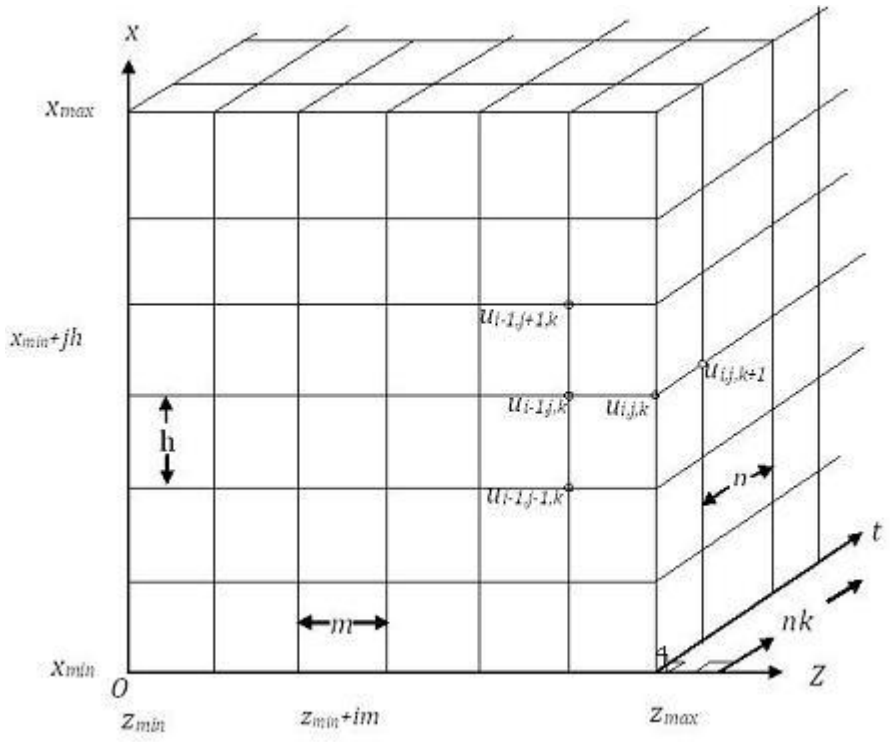

Figure 3.2 : Solution grid

3.2.2. The Finite Difference Method

The partial derivatives of U, V, C and T at each grid point are expressed using finite difference approximation. $U_{i,j,k}$, $V_{i,j,k}$, $C_{i,j,k}$ and $T_{i,j,k}$ for each i are calculated directly from the initial value condition. Thus it is natural to start from the boundary and working outwards so as to obtain $U_{i,j,k+1}$, $V_{i,j,k+1}$, $C_{i,j,k+1}$ and $T_{i,j,k+1}$ respectively. The derivatives are approximated using the Forward Time Backward Space (FTBS) finite difference scheme. The FD expressions for U, U_x and U_{xx} averaged for times k and $k+1$ and are given below.

$$\frac{\partial U}{\partial t} = \frac{U_{i,j}^{k+1} - U_{i,j}^{k}}{\Delta t} \tag{3.42}$$

$$\frac{\partial U}{\partial x} = \frac{U_{i,j}^{k+1} - U_{i-1,j}^{k+1} + U_{i,j}^{k} - U_{i-1,j}^{k}}{2\Delta x} \tag{3.43}$$

$$\frac{\partial^2 U}{\partial x^2} = \frac{U_{i+1,j}^{k+1} - 2U_{i,j}^{k+1} + U_{i-1,j}^{k+1} + U_{i+1,j}^{k} - 2U_{i,j}^{k} + U_{i-1,j}^{k}}{2(\Delta x)^2} \tag{3.44}$$

Equation (3.42) is the forward difference approximation for $\frac{\partial U}{\partial t}$ at $U_{i,j}^{k+1}$ and has a truncation error of order $O(\Delta t)$. The error can be denoted by writing this equation as

$$\frac{\partial U}{\partial t} \mid_{i,j,k+1} = \frac{U_{i,j}^{k+1} - U_{i,j}^{k}}{\Delta t} + O(\Delta t) \tag{3.45}$$

Equation (3.42) is the FTBS approximation for $\frac{\partial U}{\partial x}$ at $U_{i,j}^{k}$ and has a truncation error of order $O(\Delta x)$. The error can be denoted by writing this equation as

$$\frac{\partial U}{\partial x} \mid_{i,j,k} = \frac{U_{i,j}^{k+1} - U_{i-1,j}^{k+1} + U_{i,j}^{k} - U_{i-1,j}^{k}}{2\Delta x} + O(\Delta x) \tag{3.46}$$

Equation (3.44) is the FTBS approximation for $\frac{\partial^2 U}{\partial x^2}$ at $U_{i,j}^{k}$ has a truncation error that is of order $O(\Delta x)^2$. The error can be denoted by writing this equation as

$$\frac{\partial^2 U}{\partial x^2} \mid_{i,j,k} = \frac{U_{i+1,j}^{k+1} - 2U_{i,j}^{k+1} + U_{i-1,j}^{k+1} + U_{i+1,j}^{k} - 2U_{i,j}^{k} + U_{i-1,j}^{k}}{2\left(\Delta x\right)^2} + O(\Delta x)^2 \tag{3.47}$$

The finite difference approximations for C, C_x and C_{xx} and T, T_x and T_{xx} are:

$$\frac{\partial C}{\partial t} = \frac{C_{i,j}^{k+1} - C_{i,j}^{k}}{\Delta t} \tag{3.48}$$

$$\frac{\partial C}{\partial x} = \frac{C_{i,j}^{k+1} - C_{i-1,j}^{k+1} + C_{i,j}^{k} - C_{i-1,j}^{k}}{2\Delta x} \tag{3.49}$$

$$\frac{\partial^2 C}{\partial x^2} = \frac{C_{i+1,j}^{k+1} - 2C_{i,j}^{k+1} + C_{i-1,j}^{k+1} + C_{i+1,j}^{k} - 2C_{i,j}^{k} + C_{i-1,j}^{k}}{2(\Delta x)^2} \tag{3.50}$$

$$\frac{\partial T}{\partial t} = \frac{T_{i,j}^{k+1} - T_{i,j}^{k}}{\Delta t} \tag{3.51}$$

$$\frac{\partial T}{\partial x} = \frac{T_{i,j}^{k+1} - T_{i-1,j}^{k+1} + T_{i,j}^{k} - T_{i-1,j}^{k}}{2\Delta x} \tag{3.52}$$

$$\frac{\partial^2 T}{\partial x^2} = \frac{T_{i+1,j}^{k+1} - 2T_{i,j}^{k+1} + T_{i-1,j}^{k+1} + T_{i+1,j}^{k} - 2T_{i,j}^{k} + T_{i-1,j}^{k}}{2(\Delta x)^2} \tag{3.53}$$

The finite difference equations corresponding to equations (3.28), (2.29), (3.30), and (3.31) are as given below. The primes used in the earlier notation have been omitted for clarity.

The equation of momentum along the x-axis is

$$\begin{aligned}
\frac{U_{i,j}^{k+1} - U_{i,j}^{k}}{\Delta t} + U_{i,j}^{k}\frac{U_{i,j}^{k+1} - U_{i-1,j}^{k+1} + U_{i,j}^{k} - U_{i-1,j}^{k}}{2\Delta x} - w_o\frac{U_{i,j}^{k+1} - U_{i,j-1}^{k+1} + U_{i,j}^{k} - U_{i,j-1}^{k}}{2\Delta z} \\
-R_o(V_{i,j}^{k+1} + V_{i,j}^{k}) \\
= \frac{1}{2Re\,(\Delta x)^2}\left(U_{i+1,j}^{k+1} - 2U_{i,j}^{k+1} + U_{i-1,j}^{k+1} + U_{i+1,j}^{k} - 2U_{i,j}^{k} + U_{i-1,j}^{k}\right) \\
+\frac{1}{2Re\,(\Delta z)^2}\left(U_{i,j+1}^{k+1} - 2U_{i,j}^{k+1} + U_{i,j-1}^{k+1} + U_{i,j+1}^{k} - 2U_{i,j}^{k} + U_{i,j-1}^{k}\right) \\
-\frac{Xi}{2}(U_{i,j}^{k+1} + U_{i,j}^{k}) \\
-\frac{M}{2}(U_{i,j}^{k+1} + U_{i,j}^{k}) + \frac{Gr_\theta}{2}(T_{i,j}^{k+1} + T_{i,j}^{k}) + \frac{Gr_c}{2}(C_{i,j}^{k} + C_{i,j}^{k+1})
\end{aligned} \tag{3.54}$$

Making $U_{i,j}^{k+1}$ in equation (3.53) the subject of the formula:

$$
\begin{aligned}
U_{i,j}^{k+1} &= [U_{i,j}^{k} - \frac{\Delta t}{2\Delta x}U_{i,j}^{k}(-U_{i-1,j}^{k+1} + U_{i,j}^{k} - U_{i-1,j}^{k}) + \frac{w_o\Delta t}{2\Delta z}(-U_{i,j-1}^{k+1} + U_{i,j}^{k} - U_{i,j-1}^{k}) \\
&+R_o\Delta t(V_{i,j}^{k+1} + V_{i,j}^{k}) + \frac{\Delta t}{2Re(\Delta x)^2}(U_{i+1,j}^{k+1} + U_{i-1,j}^{k+1} + U_{i+1,j}^{k} - 2U_{i,j}^{k} + U_{i-1,j}^{k}) \\
&+\frac{\Delta t}{2Re(\Delta z)^2}(U_{i,j+1}^{k+1} + U_{i,j-1}^{k+1} + U_{i,j+1}^{k} - 2U_{i,j}^{k} + U_{i,j-1}^{k}) - \frac{Xi\Delta T}{2}U_{i,j}^{k} \\
&-M\frac{\Delta t}{2}U_{i,j}^{k} + \frac{\Delta tGr_\theta}{2}(T_{i,j}^{k+1} + T_{i,j}^{k}) + \frac{\Delta tGr_c}{2}(C_{i,j}^{k+1} + C_{i,j}^{k})]/[1 + U_{i,j}^{k}\frac{\Delta t}{2\Delta x} \\
&-\frac{w_o\Delta t}{2\Delta z} + \frac{\Delta t}{Re(\Delta x)^2} + \frac{\Delta t}{Re(\Delta z)^2} + \frac{\Delta tXi}{2} + \frac{1}{2}M\Delta t]
\end{aligned}
\tag{3.55}
$$

Equation of momentum along the y-axis is

$$
\begin{aligned}
\frac{V_{i,j}^{k+1} - V_{i,j}^{k}}{\Delta t} &+ U_{i,j}^{k}\frac{V_{i,j}^{k+1} - V_{i-1,j}^{k+1} + V_{i,j}^{k} - V_{i-1,j}^{k}}{2 * \Delta x} - w_o\frac{V_{i,j}^{k+1} - V_{i,j-1}^{k} + V_{i,j}^{k} - V_{i,j-1}^{k}}{2\Delta z} \\
&+R_o(U_{i,j}^{k+1} + U_{i,j}^{k}) \\
&= \frac{1}{2Re\,(\Delta x)^2}\left(V_{i+1,j}^{k+1} - 2V_{i,j}^{k+1} + V_{i-1,j}^{k+1} + V_{i+1,j}^{k} - 2V_{i,j}^{k} + V_{i-1,j}^{k}\right) \\
&+\frac{1}{Re}\left(\frac{V_{i,j+1}^{k+1} - 2V_{i,j}^{k+1} + V_{i,j-1}^{k+1} + V_{i,j+1}^{k} - 2V_{i,j}^{k} + V_{i,j-1}^{k}}{2\,(\Delta z)^2}\right) \\
&-\frac{Xi}{2}(V_{i,j}^{k+1} + V_{i,j}^{k}) \\
&-\frac{M}{2}(V_{i,j}^{k+1} + V_{i,j}^{k}))
\end{aligned}
\tag{3.56}
$$

Making $V_{i,j}^{k+1}$ in equation (3.56) the subject of the formula gives

$$
\begin{aligned}
V_{i,j}^{k+1} &= [V_{i,j}^{k} - \frac{\Delta t}{2\Delta x}U_{i,j}^{k}(-V_{i-1,j}^{k+1} + V_{i,j}^{k} - V_{i-1,j}^{k}) + \frac{w_o \Delta t}{2\Delta z}(-V_{i,j-1}^{k+1} + V_{i,j}^{k} - V_{i,j-1}^{k}) \\
&+ R_o \Delta t(U_{i,j}^{k+1} + U_{i,j}^{k}) + \frac{\Delta t}{2Re(\Delta x)^2}(V_{i+1,j}^{k+1} + V_{i-1,j}^{k+1} + V_{i+1,j}^{k} - 2V_{i,j}^{k} + V_{i-1,j}^{k}) \\
&+ \frac{\Delta t}{2Re(\Delta z)^2}(V_{i,j+1}^{k+1} + V_{i,j-1}^{k+1} + V_{i,j+1}^{k} - 2V_{i,j}^{k} + V_{i,j-1}^{k}) - \frac{Xi\Delta T}{2}V_{i,j}^{k} \\
&- M\frac{\Delta t}{2}V_{i,j}^{k}]/[1 + U_{i,j}^{k}\frac{\Delta t}{2\Delta x} - \frac{w_o \Delta t}{2\Delta z} + \frac{\Delta t}{Re(\Delta x)^2} + \frac{\Delta t}{Re(\Delta z)^2} \\
&+ \frac{Xi\Delta T}{2} + \frac{1}{2}M\Delta tT]
\end{aligned}
\tag{3.57}
$$

Equation of energy is

$$
\begin{aligned}
\frac{T_{i,j}^{k+1} - T_{i,j}^{k}}{\Delta t} &+ \frac{1}{2\Delta x}U_{i,j}^{k}\left(T_{i,j}^{k+1} - T_{i-1,j}^{k+1} + T_{i,j}^{k} - T_{i-1,j}^{k}\right) \\
&- \frac{w_o}{2\Delta z}\left(T_{i,j}^{k+1} - T_{i,j-1}^{k} + T_{i,j}^{k} - T_{i,j-1}^{k}\right) \\
&= \frac{1}{2PrRe\,(\Delta x)^2}\left(T_{i+1,j}^{k+1} - 2T_{i,j}^{k+1} + T_{i-1,j}^{k+1} + T_{i+1,j}^{k} - 2T_{i,j}^{k} + T_{i-1,j}^{k}\right) \\
&+ \frac{1}{2PrRe\,(\Delta z)^2}\left(T_{i,j+1}^{k+1} - 2T_{i,j}^{k+1} + T_{i,j-1}^{k+1} + T_{i,j+1}^{k} - 2T_{i,j}^{k} + T_{i,j-1}^{k}\right) \\
&+ \frac{Df}{2Re(\Delta x)^2}(C_{i+1,j}^{k+1} - 2C_{i,j}^{k+1} + C_{i-1,j}^{k+1} + C_{i+1,j}^{k} - 2C_{i,j}^{k} + C_{i-1,j}^{k}) \\
&+ \frac{Df}{2Re(\Delta z)^2}(C_{i,j+1}^{k+1} - 2C_{i,j}^{k+1} + C_{i,j-1}^{k+1} + C_{i,j+1}^{k} - 2C_{i,j}^{k} + C_{i,j-1}^{k}) \\
&+ \frac{Ec}{4Re(\Delta x)^2}(U_{i,j}^{k+1} - U_{i-1,j}^{k+1} + U_{i,j}^{k} - U_{i-1,j}^{k})^2 \\
&+ \frac{Ec\Delta t}{4Re(\Delta z)^2}(U_{i,j}^{k+1} - U_{i,j-1}^{k+1} + U_{i,j}^{k} - U_{i,j-1}^{k})^2 \\
&- \frac{2}{3NiPrRe(\Delta z)^2}(T_{i,j+1}^{k+1} - 2T_{i,j}^{k+1} + T_{i,j-1}^{k+1} + T_{i,j+1}^{k} - 2T_{i,j}^{k} + T_{i,j-1}^{k}) \\
&+ \frac{RRe}{4}((U_{i,j}^{k})^2 + (V_{i,j}^{k})^2)
\end{aligned}
\tag{3.58}
$$

Making $T_{i,j}^{k+1}$ in equation (3.58) the subject of the formula gives

$$
\begin{aligned}
T_{i,j}^{k+1} &= [T_{i,j}^{k} - \frac{\Delta t}{2\Delta x}U_{i,j}^{k}(-T_{i-1,j}^{k+1} + T_{i,j}^{k} - T_{i-1,j}^{k}) + \frac{w_o \Delta t}{2\Delta z}(-T_{i,j-1}^{k+1} + T_{i,j}^{k} - T_{i,j-1}^{k}) \\
&+ \frac{Df\Delta T}{2Re(\Delta x)^2}(C_{i+1,j}^{k+1} - 2C_{i,j}^{k+1} + C_{i-1,j}^{k+1} + C_{i+1,j}^{k} - 2C_{i,j}^{k} + C_{i-1,j}^{k}) \\
&+ \frac{Df\Delta t}{2Re(\Delta z)^2}(C_{i,j+1}^{k+1} - 2C_{i,j}^{k+1} + C_{i,j-1}^{k+1} + C_{i,j+1}^{k} - 2C_{i,j}^{k} + C_{i,j-1}^{k}) \\
&+ \frac{Ec\Delta t}{4Re(\Delta x)^2}(U_{i,j}^{k+1} - U_{i-1,j}^{k+1} + U_{i,j}^{k} - U_{i-1,j}^{k})^2 \\
&+ \frac{Ec\Delta t}{4Re(\Delta z)^2}(U_{i,j}^{k+1} - U_{i,j-1}^{k+1} + U_{i,j}^{k} - U_{i,j-1}^{k})^2]/[1 + U_{i,j}^{k} \\
&+ \frac{\Delta t}{2PrRe(\Delta x)^2}(T_{i+1,j}^{k+1} + T_{i-1,j}^{k+1} + T_{i+1,j}^{k} - 2T_{i,j}^{k} + T_{i-1,j}^{k}) \\
&+ \frac{\Delta t}{2PrRe(\Delta z)^2}(T_{i,j+1}^{k+1} + T_{i,j-1}^{k+1} + T_{i,j+1}^{k} - 2T_{i,j}^{k} + T_{i,j-1}^{k}) \\
&+ \frac{\Delta t RRe}{4}((U_{i,j}^{k})^2 + (V_{i,j}^{k})^2) \\
&- \frac{2\Delta t}{3NiPrRe(\Delta z)^2}(T_{i,j+1}^{k+1} + T_{i,j-1}^{k+1} + T_{i,j+1}^{k} - 2T_{i,j}^{k} + T_{i,j-1}^{k}) \\
&/[1 + \Delta TUi, j^k/(2\Delta x) + \frac{\Delta t}{2\Delta x} - \frac{w_o \Delta t}{2\Delta z} + \frac{\Delta t}{RePr(\Delta x)^2} \\
&+ \frac{\Delta t}{RePr(\Delta z)^2} - \frac{4\Delta T}{3NiPrRe(\Delta z)^2}]
\end{aligned}
\tag{3.59}
$$

Equation of concentration is

$$
\begin{aligned}
\frac{C_{i,j}^{k+1} - C_{i,j}^{k}}{\Delta t} &+ \frac{1}{2\Delta x}U_{i,j}^{k}(C_{i,j}^{k+1} - C_{i-1,j}^{k+1} + C_{i,j}^{k} \\
&- C_{i-1,j}^{k}) - \frac{w_o}{2\Delta z}(C_{i,j}^{k+1} - C_{i,j-1}^{k+1} + C_{i,j}^{k} - C_{i,j-1}^{k}) \\
&= \frac{1}{2ScRe(\Delta x)^2}(C_{i+1,j}^{k+1} - 2C_{i,j}^{k+1} + C_{i-1,j}^{k+1} + C_{i+1,j}^{k} - 2C_{i,j}^{k} + C_{i-1,j}^{k}) \\
&+ \frac{1}{2ScRe(\Delta z)^2}(C_{i,j+1}^{k+1} - 2C_{i,j}^{k+1} + C_{i,j-1}^{k+1} + C_{i,j+1}^{k} - 2C_{i,j}^{k} + C_{i,j-1}^{k}) \\
&+ \frac{Sr}{2Re(\Delta x)^2}\left(T_{i+1,j}^{k+1} - 2T_{i,j}^{k+1} + T_{i-1,j}^{k+1} + T_{i+1,j}^{k} - 2T_{i,j}^{k} + T_{i-1,j}^{k}\right) \\
&+ \frac{Sr}{2Re(\Delta z)^2}(T_{i,j+1}^{k+1} - 2T_{i,j}^{k+1} + T_{i,j-1}^{k+1} + T_{i,j+1}^{k} - 2T_{i,j}^{k} + T_{i,j-1}^{k})
\end{aligned}
\tag{3.60}
$$

Making $C_{i,j}^{k+1}$ in equation (3.60) the subject of the formula gives

$$
\begin{aligned}
C_{i,j}^{k+1} &= [C_{i,j}^{k} - \frac{\Delta t}{2\Delta x}U_{i,j}^{k}(-C_{i-1,j}^{k+1} + C_{i,j}^{k} - C_{i-1,j}^{k}) + \frac{w_o \Delta t}{2\Delta z}(-C_{i,j-1}^{k+1} + C_{i,j}^{k} - C_{i,j-1}^{k}) \\
&+ \frac{\Delta t}{2ScRe(\Delta x)^2}(C_{i+1,j}^{k+1} + C_{i-1,j}^{k+1} + C_{i+1,j}^{k} - 2C_{i,j}^{k} + C_{i-1,j}^{k}) \\
&+ \frac{\Delta t}{2ScRe(\Delta z)^2}(C_{i,j+1}^{k+1} + C_{i,j-1}^{k+1} + C_{i,j+1}^{k} - 2C_{i,j}^{k} + C_{i,j-1}^{k}) \\
&+ \frac{Sr\Delta T}{2Re(\Delta x)^2}(T_{i+1,j}^{k+1} - 2T_{i,j}^{k+1} + T_{i-1,j}^{k+1} \\
&+ T_{i+1,j}^{k} - 2T_{i,j}^{k} + T_{i-1,j}^{k}) + \frac{Sr\Delta T}{2Re(\Delta z)^2}(T_{i,j+1}^{k+1} - 2T_{i,j}^{k+1} \\
&+ T_{i,j-1}^{k+1} + T_{i,j+1}^{k} - 2T_{i,j}^{k} + T_{i,j-1}^{k})]/[1 + \frac{\Delta t}{2\Delta x}U_{i,j}^{k} \\
&- \frac{w_o \Delta t}{2\Delta z} + \frac{\Delta t}{ReSc(\Delta x)^2} + \frac{\Delta t}{ReSc(\Delta z)^2}]
\end{aligned}
\tag{3.61}
$$

The values of U in equation (3.55) are found at every nodal point for a particular i at $(k+1)^{th}$ time level. Similarly, the values of V are calculated from equation (3.57). The values of U and V at $(k+1)^{th}$ time level are used to compute the values of C in equation (3.61) at $(k+1)^{th}$ time level. Thus, the values of U, V and C are known on a particular i-level. Finally the values of T are calculated using equation (3.59) at every nodal point on a particular i-level at $(k+1)^{th}$ time level. Thus the values of U, V, C and T are determined, at all grid points at $(k+1)^{th}$ time level. This process is repeated for all the i-levels.

The numerical calculations have been performed by fixing the mesh sizes at $\Delta x = 0.05$, $\Delta z = 0.25$, and $\Delta t = 0.001$, where the rectangular region formed by the x-axis and z-axis has 41x41 meshes. When the mesh sizes and the time step are reduced and the results are compared, the results more or less agree up to the fourth decimal place. Hence the mesh

size is considered appropriate for the calculation of the values of the velocity, temperature and concentration. The local truncation error is of order $O(\Delta t + (\Delta z)^2 + (\Delta x)^2)$ and tends to zero as Δt, Δz and Δx tend to zero. Thus the present scheme is convergent.

3.2.3. Discussion of the results

The various parameters that have been varied include the Schmidt number Sc, Soret number Sr, Magnetic field M, Rotational parameter Ro, Permeability parameter Xi, local temperature Grashof number Gr_θ, local mass Grashof number Gr_c, time t, Dufour number Df, Reynold's number Re, Nusselt number Nu, Eckert number Ec, Schmidt number Sc, and Injection parameter w_o. These parameters are input into a computer program where each parameter is varied at a time.

Figures 3.3 and 3.4 show that increase in Magnetic field parameter M causes a decrease in the magnitude of both the primary and the secondary velocity profiles respectively. Figure 3.5 shows that increase in M causes an increase the concentration profiles. Figure 3.6 shows that increase in M causes a decrease in the temperature profiles. It is clear that increasing the value of M has a tendency to slow down the velocity of the fluid. Decreasing the velocity of the fluid slows down the movement of the species. Application of a transverse magnetic field to an electrically conducting fluid gives rise to a resistive type force called the Lorentz force. This force has the tendency to slow down the motion of the fluid in the boundary layer and to increase its concentration, Tania *et*

al. (2010). (However Tania does not explain why temperature profiles decrease with increase in M). The temperature profiles decrease with increasing M. The reduced velocity by the frictional drag due to the Lorentz force is responsible for reducing thermal viscous dissipation in the fluid leading to a thinner thermal boundary layer. Magnetic field can therefore be employed to control the velocity, temperature and concentration boundary layer characteristics of a fluid.

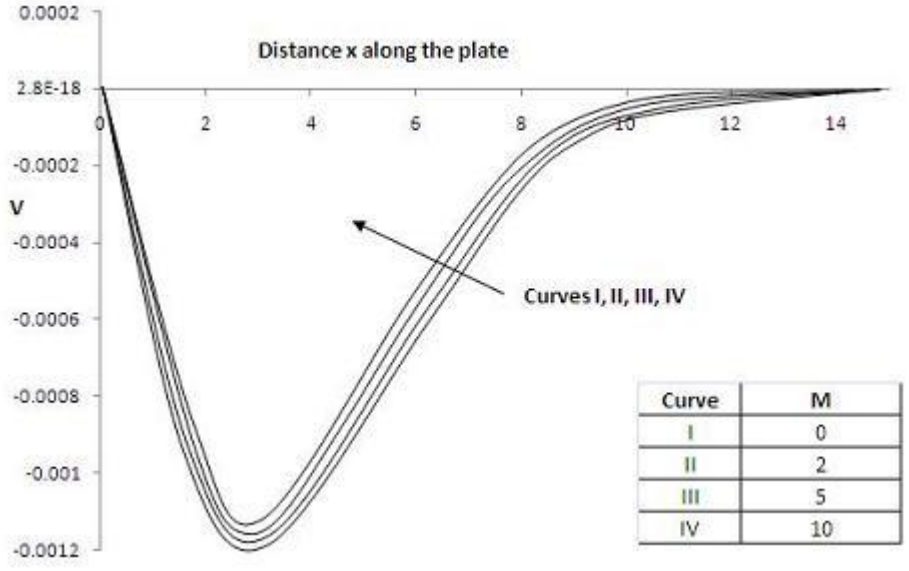

Figure 3.3: Secondary velocity field for different values of Magnetic parameter M.

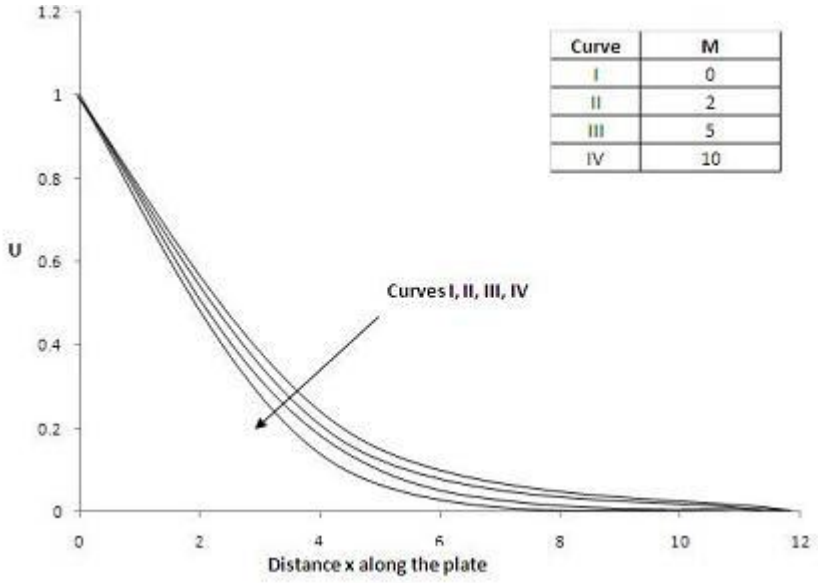

Figure 3.4 : Primary velocity field for different values of Magnetic parameter M.

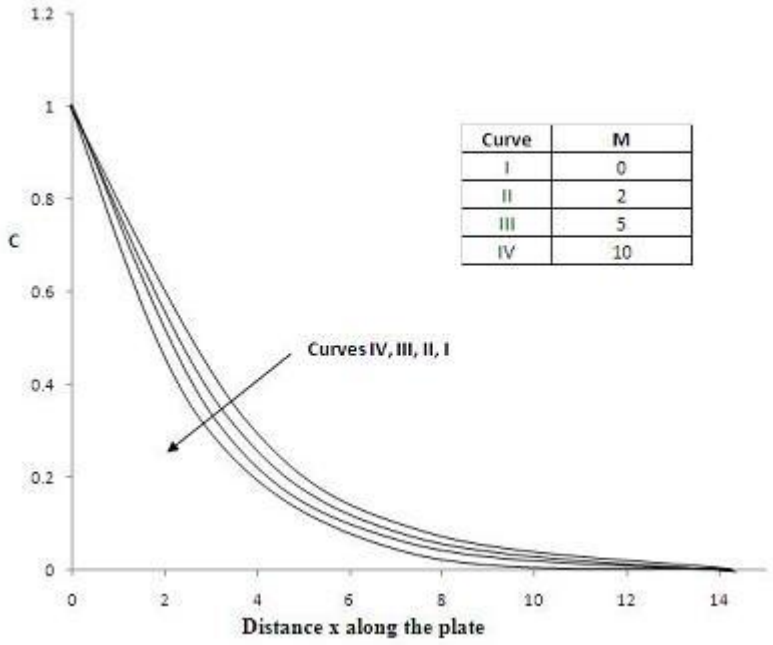

Figure 3.5 : Concentration field for different values of Magnetic parameter M.

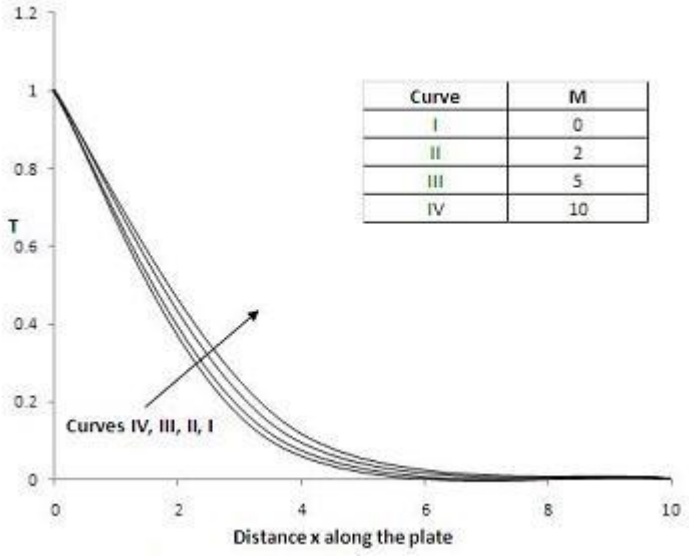

Figure 3.6 : Temperature field for different values of Magnetic parameter M.

From Figure 3.7 increase in Sr causes an increase in the primary velocity profiles. From Figure 3.8 increase in Sr causes an increase in the magnitude of the secondary velocity profiles. From Figure 3.9 increase in Sr causes an increase in the concentration profiles. Soret number (Sr) defines the effect of the temperature gradients inducing significant mass diffusion effects. Figure 3.10 shows that increase in Sr causes an increase in the temperature profiles. Increase in Soret number Sr causes an increase in the concentration, the temperature and the velocity profiles, Ferdows, *et al.* (2010).

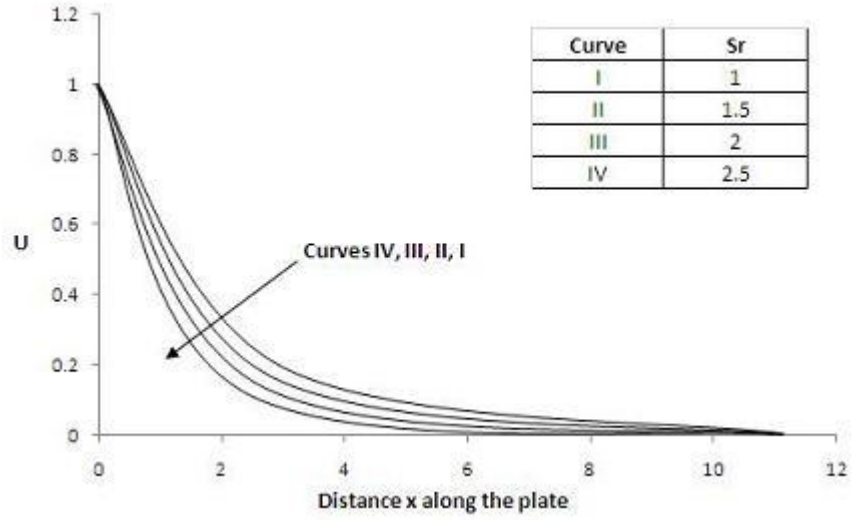

Figure 3.7 : Primary velocity field for different values of Soret number Sr.

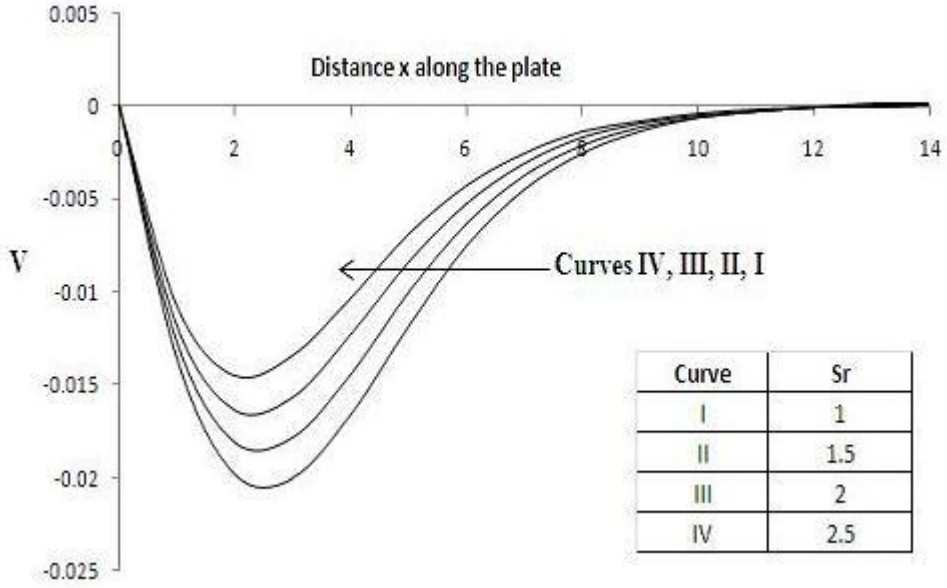

Figure 3.8 : Secondary velocity field for different values of Soret number Sr.

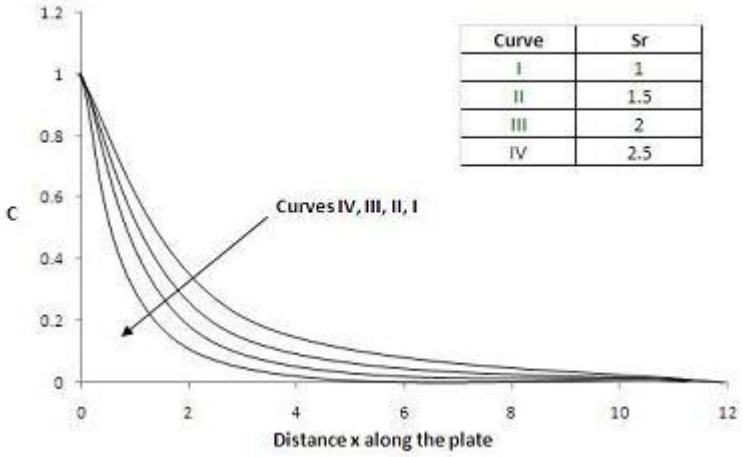

Figure 3.9 : Concentration field for different values of Soret number Sr.

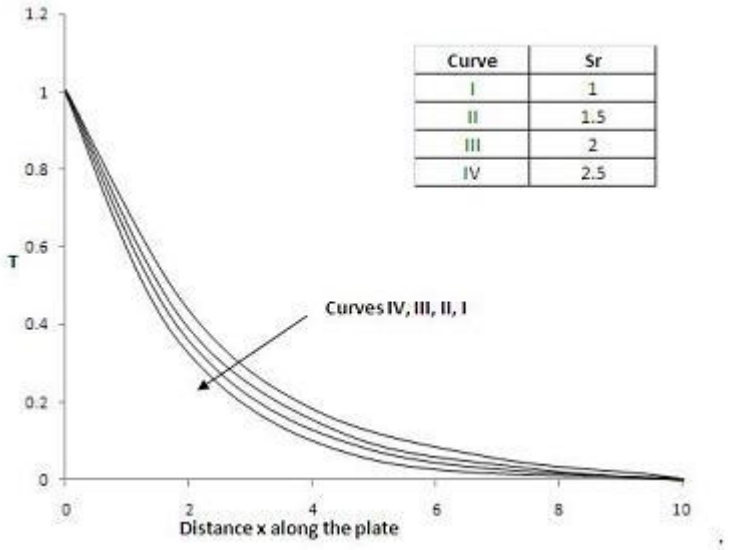

Figure 3.10 : Temperature field for different values of Soret number Sr.

From Figures Figure 3.11 and 3.12, increase in the local temperature Grashof number Gr_θ causes an increase in the primary velocity profiles and an increase in the magnitude of the secondary velocity profiles respectively. Increase in Gr_θ causes a decrease in the temperature profiles, as shown by Figure 3.13. From Figure 3.14 increase in Gr_θ causes

a decrease in the concentration profiles. The local temperature Grashof number Gr_θ represents the effects of free convection currents and physically $Gr_\theta > 0$ corresponds to heating of the fluid (or cooling of the surface). Velocity of the fluid increases because the fluid flow is assisted by the free convection currents. As expected, increase in the velocity profiles is partly due to the enhancement of thermal buoyancy force. The species concentration keeps on decreasing and finally approaches zero with increasing distance away from the fixed end of the stretching sheet. Free convection currents transport the species away from the surface of the stretching sheet resulting to lower concentration of the fluid. The observed increase in the magnitude of the secondary velocity profiles with increase in Gr_θ is as a result of emergence of secondary circulation currents due to the presence of the temperature gradient.

Figure 3.11 shows that increase in modified Grashof number Gr_c causes an increase in the primary velocity profiles. Figure 3.12 shows that increase in modified Grashof number Gr_c causes increase in the magnitude of the secondary velocity profiles. Figure 3.13 shows that increase in the modified Grashof number Gr_c causes a decrease in the temperature profiles. Physically, it means that thermal boundary layer thickness decreases with increase in Gr_c, and hence the observed decrease in the temperature profiles. Figure 3.14 shows that increase in the modified Grashof number Gr_c causes a decrease in the concentration profiles. The modified Grashof number Gr_c defines the ratio of the species buoyancy force to the viscous hydrodynamic force. Increase in Gr_c implies reduced viscous hydrodynamic forces that causes decrease in viscous

dissipation. The latter directly translates to a decrease in the temperature profiles. As expected, the fluid velocity increases due to increase in the species buoyancy force. Increase in species buoyancy force results into a higher species transportation rate away from the stretching surface, resulting into lower concentration, Shateyi (2008).

Figure 3.11 shows that increase in Permeability parameter Xi causes a decrease in the primary velocity profiles. Figure 3.12 shows that increase in Xi causes a decrease in the magnitude of the secondary velocity profiles. Figure 3.13 shows that increase in Xi causes decrease in the temperature profiles. Figure 3.14 shows that increase in Xi causes an increase in the concentration profiles. The Permeability parameter Xi is inversely proportional to the actual permeability K_p of the porous medium. Increase in Xi leads to enhanced deceleration of the flow and hence the velocity decreases. Increasing Xi increases the resistance of the porous medium (as the permeability physically becomes less with increasingXi). This decelerates the flow and reduces the magnitudes of both the primary and the secondary velocities respectively. Increase in Xi reduces the rate of species transportation from the surface of the stretching sheet, leading to the observed increase in the concentration profiles. Thus velocity, temperature and concentration of

the fluid can be controlled by varying the permeability of the porous medium.

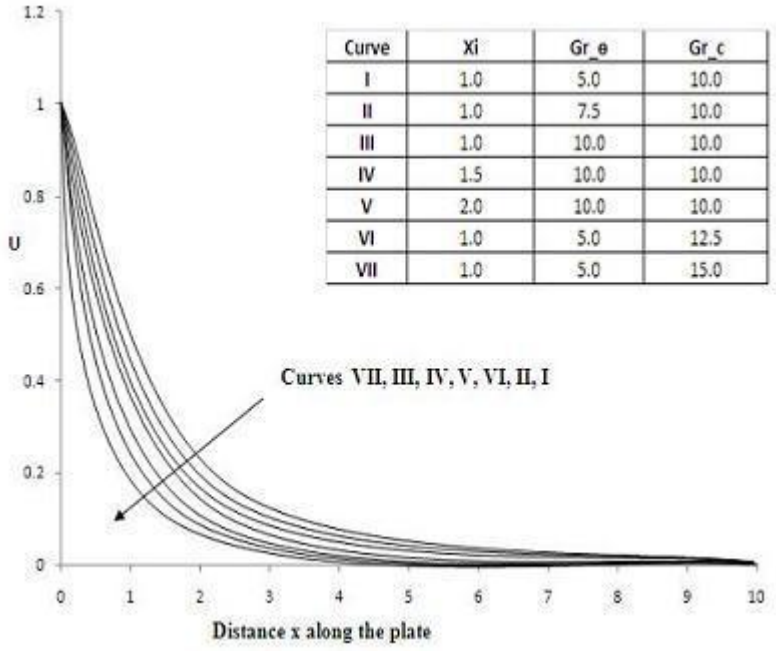

Figure 3.11 : Primary velocity field for different values of the permeability, Grashof and modified Grashof numbers.

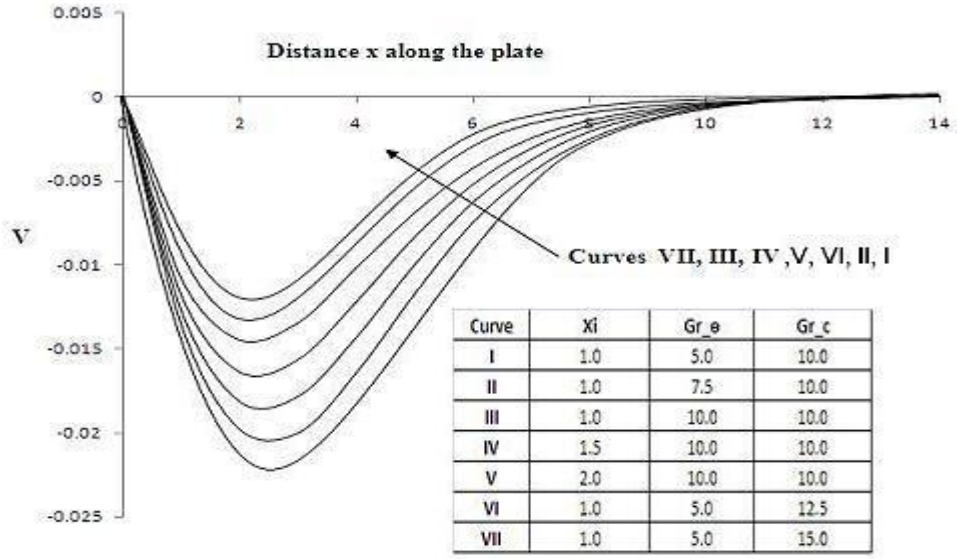

Figure 3.12 : Secondary Velocity field for different values of the permeability, Grashof and modified Grashof numbers.

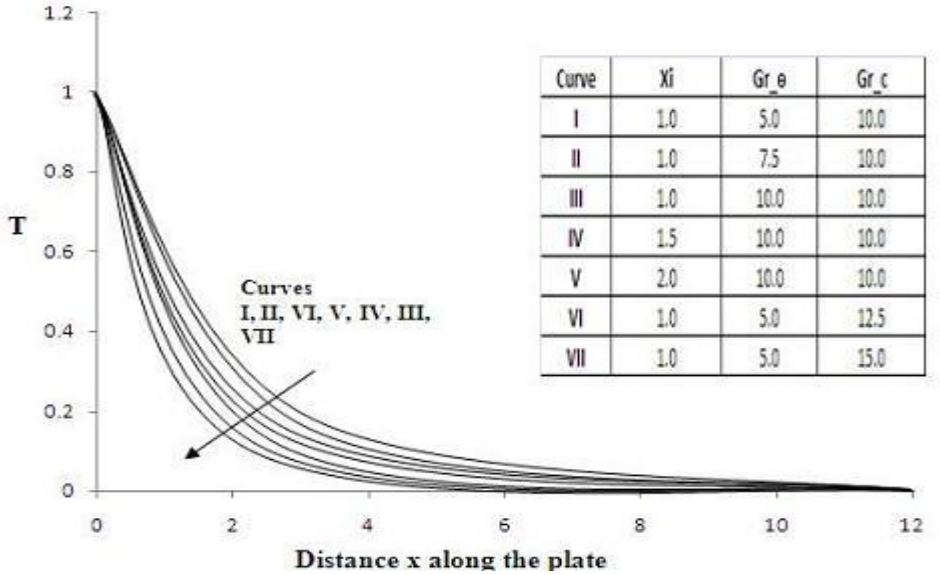

Curve	Xi	Gr_θ	Gr_c
I	1.0	5.0	10.0
II	1.0	7.5	10.0
III	1.0	10.0	10.0
IV	1.5	10.0	10.0
V	2.0	10.0	10.0
VI	1.0	5.0	12.5
VII	1.0	5.0	15.0

Figure 3.13 : Temperature field for different values of the permeability, Grashof and modified Grashof numbers.

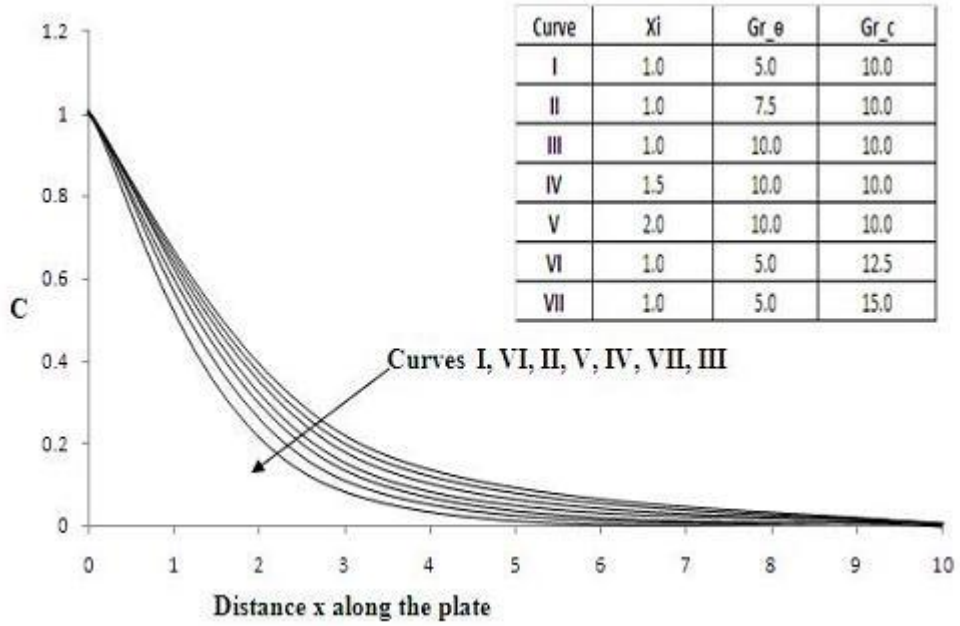

Curve	Xi	Gr_θ	Gr_c
I	1.0	5.0	10.0
II	1.0	7.5	10.0
III	1.0	10.0	10.0
IV	1.5	10.0	10.0
V	2.0	10.0	10.0
VI	1.0	5.0	12.5
VII	1.0	5.0	15.0

Figure 3.14 : Concentration field for different values of the permeability, Grashof and modified Grashof numbers.

Figure 3.15 shows that increase in time t causes an increase in the primary velocity profiles. Figure 3.16 shows that increase in time t causes an increase in the magnitude of the secondary velocity profiles. Figure 3.17 shows that increase in time causes a decrease in the concentration profiles. It means the concentration boundary layer decreases with time. Figure 3.18 shows that increase in time causes decrease in the temperature profiles. Physically, it means that thermal boundary layer thickness decreases as time increases. As time t increases the velocity, concentration and temperature of the fluid fall steeply near the fixed end of the stretching sheet, and the gradient decreases gradually as the distance from the fixed end of the stretching sheet increases.

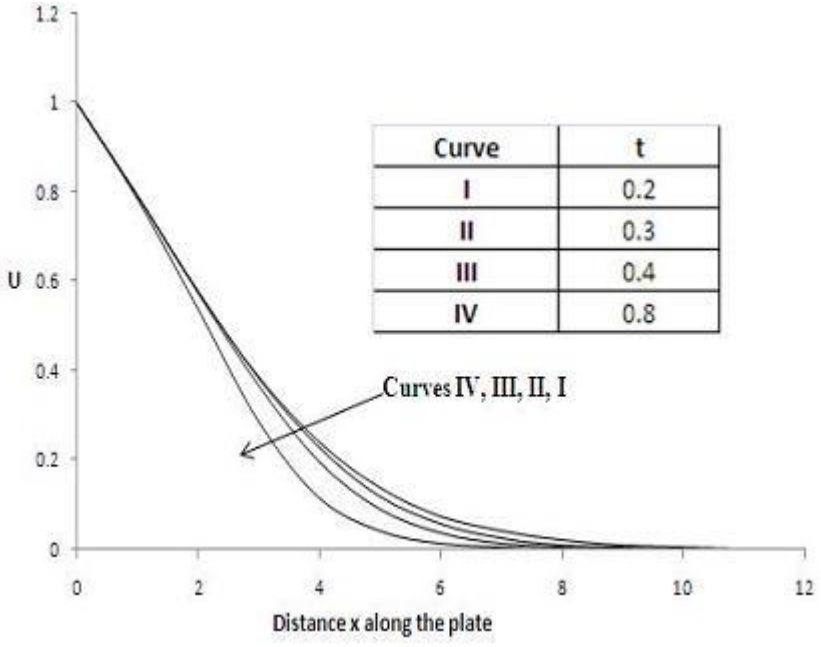

Figure 3.15 : Primary velocity profiles for different values of time t.

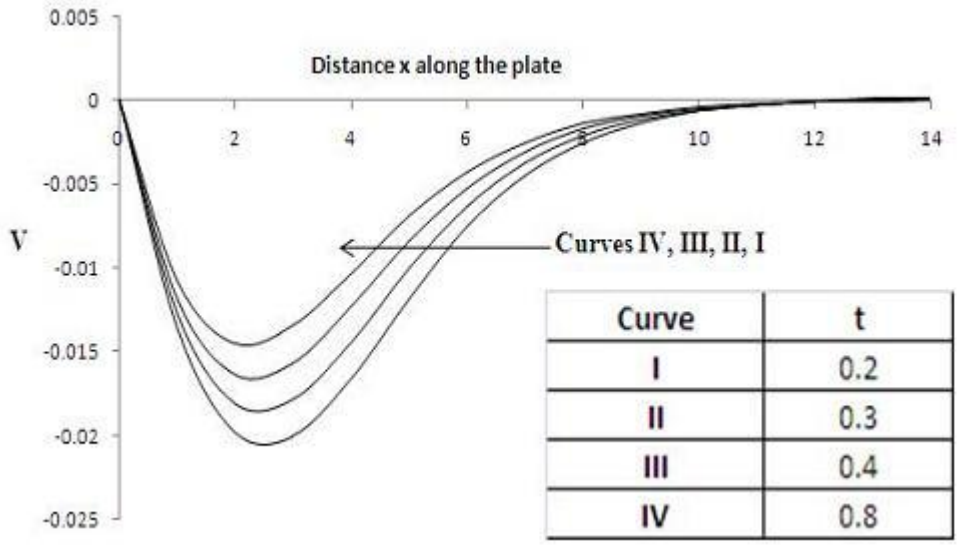

Figure 3.16 : Secondary velocity profiles for different values of time t.

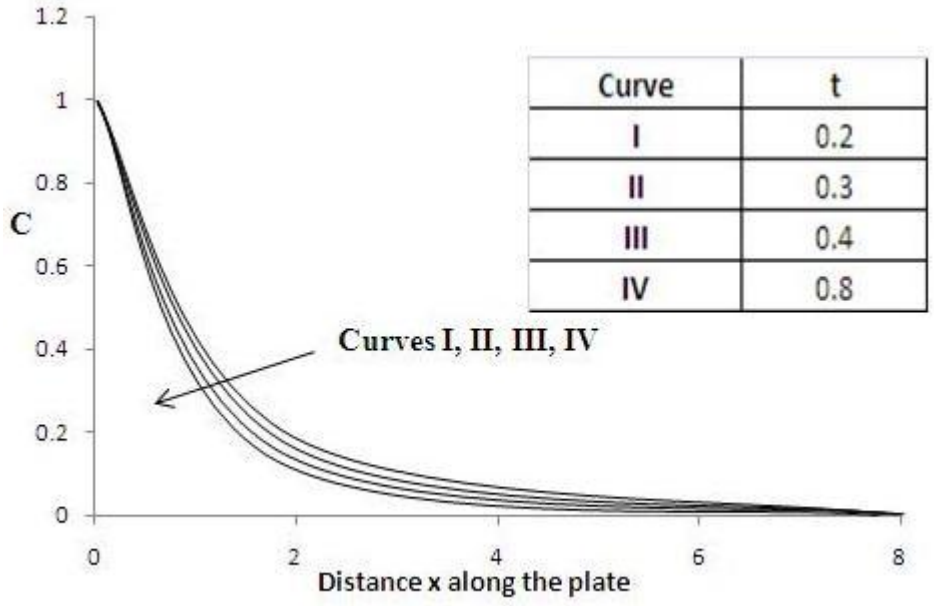

Figure 3.17 : Concentration profiles for different values of time t.

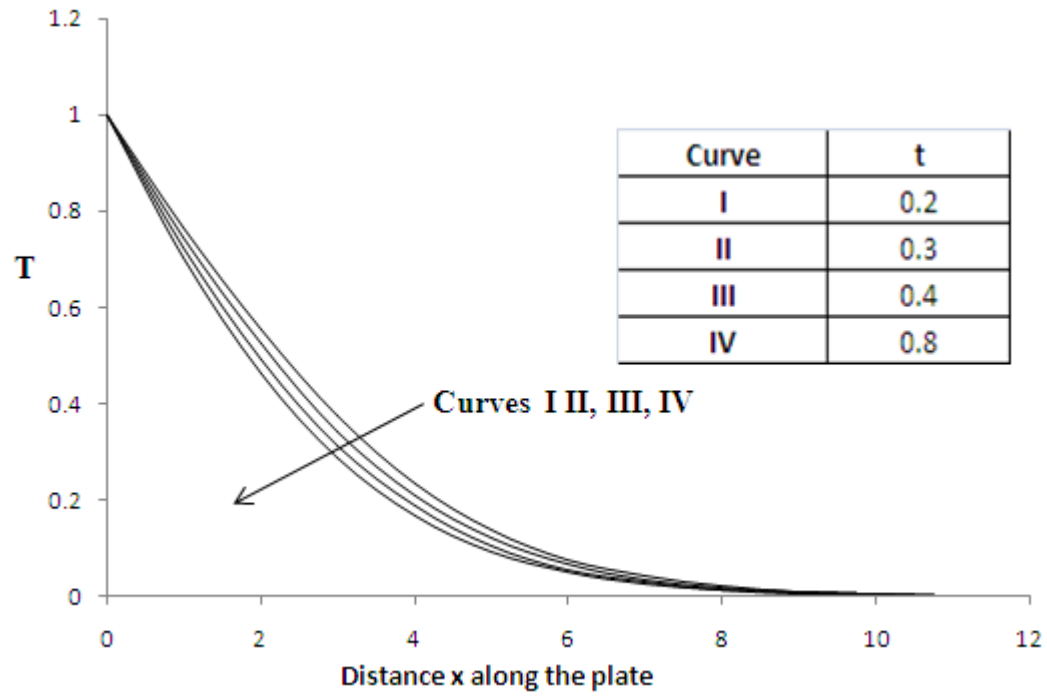

Figure 3.18 : Temperature profiles for different values of time t.

Figure 3.19 shows that increase in the Dufour number Df causes decrease in the primary velocity profiles. The figure also shows that increase in the Soret number Sr leads to an increase in the primary velocity profiles. Figure 3.20 shows that increase in Df causes a decrease in the magnitude of the secondary velocity profiles. The figure also shows that increase in Sr causes increase in the magnitude of the secondary velocity profiles. Figure 3.21 shows that increase in Df causes an increase in the concentration profiles. The figure also shows that increase in Sr causes an increase in the concentration profiles. Figure 3.22 shows that increase in Df causes a decrease in the temperature profiles. The figure also shows that increase in Sr causes a decrease in the temperature profiles. The Dufour number signifies the contribution of the concentration gradients to the thermal energy flux in the flow. From the definition of the Dufour number, an increase in Df

translates directly to a decrease in the temperature profiles of the fluid, or to an increase in the concentration profiles of the fluid.

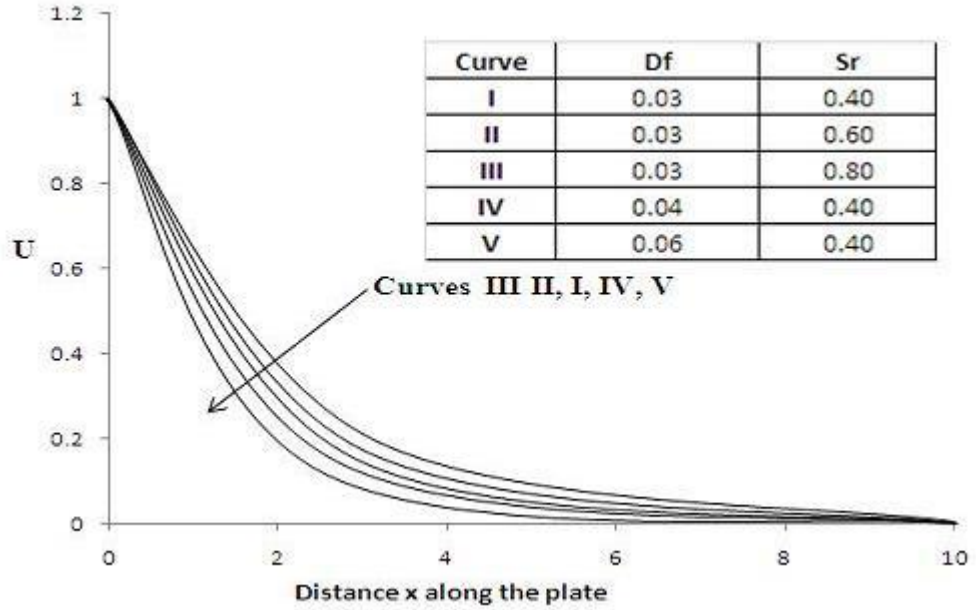

Figure 3.19 : Primary velocity field for different values of Dufour number.

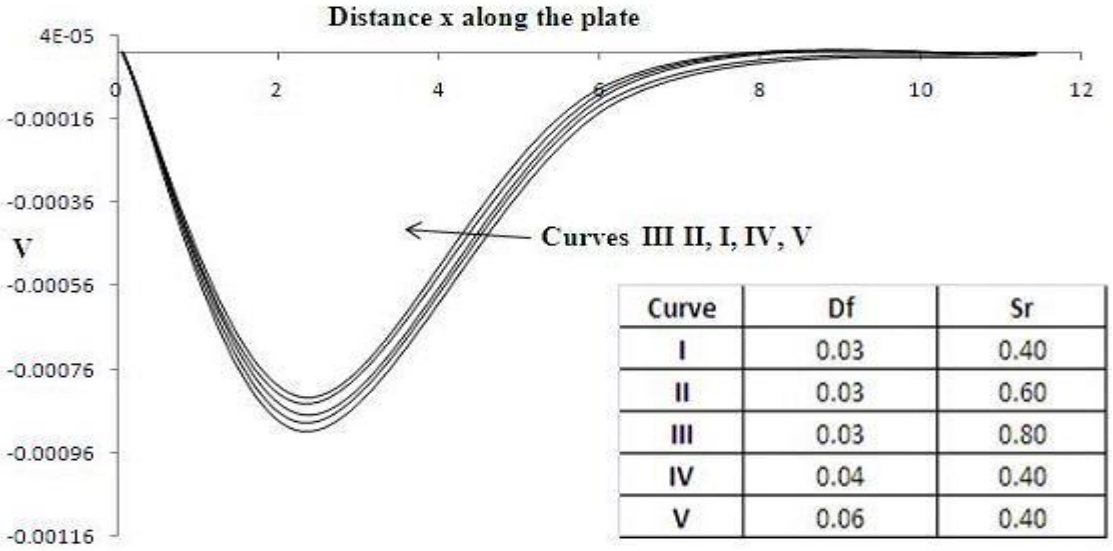

Figure 3.20 : Secondary velocity field for different values of Dufour number.

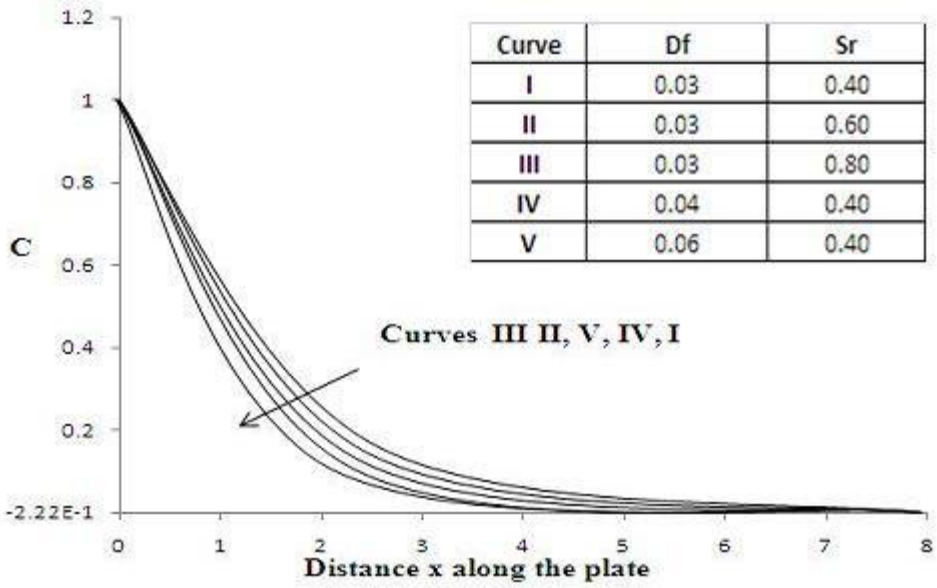

Figure 3.21 : Concentration field for different values of Dufour number.

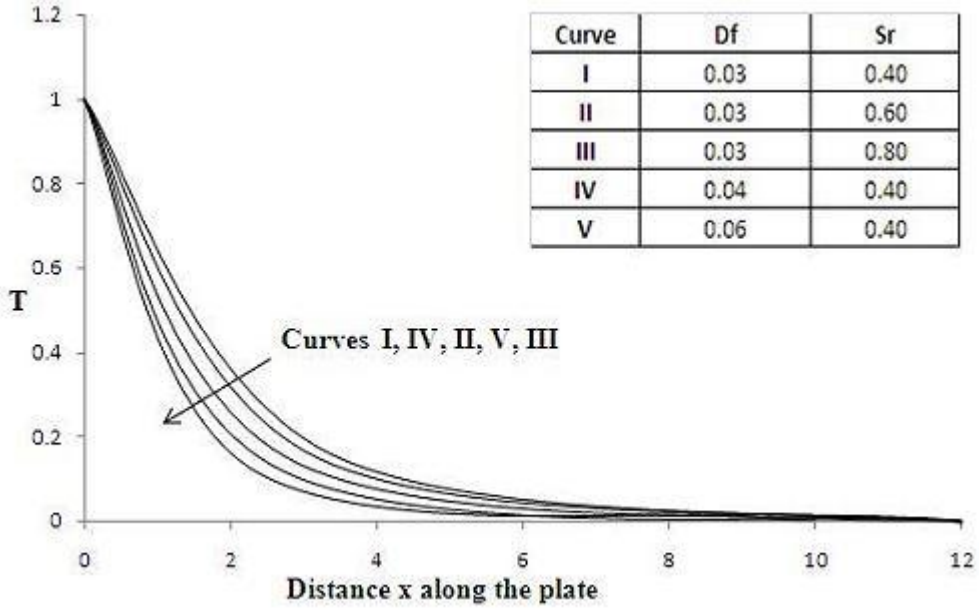

Figure 3.22 : Temperature field for different values of Dufour number.

Figures 3.23 and 3.24 show that increase in Reynold's number Re causes an increase in the primary velocity profiles and increase in the magnitude of the secondary velocity profiles respectively. The Reynolds number represents the ratio of the inertial to viscosity forces. Increase in Re results to a larger inertia force that in turn translates to higher velocities. Figure 3.25 and Figure 3.26 show that increase in Re causes a decrease in the concentration profiles but an increase in the temperature profiles. A higher velocity of the fluid takes away more species from the surface of the stretching sheet thereby reducing the species concentration.

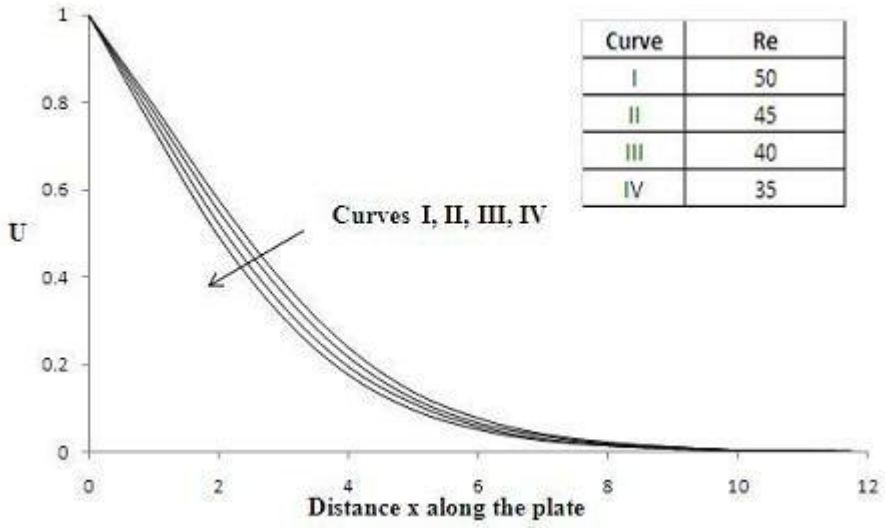

Figure 3.23 : Primary velocity field for different values of Re.

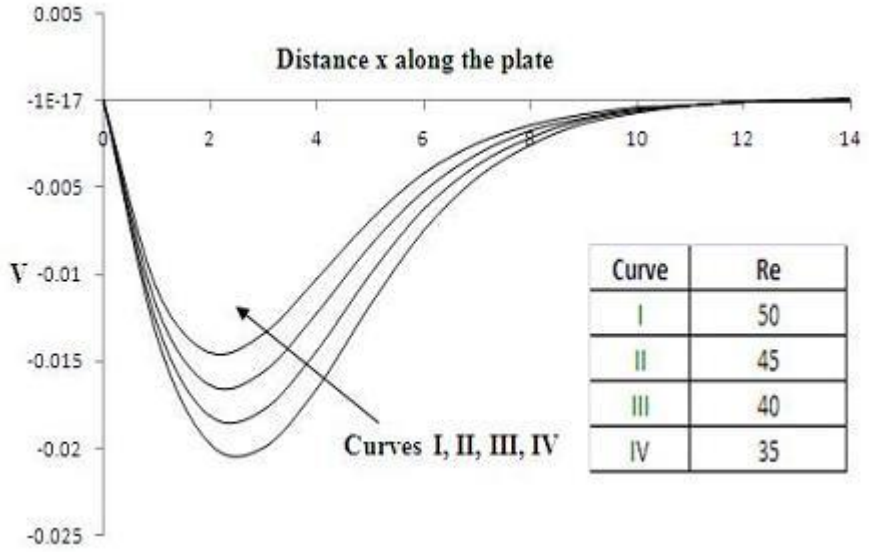

Figure 3.24 : Secondary velocity field for different values of Re.

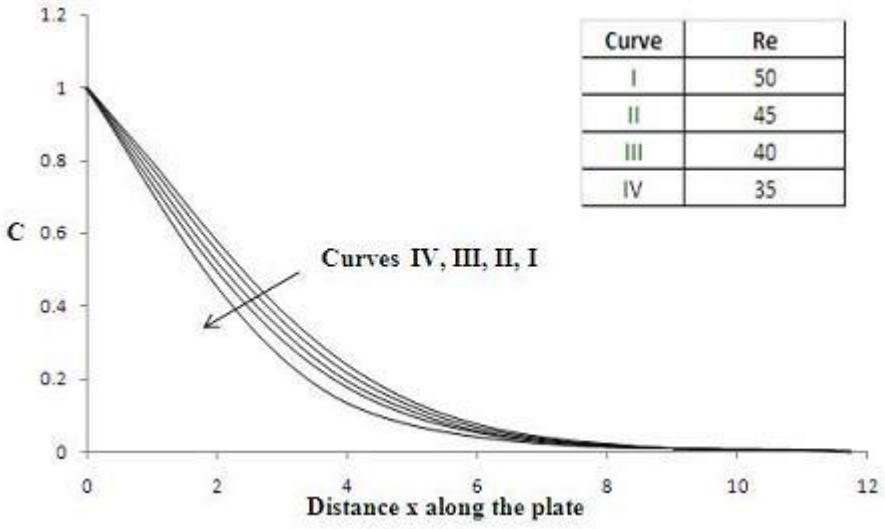

Figure 3.25 : Concentration field for different values of Re.

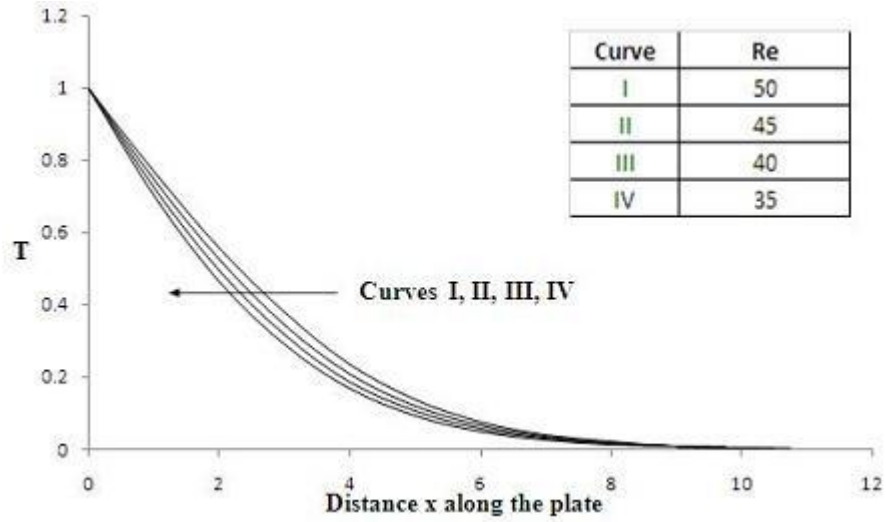

Figure 3.26 : Temperature field for different values of Re.

Figure 3.27 and Figure 3.28 show that increase in Radiation parameter N leads to a decrease in the primary velocity profiles but to an increase in the magnitude of the secondary velocity profiles. Figure 3.29 show that increase in N leads to an increase in the concentration profiles. Figure 3.30 shows that increase in N leads to a decrease in the temperature profiles. So radiation can be used to control the velocity, concentration and the thermal boundary layers quite effectively. So decreasing the value of N lowers both the flow velocity and the temperature of the fluid. The rate of the respective boundary layer growth for the temperature, concentration and primary and secondary velocities is higher near the fixed end of stretching sheet.

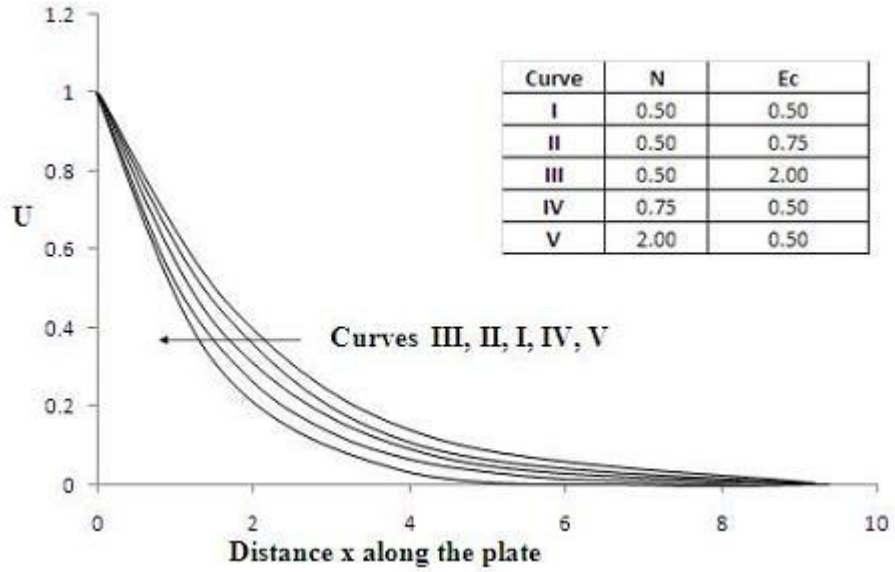

Figure 3.27 : Primary velocity profiles for different values of N and Ec.

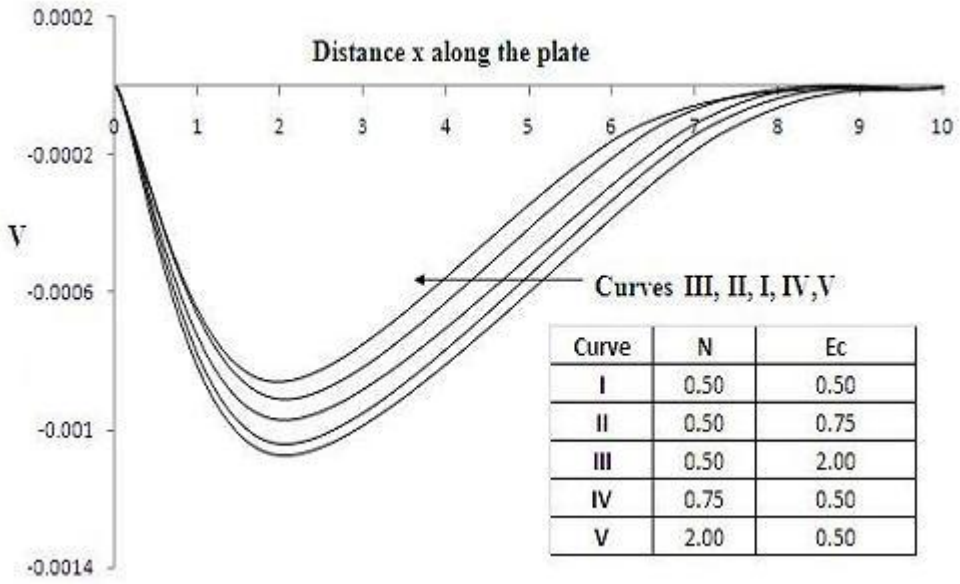

Figure 3.28 : Secondary velocity profiles for different values of N and Ec.

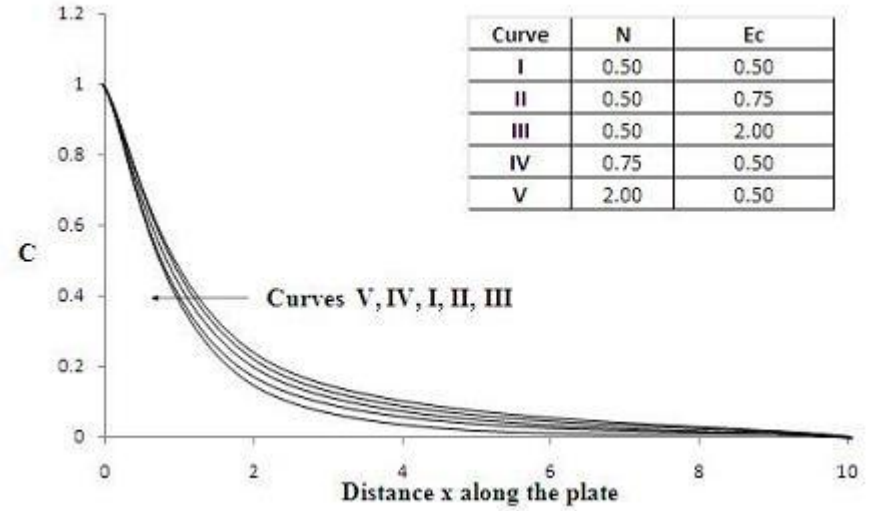

Figure 3.29 : Concentration profiles for different values of N and Ec.

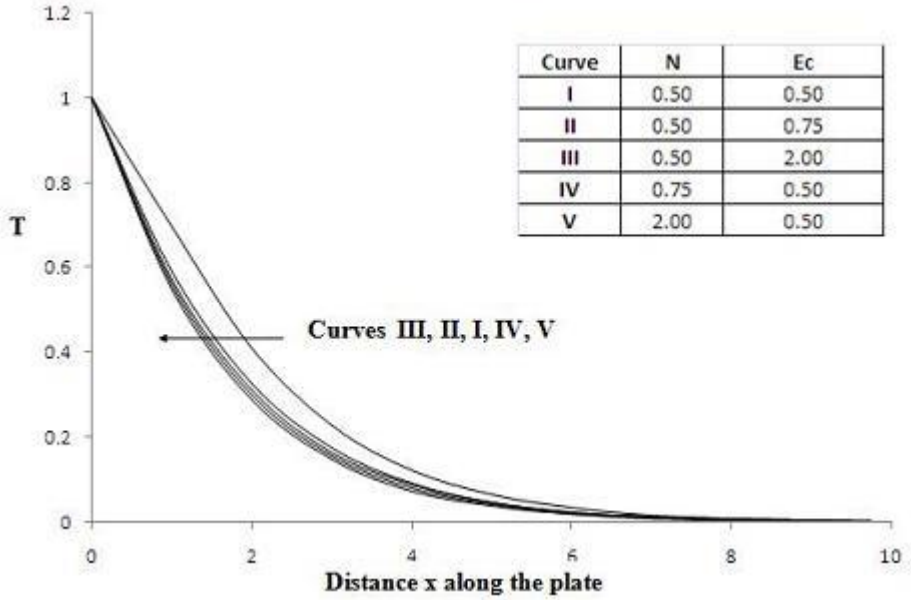

Figure 3.30 : Temperature profiles for different values of N and Ec.

Figure 3.27 shows that increase in Eckert number Ec causes an increase in the primary velocity profiles. From Figure 3.28 increase in Ec leads to an increase in the magnitude

of the secondary velocity profiles. Figure 3.29 shows that concentration profiles decrease with increase in the Eckert number. Figure 3.30 shows that increase in Eckert number Ec causes an increase in the temperature profiles. Thus increasing Eckert number boosts both the velocity and the temperature of the fluid flowing in a porous medium. The Eckert number expresses the relationship between the kinetic energy in the flow and the enthalpy. It embodies the conversion of kinetic energy into internal energy by work done against the viscous fluid stresses. A positive Eckert number implies cooling the sheet, implying heating the fluid. This causes a rise in the temperature and the velocity of the fluid respectively. So introducing radiation can be used to control the velocity, concentration and thermal boundary layers in porous media.

Figure 3.31 and Figure 3.32 show that increase in Schmidt number Sc causes a decrease in primary profiles and in the magnitude of the secondary velocity profiles respectively. Figure 3.33 shows that an increase in Schmidt number Sc causes decrease in the concentration profiles near the fixed end of the stretching sheet, and causes a cross-over of the concentration profiles further away along the stretching sheet. The effect of stretching on velocity is overcome by freestream velocity, leading to the observed cross-over of concentration profiles. Figure 3.34 shows that increase in Sc leads to a decrease in the temperature profiles. An increase in Sc leads to thinning of the velocity and the concentration boundary layers respectively, Abo-Eldahab (2005). A large value of Sc means a presence of a heavier fluid and this implies a lower velocity of the fluid.

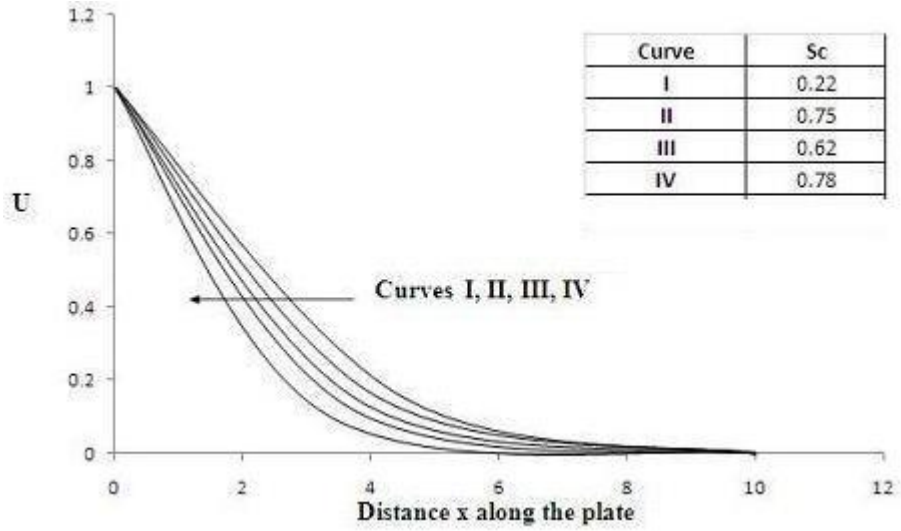

Figure 3.31 : Primary velocity profiles for different values of Sc.

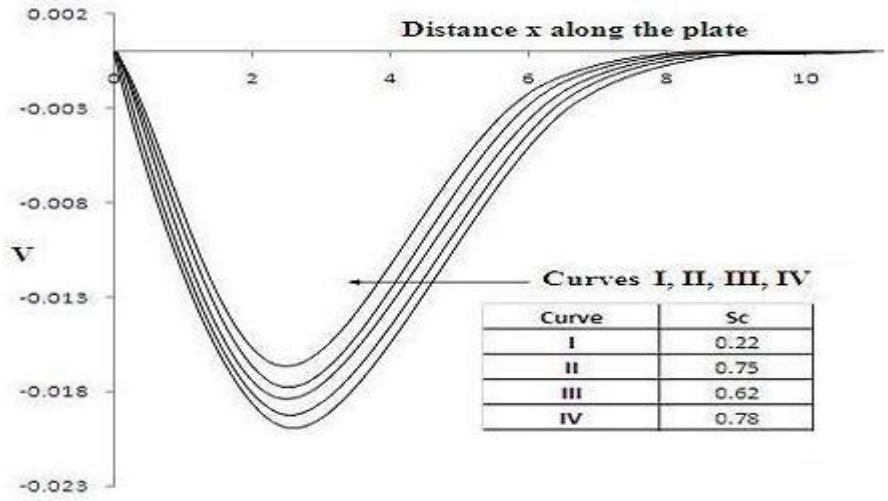

Figure 3.32 : Secondary velocity profiles for different values of Sc.

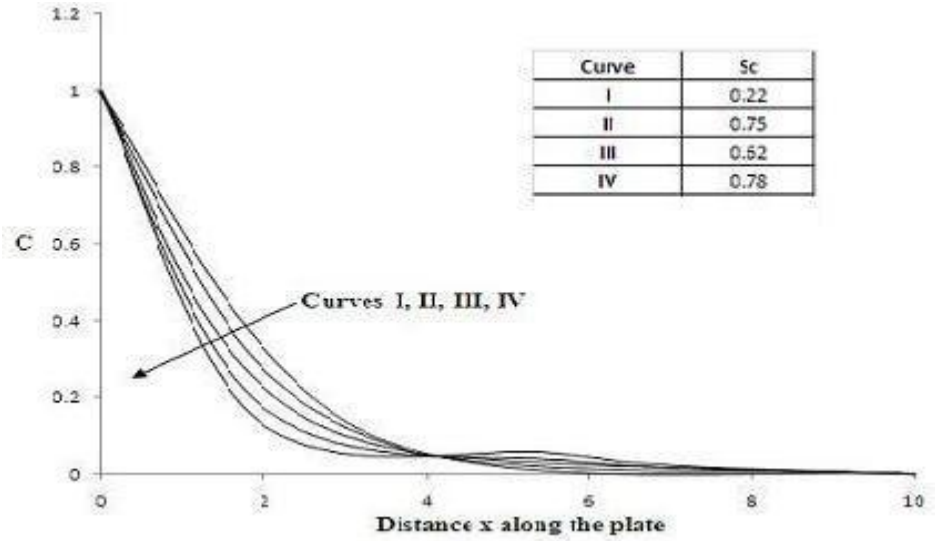

Figure 3.33 : Concentration profiles for different values of Sc.

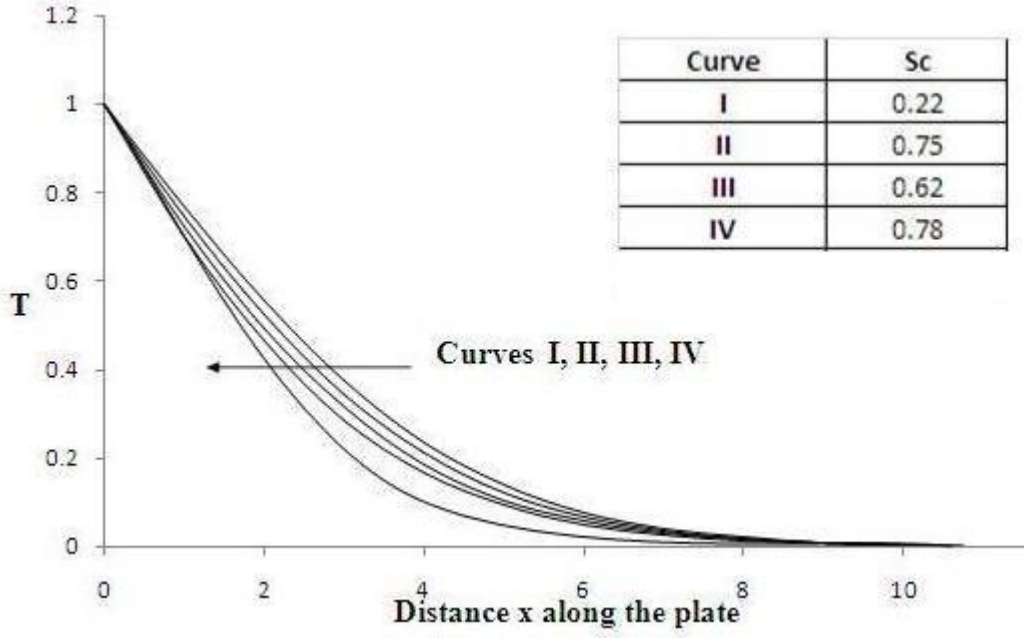

Figure 3.34 : Temperature profiles for different values of Sc.

Figure 3.35 shows that an increase in the magnitude of the Injection parameter w_o causes a decrease in the primary velocity profiles near the fixed end of the stretching sheet but there is a cross-over of the velocity profiles further away from the fixed end of the sheet.

The cross-over occurs when the effect of stretching on velocity is overcome by the effects of the freestream velocity on the boundary layer. Figure 3.36 shows that an increase in the magnitude of the injection parameter w_o causes a decrease in the magnitude of the secondary velocity profiles near the fixed end of the stretching sheet but there is a cross-over of the velocity profiles at around x=5.5. Figure 3.37 shows that an increase in the magnitude of the Injection parameter w_o causes a decrease in the concentration profiles. Figure 3.38 shows that an increase in the magnitude of the injection parameter w_o causes a decrease in the temperature profiles, but there is a cross-over of profiles at around x=3. The results show that introducing injection can be used to destabilize the velocity and the temperature boundary layers away from the fixed end of the stretching sheet; but can also be used to stabilize the two boundary layers near the fixed end of the sheet. This indicates the usual fact that blowing destabilizes the growth of the velocity and temperature the boundary layers respectively.

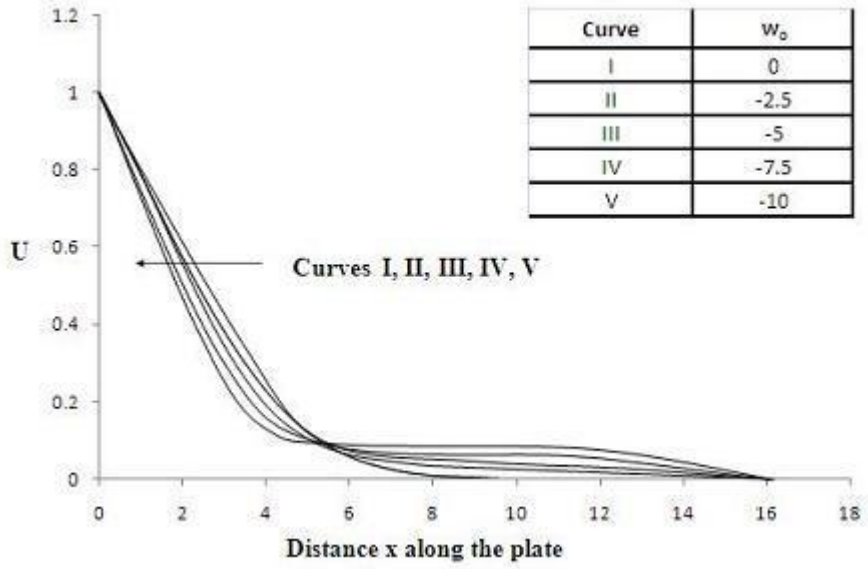

Figure 3.35 : Primary velocity profiles for various values of Injection parameter, w_o.

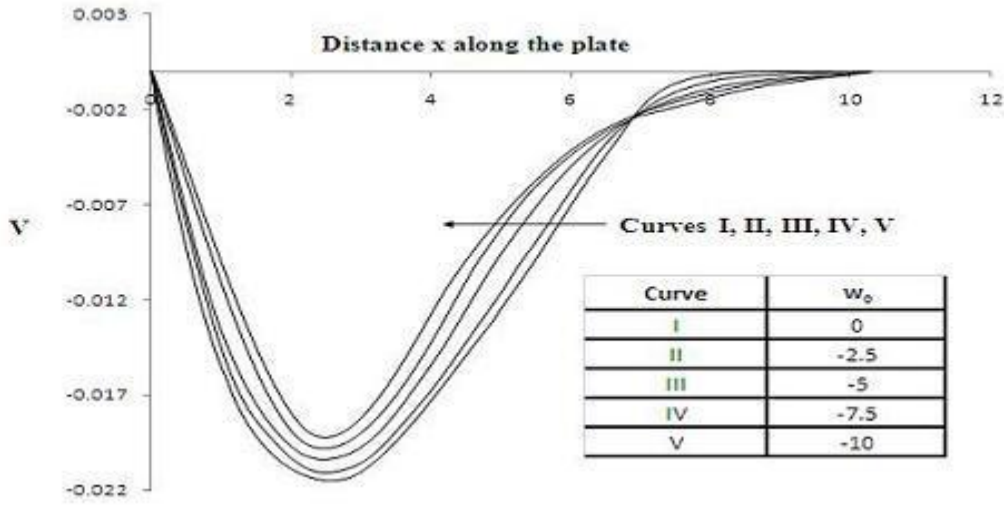

Figure 3.36 : Secondary velocity profiles for various values of injection parameter, w_o.

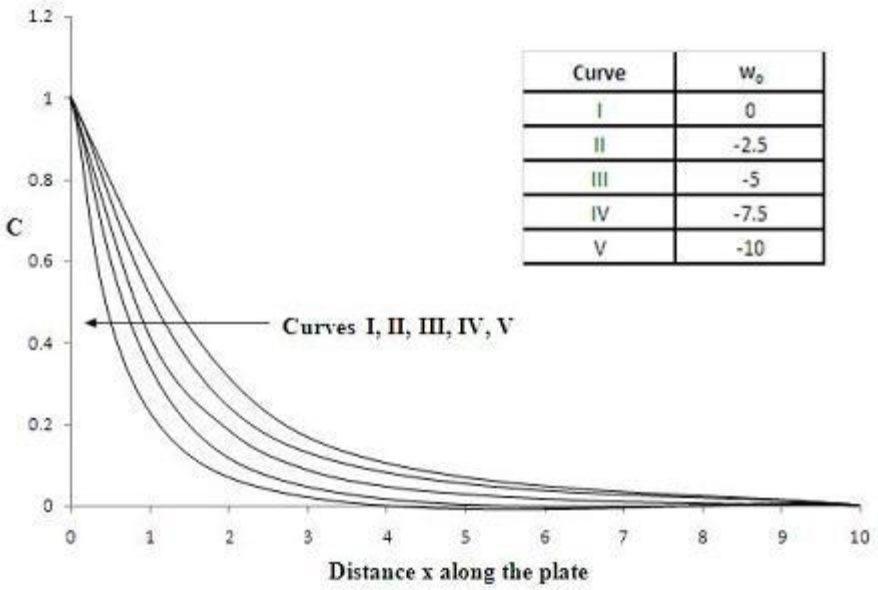

Figure 3.37 : Concentration profiles for various values of injection parameter, w_o.

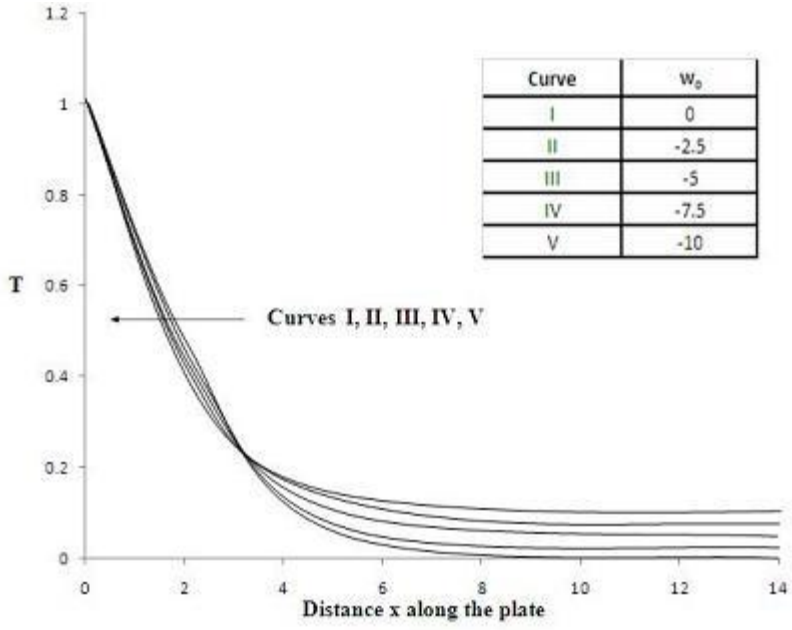

Figure 3.38 : Temperature profiles for various values of injection parameter, w_o

Figure 3.39 shows that primary velocity profiles decrease with increase in the value of the Rotation parameter Ro. Figure 3.40 shows that the magnitude of the secondary

velocity profiles decrease with increase in Ro; and absence of rotation translates to absence of the secondary velocity profiles. This means rotation can be used to control emergence of the secondary velocity profiles in a rotating system. Figure 3.41 shows that increase in Ro leads to an increase in the concentration profiles. Figure 3.42 shows that increase in Ro leads to a decrease in the temperature profiles. An increase in Ro, which leads to a decrease in the primary velocity profiles, leads to slowing down of the fluid thus retarding the movement of the species away from the stretching sheet, leading to the observed increase in the concentration profiles.

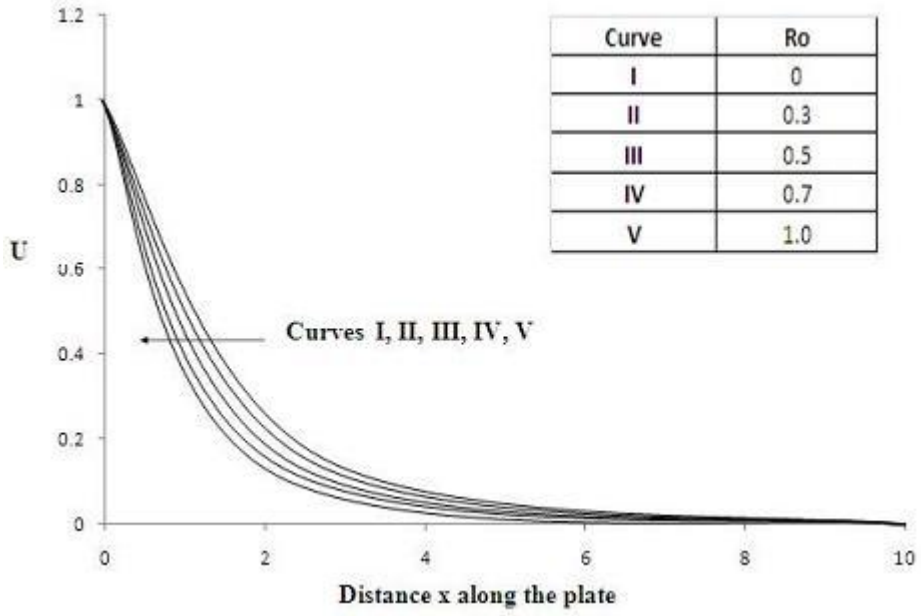

Figure 3.39 : Primary velocity profiles for various values of Rotation parameter, Ro.

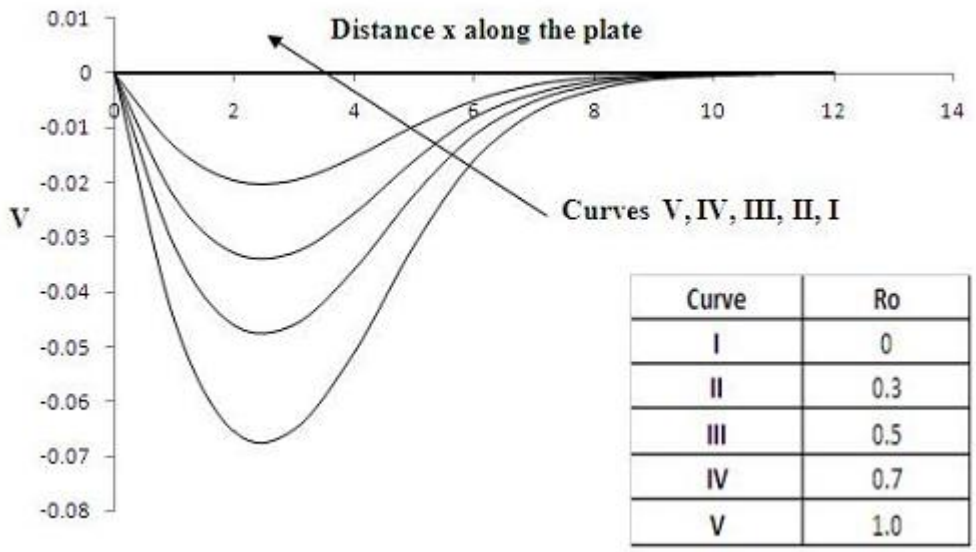

Figure 3.40 : Secondary velocity profiles for various values of Rotation parameter, Ro.

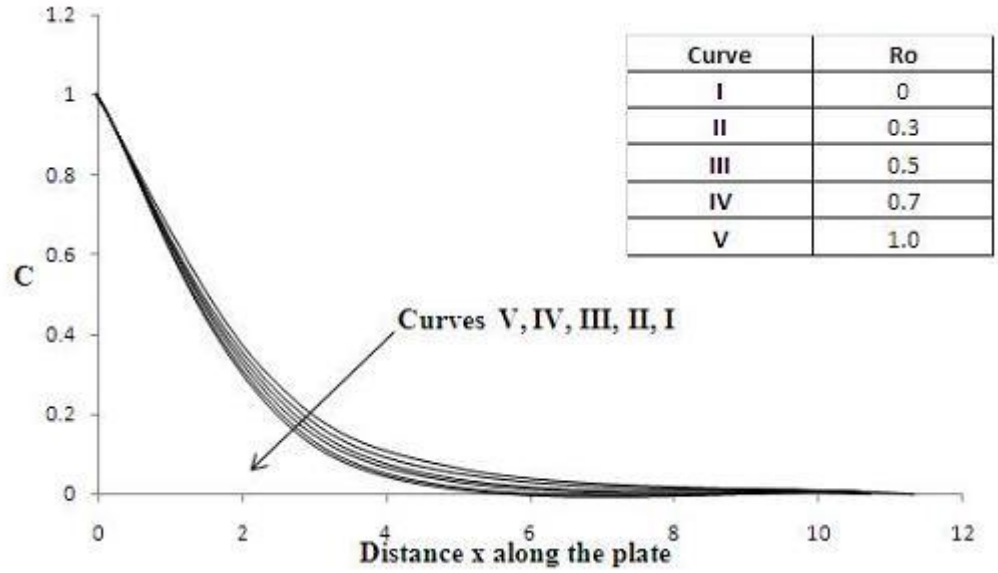

Figure 3.41 : Concentration profiles for various values of Rotation parameter, Ro.

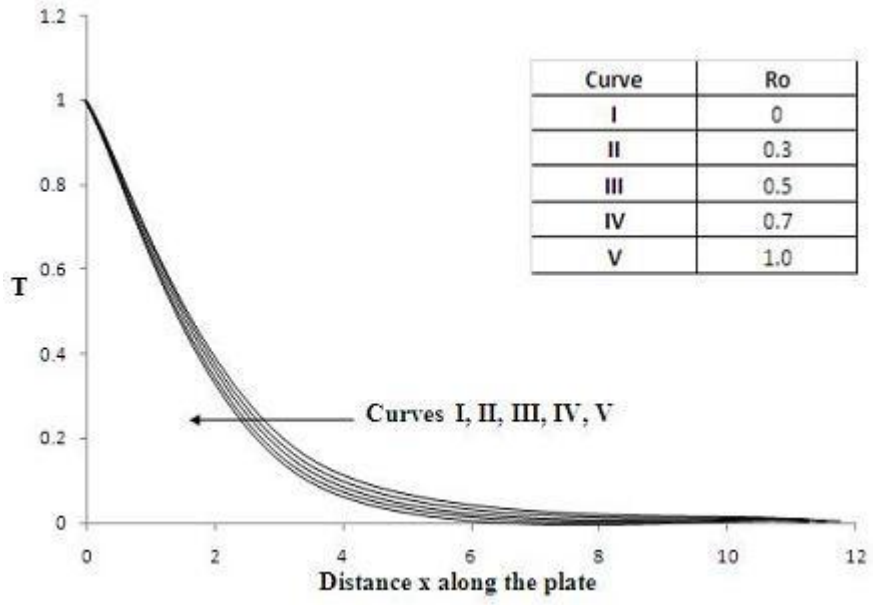

Figure 3.42 : Temperature profiles for various values of Rotation parameter, Ro.

3.3. Nusselt number, Sherwood number and Local Skin-friction Coefficient

The quantities of main engineering interest in the problem at hand are the local Nusselt number, the local Sherwood number, and the shearing stress on the stretching sheet. The Nusselt number and the local Sherwood number physically indicate the rate of heat transfer and the rate of mass transfer respectively. The shearing stress on the surface of the stretching sheet is defined as

$$\tau_x = -\mu \left(\frac{\partial u}{\partial z}\right)_{z=0} = -\frac{\mu U_\infty}{H} \left(\frac{\partial u'}{\partial z'}\right)_{z'=0} \tag{3.62}$$

$$\tau_y = -\mu \left(\frac{\partial v}{\partial z}\right)_{z=0} = -\frac{\mu U_\infty}{H} \left(\frac{\partial v'}{\partial z'}\right)_{z'=0} \tag{3.63}$$

The local skin friction coefficients are defined as

$$C_{fx} = -\frac{\tau_x}{\frac{1}{2}\rho U^2} = -\frac{2}{Re}\left(\frac{\partial u'}{\partial z'}\right)_{z'=0} \tag{3.64}$$

$$C_{fy} = -\frac{\tau_x}{\frac{1}{2}\rho U^2} = -\frac{2}{Re}\left(\frac{\partial v'}{\partial z'}\right)_{z'=0} \tag{3.65}$$

Equations (3.64) and (3.65) represent the respective local skin friction coefficients due to the primary and the secondary velocity profiles. The local surface mass flux is defined by

$$\begin{aligned} Q_w &= -D_M\left(\frac{\partial C}{\partial z}\right)_{z=0} \\ &= -D_M\frac{(C_W - C_\infty)}{H}\left(\frac{\partial C'}{\partial z'}\right)_{z'=0} \end{aligned} \tag{3.66}$$

At characteristic length H units along the x-axis from the fixed end of the stretching sheet, the local Sherwood number Sh is expressed as

$$Sh = \frac{Q_w}{C_W - C_\infty}\cdot\frac{H}{D_M} = -\left(\frac{\partial C'}{\partial z'}\right)_{z'=0} \tag{3.67}$$

Assuming the no-slip condition at the wall, and that heat transfer at the wall is by conduction, the local surface heat flux is expressed as

$$q_w = -k_f\frac{\partial T}{\partial z} \tag{3.68}$$

where k_f is the thermal conductivity of the saturated porous medium. The local Nusselt number Nu is expressed as

$$\begin{aligned} Nu &= \frac{q_w}{T_W - T_\infty}\cdot\frac{H}{k_f} \\ &= -\left(\frac{\partial T'}{\partial z'}\right)_{z'=0} \end{aligned} \tag{3.69}$$

3.3.1. The Least Squares Approximation Method

The method of least squares approximation has been used to determine a quadratic bivariate polynomial that is a function of z and t; say, $P_1(z,t)$, $P_2(z,t)$, $P_3(z,t)$ and $P_4(z,t)$ where each polynomial approximates the continuous functions $U(z,t)$, $V(z,t)$, $C(z,t)$ and $T(z,t)$ respectively. The method of least squares is used in order to minimize the difference between each of the following functions:

$$|P_1(z,t) - U(z,t)|, |P_2(z,t) - V(z,t)|, |P_3(z,t) - C(z,t)|, \quad and \quad |P_4(z,t) - T(z,t)| \tag{3.70}$$

Since $P_i(z,t)$ is a second degree bivariate approximating polynomial, then

$P_i(z,t) = a_1 + b_1 z + c_1 t + d_1 z^2 + e_1 t^2 + f_1 zt$;

where a_1, b_1, c_1, d_1, e_1 and f_1 are real constants. In order to obtain an approximating polynomial for $U(z,t)$, the following equation is minimized:

$$I(a_1, b_1, c_1, d_1, e_1, f_1) = \sum_{n}^{i=1} \left[U(z_i, t_i) - (a_1 + b_1 z_i + c_1 t_i + d_1 z_i^2 + e_1 t_i^2 + f_1 z_i t_i)\right]^2 \tag{3.71}$$

where n is the number of points used. The respective partial derivatives with respect to $a_1, b_1, c_1, d_1, e_1, f_1$ are given below.

$$\frac{\partial I}{\partial a_1} = -\sum_{i=1}^{n} \left[U(z_i, t_i) - (a_1 + b_1 z_i + c_1 t_i + d_1 z_i^2 + e_1 t_i^2 + f_1 z_i t_i)\right] = 0$$

$$\frac{\partial I}{\partial b_1} = -\sum_{i=1}^{n} \left[U(z_i, t_i) - (a_1 + b_1 z_i + c_1 t_i + d_1 z_i^2 + e_1 t_i^2 + f_1 z_i t_i)\right] z_i = 0$$

$$\frac{\partial I}{\partial c_1} = -\sum_{i=1}^{n} \left[U(z_i, t_i) - (a_1 + b_1 z_i + c_1 t_i + d_1 z_i^2 + e_1 t_i^2 + f_1 z_i t_i)\right] t_i = 0$$

$$\frac{\partial I}{\partial d_1} = -\sum_{i=1}^{n} \left[U(z_i, t_i) - (a_1 + b_1 z_i + c_1 t_i + d_1 z_i^2 + e_1 t_i^2 + f_1 z_i t_i)\right] z_i^2 = 0$$

$$\frac{\partial I}{\partial e_1} = -\sum_{i=1}^{n} \left[U(z_i, t_i) - (a_1 + b_1 z_i + c_1 t_i + d_1 z_i^2 + e_1 t_i^2 + f_1 z_i t_i)\right] t_i^2 = 0$$

$$\frac{\partial I}{\partial f_1} = -\sum_{i=1}^{n} \left[U(z_i,t_i) - (a_1 + b_1 z_i + c_1 t_i + d_1 z_i^2 + e_1 t_i^2 + f_1 z_i t_i)\right] z_i z_i = 0$$

Using the preceding six partial derivatives using $n = 9$ the flowing six respective normal equations are obtained:

$$\sum U(z_i,t_i) \quad = 10a_1 + b_1 \sum z_i + c_1 \sum t_i + d_1 \sum z_i^2 + e_1 \sum t_i^2 + f_1 \sum z_i t_i$$

$$\sum (z_i U(z_i,t_i) = a_1 \sum z_i + b_1 \sum z_i^2 + c_1 \sum z_i t_i + d_1 \sum z_i^3 + e_1 \sum z_i t_i^2 + f_1 \sum z_i^2 t_i$$

$$\sum (t_i U(z_i,t_i)) = a_1 \sum t_i + b_1 \sum z_i t_i + c_1 \sum t_i^2 + d_1 \sum t_i z_i^2 + e_1 \sum t_i^3 + f_1 \sum z_i t_i^2$$

$$\sum (z_i^2 U(z_i,t_i)) = a_1 \sum z_i^2 + b_1 \sum z_i^3 + c_1 \sum t_i z_i^2 + d_1 \sum z_i^4 + e_1 \sum t_i^2 z_i^2 + f_1 \sum t_i z_i^3$$

$$\sum (t_i^2 U(z_i,t_i)) = a_1 \sum t_i^2 + b_1 \sum z_i t_i^2 + c_1 \sum t_i^3 + d_1 \sum t_i^2 z_i^2 + e_1 \sum t_i^4 + f_1 \sum z_i t_i^3$$

$$\sum (z_i t_i U(z_i,t_i)) = a_1 \sum t_i z_i + b_1 \sum t_i z_i^2 + c_1 \sum z_i t_i^2 + d_1 \sum z_i^3 t_i + e_1 \sum z_i t_i^3 + f_1 \sum z_i^2 t_i^2$$

For instance when x = 3, the values shown in Table 3.1 are obtained.

Table 3.1 : Values of t, z and U(z,t) Sc = 0.22, Sr = 0.4, M = 1.0, Xi =0.5 , Ro = 0.5, N = 0.5, w_o = 0.5, Re = 50, Df = 0.03, Ec = 0.5, R = 0.2, Gr_θ= 5, Gr_c = 10, Pr = 0.71**.**

t	0.399	0.400	0.401	0.402	0.403	0.404
z	0	0.03	0.06	0.09	0.12	0.15
U(z,t)	0.46335	0.42591	0.42881	0.42887	0.42888	0.42894

[Table continued]

t	0.405	0.406	0.407
z	0.18	0.21	0.24
U(z,t)	0.42899	0.42904	0.42909

The matrix A of coefficients $a_1, b_1, c_1, d_1, e_1, f_1$ derived from the normal equations is

$$A = \begin{pmatrix} 10 & 1.08 & 3.62700 & 0.18360 & 1.46174 & 0.43704 \\ 1.08 & 0.18360 & 0.43704 & 0.03499 & 0.17686 & 0.07442 \\ 3.627 & 0.43704 & 1.46174 & 0.07442 & 0.58913 & 0.17686 \\ 0.18360 & 0.03499 & 0.07442 & 0.00711 & 0.03017 & 0.0142 \\ 1.46174 & 0.17686 & 0.58913 & 0.03017 & 0.23745 & 0.07157 \\ 0.43704 & 0.07442 & 0.17686 & 0.0142 & 0.07157 & 0.03017 \end{pmatrix} \tag{3.72}$$

The column matrix given by the left-hand side of the respective normal equations is given by matrix C below.

$$C = \begin{pmatrix} 3.891896 \\ 0.463212 \\ 1.568307 \\ 0.078764 \\ 0.632003 \\ 0.187447 \end{pmatrix} \tag{3.73}$$

The column matrix of the constants $a_1, b_1 \cdots f_1$ is given as matrix B below:

$$B = \begin{pmatrix} a_1 \\ b_1 \\ c_1 \\ d_1 \\ e_1 \\ f_1 \end{pmatrix} \tag{3.74}$$

Solving the matrix equation $\mathbf{AB=C}$ using Matlab's command $B = A\backslash C$ leads to the following approximating polynomial.

$$U(z,t) = -0.1043z + 0.9351t + 1.166z^2 + 0.4863t^2 0.7636zt.$$

Similarly the approximating polynomials for $V(z,t)$, $C(z,t)$ and $T(z,t)$ are:

$$V(z,t) = 0.1957z + 0.035t - 0.2072z^2 - 0.3567t^2 - 0.3052zt.$$

$$C(z,t) = 4895z + 0.6034t - 2.1533z^2 - 1.4022t^2 + 0.4452zt.$$

$$T(z,t) = 0.3984z + 1.2739t - 2.5022z^2 - 1.0473t^2 + 0.8446zt.$$

The bivariates for U, V, C and T are used in obtaining the results shown in Table 3.2.

Table 3.2 : Variation of Coefficients of friction, Sherwood and Nusselt numbers with various parameters.

M	Xi	Ro	N	t	w_o	Ec	C_{fx}	C_{fy}	Sh	Nu
1.0	0.50	0.50	0.50	0.40	0.5	0.50	0.01556	-0.00296	-0.66713	-0.73540
2.0	0.50	0.50	0.50	0.40	0.5	0.50	0.01089	-0.00260	-0.69767	-0.83061
3.0	0.50	0.50	0.50	0.40	0.5	0.50	0.00686	-0.00168	-0.70727	-0.91100
1.0	1.50	0.50	0.50	0.40	0.5	0.50	0.01089	-0.00260	-0.69767	-0.83061
1.0	2.50	0.50	0.50	0.40	0.5	0.50	0.00686	-0.00168	-0.70727	-0.91100
1.0	0.50	2.50	0.50	0.40	0.5	0.50	0.01120	-0.01344	-0.68330	-0.76090
1.0	0.50	4.50	0.50	0.40	0.5	0.50	0.00175	-0.01947	-0.71278	-0.87060
1.0	0.50	0.50	2.50	0.40	0.5	0.50	0.01719	-0.00298	-0.68550	-0.41046
1.0	0.50	0.50	4.50	0.40	0.5	0.50	0.01787	-0.00313	-0.69598	-0.35613
1.0	0.50	0.50	0.50	0.40	0.4	0.50	0.01209	-0.00187	-0.48325	-0.65535
1.0	0.50	0.50	0.50	0.40	0.3	0.50	0.00809	-0.00137	-0.29031	-0.55647
1.0	0.50	0.50	0.50	0.40	0.5	1.00	0.01641	-0.00255	-0.67420	-0.71822
1.0	0.50	0.50	0.50	0.40	0.5	1.50	-0.01761	-0.00354	-0.67118	-0.34306
1.0	0.50	0.50	0.50	5.00	0.5	0.50	0.01421	-0.00325	-0.56666	-0.64909
1.0	0.50	0.50	0.50	6.00	0.5	0.50	0.00865	0.00542	-0.04937	-0.42828

3.3.2. Discussion of the results

From Table 3.2 the following observations can be made:

1. Increase in Magnetic parameter M results in decrease in the magnitudes of both shear stresses, C_{fx} and C_{fy} respectively; but to an increase in the magnitude of the Sherwood number Sh and Nusselt number Nu. The magnitude of shear stress is proportional to velocity and since both velocity profiles decrease with increase in M, the shear stress is expected to decrease. Increase in the value of M causes thickening of the concentration boundary layer, resulting to a lower rate of transportation of the species in the concentration boundary layer. Thermal boundary layer thickness decreases with increase in M resulting to the observed increase in the Nusselt number.
2. Increase in the Permeability parameter Xi causes a decrease in the magnitudes of C_{fx} and C_{fy} respectively. This is explained by the fact that increase in Xi means a decrease in the size of the pores of the porous medium and this causes an increased resistance to the flow, leading to lower velocity, and consequently to a decrease in the two respective coefficients of friction. An increase in Xi leads to an increase in the magnitude of Nusselt number Nu and Sherwood number Sh. This observation is due to the fact that increase in Xi leads to thinner temperature boundary layer, thereby leading to an increase in the rate of heat transfer. Decrease in velocity of the fluid results to a reduced rate of transportation of species away from the surface of the stretching sheet, leading to the observed increase in the value of Sh.

3. Increase in the Rotational parameter Ro leads to a decrease in the magnitude of C_{fx} but to an increase in the magnitude of C_{fy}. Increase in Ro causes an increase in the magnitude of the secondary velocity profiles that in turn lead to increase in the magnitude of C_{fy}. Increase in Ro leads to an increase in the magnitude of Sh and Nu respectively. Increase in Ro leads to a thinner thermal boundary layer, resulting to an increased rate of heat transfer. Decrease in the primary velocity profiles leads to a reduced rate of transportation of species away from the surface of the stretching sheet, leading to the observed increase in the value of Sh.
4. Increase in the Radiation parameter N leads to an increase in the magnitudes of C_{fx}, C_{fy}, Nu and Sh respectively. Increase in N leads to an increase in the rate of species transportation. Increase in Radiation parameter N leads to a thinner thermal boundary layer, resulting to an increase in the rate of heat transfer. Increase in N also enhances the flow of convection currents on the surface of the sheet, leading to an increase in C_{fx} and C_{fy} respectively.
5. Increase in the magnitude of the suction parameter w_o leads to an increase in the magnitudes of C_{fx}, C_{fy}, Sh and Nu. Suction accelerates the velocity of the fluid particles leading to higher flow velocities. Thermal boundary layer thickness decreases with increase in w_o, leading to an increased rate of heat transfer. Decrease in concentration boundary layer thickness leads to an increased rate of species transportation, and hence to increase in the Sherwood number Sh.
6. Increase in the Eckert number Ec leads to an increase in the magnitudes of C_{fx} and C_{fy} respectively; but to a decrease in the magnitude of the Nusselt number Nu and

Sherwood number Sh respectively. Increasing the value of Ec leads to an increase in the velocity of the fluid and hence the observed increase in the magnitude of the values of both shear stresses. Increasing Ec results to a lower rate of species transportation leading to a decrease in Sh. Increase in Ec translates to a lower value of the temperature difference, and to a reduced rate of heat transfer.

7. Increase in time t leads to a decrease in the magnitudes of C_{fx}, Sh and Nu respectively; but to an increase in the magnitude of C_{fy}. The respective transient temperature and concentration differences within the fluid decrease with time, leading to a decreased rate of mass transfer and heat transfer respectively. The transient shear stress due to secondary velocity increases with time while that due to the primary velocity profiles decrease with time. The effect of rotation on the secondary velocity profiles increases with time hence the observed increase the magnitude of C_{fy} with time t.

3.4. Conclusion

Tania and Samad (2010) analyzed the effects Magnetic field parameter, Suction parameter, Schmidt number, Radiation parameter, buoyancy force, viscous stress and Eckert number on a steady two-dimensional magneto-hydrodynamics free convection flow along a stretching sheet in the presence of a heat source. The problem at hand has in addition considered the effects of the Dufour number, Soret number, Reynold's number, Nusselt number, rotation and porosity on the flow variables. To validate the present results, the additional flow parameters are removed from the governing

equations by giving each of them a value of zero. The results are compared with those of Tania and Samad; and the results agree. However, the important part of this work in comparison with the previous work is that there are sharp rises in the momentum, concentration and thermal boundary layers near the fixed end of the stretching sheet. This can easily be explained as the usual effect of the stretching, buoyancy force, radiation, magnetic field, rotation, permeability and viscous dissipation on the flow variables.

The next chapter considers MHD flow over a stretching sheet in a rotating system in porous media with Hall currents, heat and mass transfer.

CHAPTER 4

4.0 MHD Flow over a Stretching Sheet in Porous Media in a Rotating System with Hall Currents, Heat and Mass Transfer

4.1. Introduction

MHD is the study of the motion of electrically conducting fluids. In Chapter 3, unsteady laminar boundary layer flow of an incompressible, electrically conducting, viscous Newtonian fluid past an electrically non-conducting stretching sheet embedded in porous media in a rotating system with heat and mass transfer has been discussed. In this chapter the effects of Hall currents and heat flux have been considered. In addition, the heat source effect, thermal diffusion effect (commonly known as Soret effect) and mass diffusion effect (commonly known as Dufour effect) have been considered. The problem of heat source is important for it has applications in areas such as effective cooling of electronic equipment, design of heaters and combustion engines. Possible heat generation effects may alter the temperature distribution and consequently, alter the rate of particle deposition in a nuclear reactor, electronic chips and semi conductor wafers. The magnitude of thermal diffusion effect may be considerably large, and as such it can be utilized in the separation of isotopes in a mixture of gases with very light molecular weight (hydrogen, helium) and gases with medium molecular weight (nitrogen, air). MHD free convection flow has applications in the fields of stellar and planetary magnetospheres, Tania and Samad (2010). MHD flows with Hall and ion-slip currents have applications in the design of MHD generators, Hall accelerators and flight magnetohydrodynamics. In this work the combined effect of thermal radiation, heat generation, free convection and viscous dissipation on unsteady free convection heat and mass transfer flow over a stretching sheet in the presence of a

transverse magnetic field in a rotating system has been investigated. A computer program, appended to this work, has been employed to solve the coupled non-linear PDEs.

4.1.1. Mathematical formulation

Consider an unsteady MHD flow of an electrically conducting Newtonian fluid between two vertical parallel sheets embedded in a porous medium in a rotating system. The configuration of this type of flow is shown by Figure 3.1 in Section 3.1 of Chapter 3. The equation of continuity for the problem at hand is $w = -w_o$. A negative value of w_o therefore represents injection. The equation of conservation of electric charge is $\nabla \cdot \mathbf{J} = 0$. The components of the electric current density **J** along the x, y, and z-axes are $J_x, J_y,$ and J_z respectively. Since both sheets are electrically non-conducting $\mathbf{E} = 0$. Thus J_z is zero everywhere in the flow. Taking Hall current into account, the generalized Ohm's law can be written as

$$\mathbf{J} + \frac{\omega_e \tau_e}{H_o}\mathbf{J} \times \mathbf{H} = \sigma(\mathbf{E} + \mu_e \mathbf{q} \times \mathbf{H}) \tag{4.1}$$

In equation (4.1) the electron pressure gradient (for weakly ionized fluid), ion-slip and thermo-electric effects are neglected. Under these assumptions, and in the absence of electric field, equation (4.1) becomes

$$J_x + mJ_y = \sigma \mu_e H_o v \tag{4.2}$$

$$J_y - mJ_x = -\sigma \mu_e H_o u \tag{4.3}$$

where $m = \omega_e \tau_e$ is the Hall parameter. Solving equations (4.2) and (4.3) for J_x and J_y yields

$$J_x = \frac{\sigma \mu_e H_o}{1 + m^2}(v + mu) \tag{4.4}$$

$$J_y = \frac{\sigma \mu_e H_o}{1 + m^2}(mv - u) \tag{4.5}$$

The Lorentz force $\mathbf{J} \times \mathbf{B}$ yields

$$J_y B_o \mathbf{i} - J_x B_o \mathbf{j} \tag{4.6}$$

When there is an appreciable temperature difference between the stretching surface and the ambient fluid, it is important to consider the temperature dependent heat source or sink which may exert a strong influence on the heat transfer characteristics within the fluid. If Q is the temperature dependent volumetric heat generation parameter, then $Q > 0$ represents a heat source, and $Q < 0$ represents a heat sink. Incorporating equations (4.4) to (4.6) into the equations of momentum discussed in Chapter 3 in Section 3.1, the following respective equations of momentum, energy and concentration are obtained:

Equations of momentum:

$$\frac{\partial u}{\partial t} + u\frac{\partial u}{\partial x} - w_o\frac{\partial u}{\partial z} - 2\Omega v = \nu\left(\frac{\partial^2 u}{\partial x^2} + \nu\frac{\partial^2 u}{\partial z^2}\right) - \frac{\nu}{K_p}u + \frac{\sigma B_o^2}{\rho(1+m^2)}(mv - u) + \beta g(T - T_\infty) + \beta^* g(C - C_\infty) \tag{4.7}$$

$$\frac{\partial v}{\partial t} + u\frac{\partial v}{\partial x} - w_o\frac{\partial v}{\partial z} + 2\Omega u = \nu\left(\frac{\partial^2 v}{\partial x^2} + \frac{\partial^2 v}{\partial z^2}\right) - \frac{\nu}{K_p}v - \frac{\sigma B_o^2}{\rho(1+m^2)}(v + mu) \tag{4.8}$$

Equation of energy:

$$\begin{aligned}\frac{\partial T}{\partial t} + u\frac{\partial T}{\partial x} - w_o\frac{\partial T}{\partial z} &= \frac{k_f}{\rho C_p}\left(\frac{\partial^2 T}{\partial x^2} + \frac{\partial^2 T}{\partial z^2}\right) + \frac{D_M k_T}{c_s C_p}\left(\frac{\partial^2 C}{\partial z^2} + \frac{\partial^2 C}{\partial x^2}\right) \\ &+ \frac{\sigma}{\rho C_p}B_0^2\left(u^2 + v^2\right) + \frac{Q_o}{\rho C_p}(T - T_\infty) \\ &+ \frac{\mu}{\rho C_p}\left[\left(\frac{\partial u}{\partial z}\right)^2 + \left(\frac{\partial v}{\partial z}\right)^2\right] - \frac{16\sigma^* T_\infty^3}{3\rho C_p k^*}\frac{\partial^2 T}{\partial z^2}\end{aligned} \tag{4.9}$$

Equation of concentration:

$$\frac{\partial C}{\partial t} = D_M\left(\frac{\partial^2 C}{\partial x^2} + \frac{\partial^2 C}{\partial z^2}\right) + \frac{D_M k_T}{T_m}\left(\frac{\partial^2 T}{\partial x^2} + \frac{\partial^2 T}{\partial z^2}\right) - u\frac{\partial C}{\partial x} + w_o\frac{\partial C}{\partial z} \tag{4.10}$$

The initial and boundary conditions of the problem are:

$$
\begin{aligned}
t \leq 0 \quad &: \quad u = 0, v = 0, w = 0, C = 0, T = 0 \quad at \quad 0 \leq z \leq H \\
t > 0 \quad &: \quad C = C_\infty, T = T_\infty \qquad at \qquad x = 0 \quad (Channel \quad entrance) \\
t > 0 \quad &: \quad u = cx, v = 0, C = C_W, T = T_W, w = w_0 \qquad at \quad z = 0 \quad (Porous \quad wall) \\
t > 0 \quad &: \quad u = U, v = 0, C = C_\infty, T = T_\infty \quad at \quad z = H \quad (Impermeable \quad wall).
\end{aligned}
$$

4.1.2. Non-dimensionalization

The equations of momentum, energy and concentration have been derived in Chapter 3. The non-dimensionalization process discussed in Chapter 3 in Section 3.11 has been used in transforming the equations governing the flow to their respective non-dimensionalized form. Thus the respective non-dimensionalized form of equations (4.7) and (4.8) is

$$
\frac{\partial u'}{\partial t'} - w_o \frac{\partial u'}{\partial z'} - 2R_o v' = \frac{1}{Re} \frac{\partial^2 u'}{\partial z'^2} - Xiu' - Mu' + \frac{M}{1+m^2}(mv' - u') + Gr_\theta T' + Gr_c C' \tag{4.11}
$$

$$
\frac{\partial v'}{\partial t'} - w_o \frac{\partial v'}{\partial z'} + 2R_o u' = \frac{1}{Re} \frac{\partial^2 v'}{\partial z'^2} - Xiv' - Mv' - \frac{M}{1+m^2}(v' + mu') \tag{4.12}
$$

Similarly non-dimensional form of the equation of energy (4.9) is

$$
\begin{aligned}
\frac{\partial T'}{\partial t'} - w_o \frac{\partial T'}{\partial z'} \quad &= \quad \frac{1}{PrRe} \frac{\partial^2 T'}{\partial z'^2} + D_f Re \frac{\partial^2 C'}{\partial z'^2} + \frac{Ec}{Re} \left[\left(\frac{\partial u'}{\partial z'} \right)^2 + \left(\frac{\partial v'}{\partial z'} \right)^2 \right] \\
&+ \quad QT' - \frac{4}{3NPrRe} \left(\frac{\partial^2 T'}{\partial z'^2} \right) + RRe \left(u'^2 + v'^2 \right)
\end{aligned} \tag{4.13}
$$

where $Q = \frac{Q_o H}{\rho U C_p}$ is the non-dimensional heat source/sink parameter. The non-dimensional parameters appearing in these equations, namely M, Re, R_o, Xi , Gr_θ and Gr_c have been discussed in Chapter 3.

The non-dimensional form of the equation of concentration (4.10) is

$$
\frac{\partial C'}{\partial t'} + u' \frac{\partial C'}{\partial x'} - w_o \frac{\partial C'}{\partial z'} = \frac{1}{ReSc} \left(\frac{\partial^2 C'}{\partial x'^2} + \frac{\partial^2 C'}{\partial z'^2} \right) + \frac{Sr}{Re} \left(\frac{\partial^2 T'}{\partial x'^2} + \frac{\partial^2 T'}{\partial z'^2} \right) \tag{4.14}
$$

where Sc and Sr are the Schmidt number and Soret number respectively. The non-dimensional form of the initial and boundary conditions for this problem is

$$
\begin{aligned}
t^{'} \leq 0 \quad &: \quad u^{'} = 0, v^{'} = 0, w^{'} = 0, T^{'} = 0, C^{'} = 0 \qquad at \qquad 0 \leq z^{'} \leq H \\
t^{'} > 0 \quad &: \quad C^{'} = 0, T^{'} = 0 \qquad at \qquad x^{'} = 0 \quad (At \quad Entry) \\
t^{'} > 0 \quad &: \quad u^{'} = \frac{cH}{U_{\infty}} x^{'}, v^{'} = 0, C^{'} = 1, T^{'} = 1 \quad at \quad z^{'} = 0 \quad (Stretching \quad sheet) \\
t^{'} > 0 \quad &: \quad u^{'} = 1, v^{'} = 0, w^{'} = 0, C^{'} = 0, T^{'} = 0 \quad at \quad z^{'} = H \quad (Impermeable \quad sheet).
\end{aligned}
$$

4.2. Methodology

The equations that govern the flow in porous media over a stretching surface in the presence of heat source/sink are coupled and highly non-linear. They are represented by equations (4.11), (4.12), (4.13) and (4.14).

4.2.1. Definition of the mesh

The discretised domain for this problem is same as the one discussed Section 3.2 of Chapter 3.

4.2.2. The Finite Difference Method

The numerical method used to solve the equations governing the flow together with the initial and boundary conditions applies Crank-Nicholson algorithm. This method has been discussed in Section 3.22 of Chapter 3.

The FD form of the equation of momentum along the x-axis is

$$
\begin{aligned}
U_{i,j}^{k+1} &= [U_{i,j}^{k} - \frac{\Delta T}{2\Delta X}U_{i,j}^{k}(-U_{i-1,j}^{k+1} + U_{i,j}^{k} - U_{i-1,j}^{k}) + \frac{w_o \Delta T}{2\Delta Z}(-U_{i,j-1}^{k+1} + U_{i,j}^{k} - U_{i,j-1}^{k}) \\
&\quad + R_o \Delta T(V_{i,j}^{k+1} + V_{i,j}^{k}) + \frac{\Delta T}{2Re(\Delta X)^2}(U_{i+1,j}^{k+1} + U_{i-1,j}^{k+1} + U_{i+1,j}^{k} - 2U_{i,j}^{k} + U_{i-1,j}^{k}) \\
&\quad + \frac{\Delta T}{2Re(\Delta Z)^2}(U_{i,j+1}^{k+1} + U_{i,j-1}^{k+1} + U_{i,j+1}^{k} - 2U_{i,j}^{k} + U_{i,j-1}^{k}) - \frac{Xi\Delta T}{2}U_{i,j}^{k} \\
&\quad - M\frac{\Delta T}{2}U_{i,j}^{k} + \frac{M\Delta T}{2+2m^2}(mV_{i,j}^{k+1} + mV_{i,j}^{k} - U_{i,j}^{k}) \\
&+ \quad \frac{\Delta T Gr_\theta}{2}(T_{i,j}^{k+1} + T_{i,j}^{k}) + \frac{\Delta T Gr_c}{2}(C_{i,j}^{k+1} + C_{i,j}^{k})]/[1 + U_{i,j}^{k}\frac{\Delta T}{2\Delta X} \\
&\quad - \frac{w_o \Delta T}{2\Delta Z} + \frac{\Delta T}{Re(\Delta X)^2} + \frac{\Delta T}{Re(\Delta Z)^2} + \frac{\Delta T Xi}{2} + \frac{1}{2}M\Delta T + \frac{M\Delta T}{2+2m^2}]
\end{aligned}
$$

(4.16)

The FD form of the equation of momentum along the y-axis is

$$
\begin{aligned}
V_{i,j}^{k+1} &= [V_{i,j}^{k} - \frac{\Delta T}{2\Delta X}U_{i,j}^{k}(-V_{i-1,j}^{k+1} + V_{i,j}^{k} - V_{i-1,j}^{k}) + \frac{w_o \Delta T}{2\Delta Z}(-V_{i,j-1}^{k+1} + V_{i,j}^{k} - V_{i,j-1}^{k}) \\
&\quad + R_o \Delta T(U_{i,j}^{k+1} + U_{i,j}^{k}) + \frac{\Delta T}{2Re(\Delta X)^2}(V_{i+1,j}^{k+1} + V_{i-1,j}^{k+1} + V_{i+1,j}^{k} - 2V_{i,j}^{k} + V_{i-1,j}^{k}) \\
&\quad + \frac{\Delta T}{2Re(\Delta Z)^2}(U_{i,j+1}^{k+1} + V_{i,j-1}^{k+1} + V_{i,j+1}^{k} - 2V_{i,j}^{k} + V_{i,j-1}^{k}) - \frac{Xi\Delta T}{2}V_{i,j}^{k} \\
&\quad - M\frac{\Delta T}{2}V_{i,j}^{k} + \frac{M\Delta T}{2+2m^2}(V_{i,j}^{k} + m(U_{i,j}^{k+1} + U_{i,j}^{k})]/[1 + U_{i,j}^{k}\frac{\Delta T}{2\Delta X} - \frac{w_o \Delta T}{2\Delta Z} \\
&\quad + \frac{\Delta T}{Re(\Delta X)^2} + \frac{\Delta T}{Re(\Delta Z)^2} + \frac{Xi\Delta T}{2} + \frac{1}{2}M\Delta T - M\frac{\Delta T}{2+2m^2}]
\end{aligned}
$$

(4.17)

The FD form of the equation of energy is

$$
\begin{aligned}
T_{i,j}^{k+1} &= [T_{i,j}^{k} + \frac{Q\Delta t}{2}T_{i,j}^{k} - \frac{\Delta t}{2\Delta X}U_{i,j}^{k}(-T_{i-1,j}^{k+1} + T_{i,j}^{k} - T_{i-1,j}^{k}) \\
&+ \frac{w_o\Delta t}{2\Delta Z}(-T_{i,j-1}^{k+1} + T_{i,j}^{k} - T_{i,j-1}^{k}) \\
&+ \frac{Df\Delta t}{2Re(\Delta X)^2}(C_{i+1,j}^{k+1} - 2C_{i,j}^{k+1} + C_{i-1,j}^{k+1} + C_{i+1,j}^{k} - 2C_{i,j}^{k} + C_{i-1,j}^{k}) \\
&+ \frac{Df\Delta t}{2Re(\Delta Z)^2}(C_{i,j+1}^{k+1} - 2C_{i,j}^{k+1} + C_{i,j-1}^{k+1} + C_{i,j+1}^{k} - 2C_{i,j}^{k} + C_{i,j-1}^{k}) \\
&+ \frac{Ec\Delta t}{4Re(\Delta X)^2}(U_{i,j}^{k+1} - U_{i-1,j}^{k+1} + U_{i,j}^{k} - U_{i-1,j}^{k})^2 \\
&+ \frac{Ec\Delta t}{4Re(\Delta Z)^2}(U_{i,j}^{k+1} - U_{i,j-1}^{k+1} + U_{i,j}^{k} - U_{i,j-1}^{k})^2]/[1 + U_{i,j}^{k} \\
&+ \frac{\Delta t}{2PrRe(\Delta X)^2}(T_{i+1,j}^{k+1} + T_{i-1,j}^{k+1} + T_{i+1,j}^{k} - 2T_{i,j}^{k} + T_{i-1,j}^{k}) \\
&+ \frac{\Delta t}{2PrRe(\Delta Z)^2}(T_{i,j+1}^{k+1} + T_{i,j-1}^{k+1} + T_{i,j+1}^{k} - 2T_{i,j}^{k} + T_{i,j-1}^{k}) \\
&+ \frac{\Delta tRRe}{4}((U_{i,j}^{k})^2 + (V_{i,j}^{k})^2) \\
&- \frac{2\Delta t}{3NiPrRe(\Delta Z)^2}(T_{i,j+1}^{k+1} - 2T_{i,j}^{k+1} + T_{i,j-1}^{k+1} + T_{i,j+1}^{k} - 2T_{i,j}^{k} + T_{i,j-1}^{k}) \\
&\frac{\Delta t}{2\Delta X} - \frac{w_o\Delta t}{2\Delta Z} + \frac{\Delta t}{RePr(\Delta X)^2} + \frac{\Delta t}{RePr(\Delta Z)^2} - \frac{Q\Delta t}{2} - \frac{4\Delta t}{3NiPrRe(\Delta Z)^2}]
\end{aligned}
$$

(4.18)

The FD form of the equation of concentration is

$$
\begin{aligned}
C_{i,j}^{k+1} &= [C_{i,j}^{k} - \frac{\Delta t}{2\Delta X}U_{i,j}^{k}(-C_{i-1,j}^{k+1} + C_{i,j}^{k} - C_{i-1,j}^{k}) + \frac{w_o\Delta t}{2\Delta Z}(-C_{i,j-1}^{k+1} + C_{i,j}^{k} - C_{i,j-1}^{k}) \\
&+ \frac{\Delta t}{2ScRe(\Delta X)^2}(C_{i+1,j}^{k+1} + C_{i-1,j}^{k+1} + C_{i+1,j}^{k} - 2C_{i,j}^{k} + C_{i-1,j}^{k}) \\
&+ \frac{\Delta t}{2ScRe(\Delta Z)^2}(C_{i,j+1}^{k+1} + C_{i,j-1}^{k+1} + C_{i,j+1}^{k} - 2C_{i,j}^{k} + C_{i,j-1}^{k}) \\
&+ \frac{Sr\Delta t}{2Re(\Delta X)^2}(T_{i+1,j}^{k+1} - 2T_{i,j}^{k+1} + T_{i-1,j}^{k+1} \\
&+ T_{i+1,j}^{k} - 2T_{i,j}^{k} + T_{i-1,j}^{k}) + \frac{Sr\Delta t}{2Re(\Delta Z)^2}(T_{i,j+1}^{k+1} - 2T_{i,j}^{k+1} \\
&+ T_{i,j-1}^{k+1} + T_{i,j+1}^{k} - 2T_{i,j}^{k} + T_{i,j-1}^{k})]/[1 + \frac{\Delta t}{2\Delta X}U_{i,j}^{k} \\
&- \frac{w_o\Delta t}{2\Delta Z} + \frac{\Delta t}{ReSc(\Delta X)^2} + \frac{\Delta t}{ReSc(\Delta Z)^2}]
\end{aligned}
$$

(4.19)

The values of U in equation (4.15) are computed at every nodal point for a particular i at the $(k+1)^{th}$ time level. This is followed by computing the values of V in equation (4.16). Using the values of U and V at $(k+1)^{th}$ time level, the values of C at $(k+1)^{th}$ time level in equation (4.18) are also computed. At this point the values of U, V and C are known on a particular i-level. Finally the known values of U, V and C are employed in computing the values of T in equation (4.17) at every nodal point on a particular i-level at $(k+1)^{th}$ time level. This process is repeated for all the i-levels. Thus the values of U, V, C and T are determined at every grid point in the domain at all time levels.

The numerical calculations have been performed by fixing the mesh sizes at $\Delta x = 0.05$, $\Delta z = 0.25$, and $\Delta t = 0.001$ where the region formed by the x-axis and the z-axis is a 41 x 41 mesh. The suitability of the mesh sizes has been discussed in Section 3.22 of Chapter 3.

4.2.3. Discussion of the results

In order to get a physical insight into the problem at hand, the velocity, temperature and concentration fields have been discussed by assigning numerical values to various non-dimensional parameters. For instance the following parameters have been used: M = 1, Pr = 0.71, m = 0.5, N = 0.45, Q = 0.8, R = 0.2, Ec = 0.4, Sc = 0.78, Xi = 0.5, Sr = 1, Ro = 0.3, w_o = -0.5, Re = 50, Df = 0.03, $Gr_\theta = 5$, and $Gr_c = 2$. The values of Prandtl number Pr used are 0.64, 0.71, and 7.00 and represent flue gas, air, and water respectively at 20^oC and one atmosphere pressure. The values of Schmidt number used are 0.22, 0.62, and 0.78 and represent hydrogen, water vapour and ammonia respectively at 20^oC and one atmosphere pressure. A positive value of thermal Grashof number ($Gr_\theta > 0$) corresponds to a cooled sheet.

Figures 4.1 and 4.2 show that in the presence of a heat source, increase in Hall parameter m leads to an increase in the magnitude of primary velocity profiles and secondary velocity profiles respectively. Increase in Magnetic parameter M leads to a decrease in the magnitude of primary velocity profiles and secondary velocity profiles respectively. A large value of M causes a reversal in the direction of the secondary velocity profiles. The fluid velocity increases with increasing m due to the fact that the effective conductivity of the fluid decreases with increase in the Hall parameter m, since the magnetic damping force is reduced. However the magnetic damping force increases with increasing M, causing a decrease in the velocity profiles. Increase in time t leads to an increase in the magnitude of the primary and secondary velocity profiles respectively.

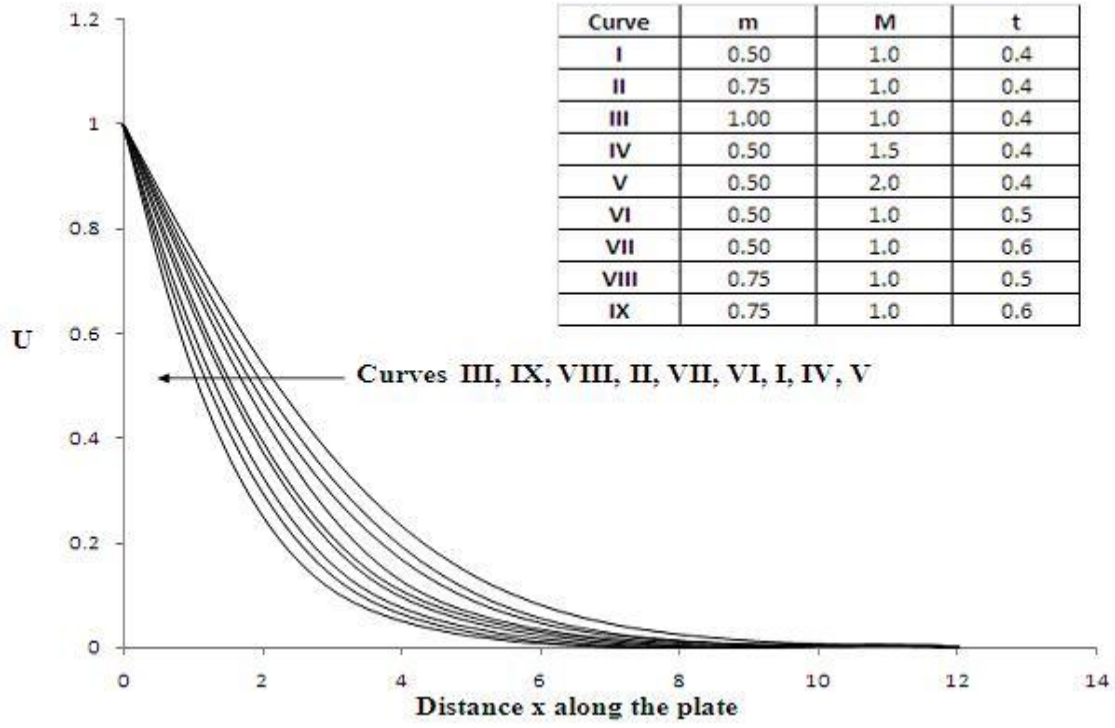

Figure 43 : Primary velocity profiles when m, M and t are varied.

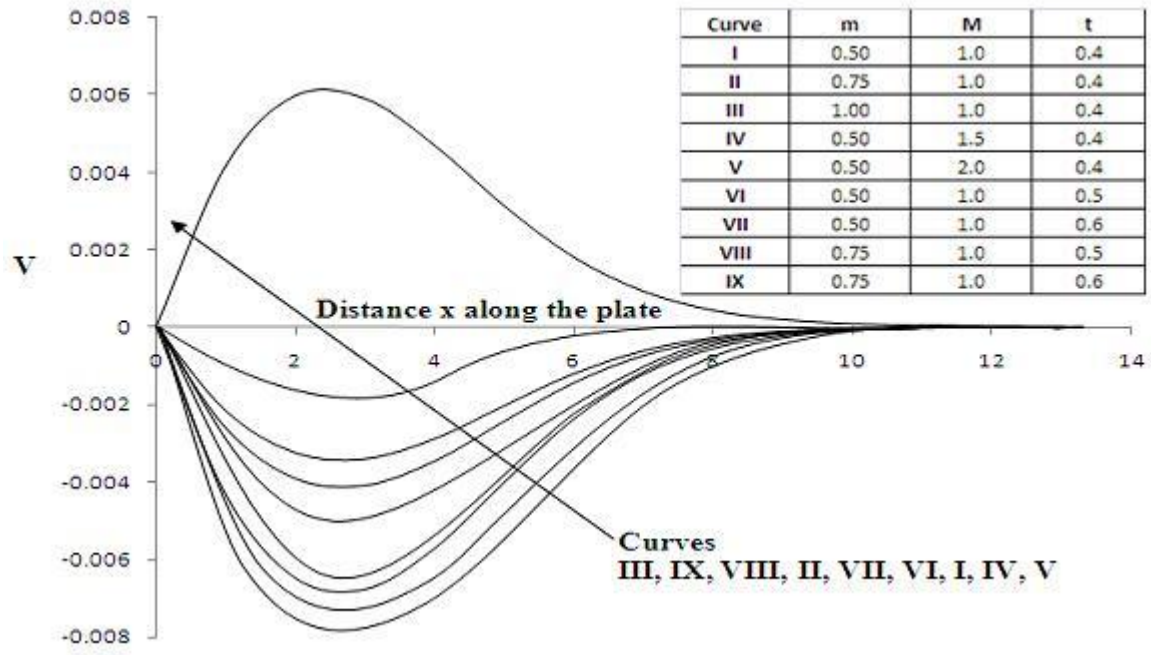

Curve	m	M	t
I	0.50	1.0	0.4
II	0.75	1.0	0.4
III	1.00	1.0	0.4
IV	0.50	1.5	0.4
V	0.50	2.0	0.4
VI	0.50	1.0	0.5
VII	0.50	1.0	0.6
VIII	0.75	1.0	0.5
IX	0.75	1.0	0.6

Figure 44 : Secondary velocity profiles when m, M and t are varied.

Figure 4.3 shows that an increase in Hall parameter m leads to a decrease in the concentration profiles. An increase in the Magnetic parameter M leads to an increase in the concentration profiles. Increase in m leads to decrease in the conductivity of the fluid, reducing the magnetic damping force. This increases the rate of transportation of the species by convection away from the boundary layer region, leading to lower species concentration. Similarly, increase in M leads to an increase in the magnetic damping force, resulting to an increase in the concentration profiles. Increase in the concentration profiles is as a result of reduced rate of species transportation. Increase in time t leads to a decrease in the concentration profiles. Thus concentration of the fluid decreases with time.

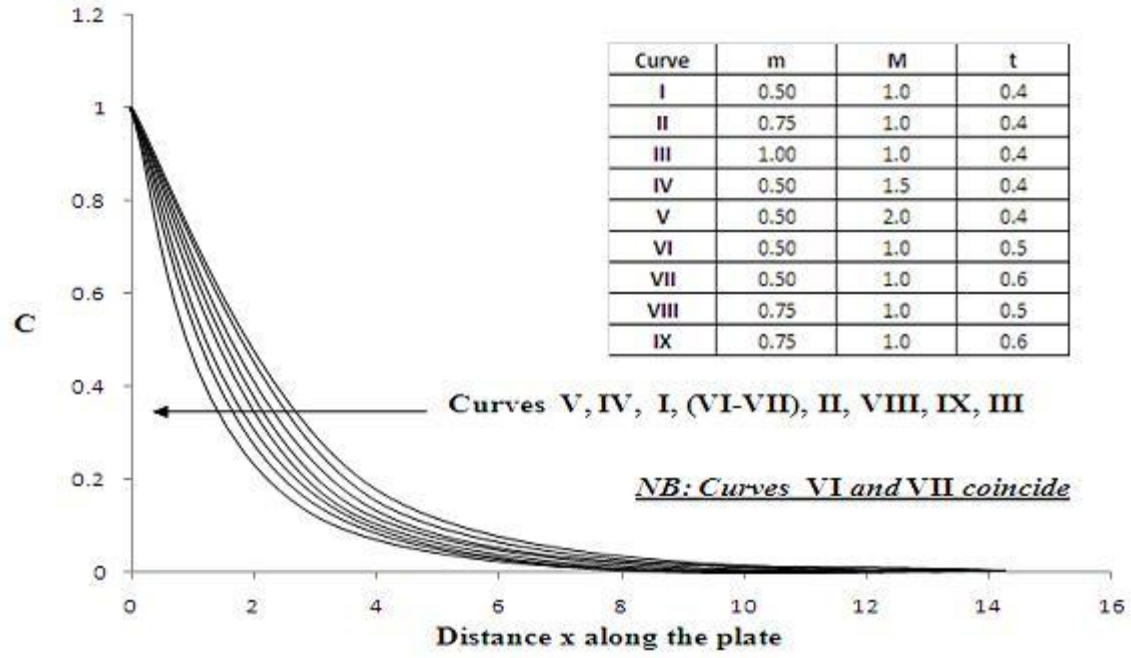

Curve	m	M	t
I	0.50	1.0	0.4
II	0.75	1.0	0.4
III	1.00	1.0	0.4
IV	0.50	1.5	0.4
V	0.50	2.0	0.4
VI	0.50	1.0	0.5
VII	0.50	1.0	0.6
VIII	0.75	1.0	0.5
IX	0.75	1.0	0.6

Figure 45 : Concentration profiles when m, M and t are varied.

From Figure 4.4 increase in the Hall parameter m causes increase in the temperature profiles. Increasing m decreases the conductivity of the fluid, resulting in increase in Joule heating, leading to a thicker thermal boundary layer. Increase in the Magnetic parameter M leads to a decrease in the temperature profiles. Reduced velocity implies lower viscous dissipation and hence the observed decrease in the temperature profiles.

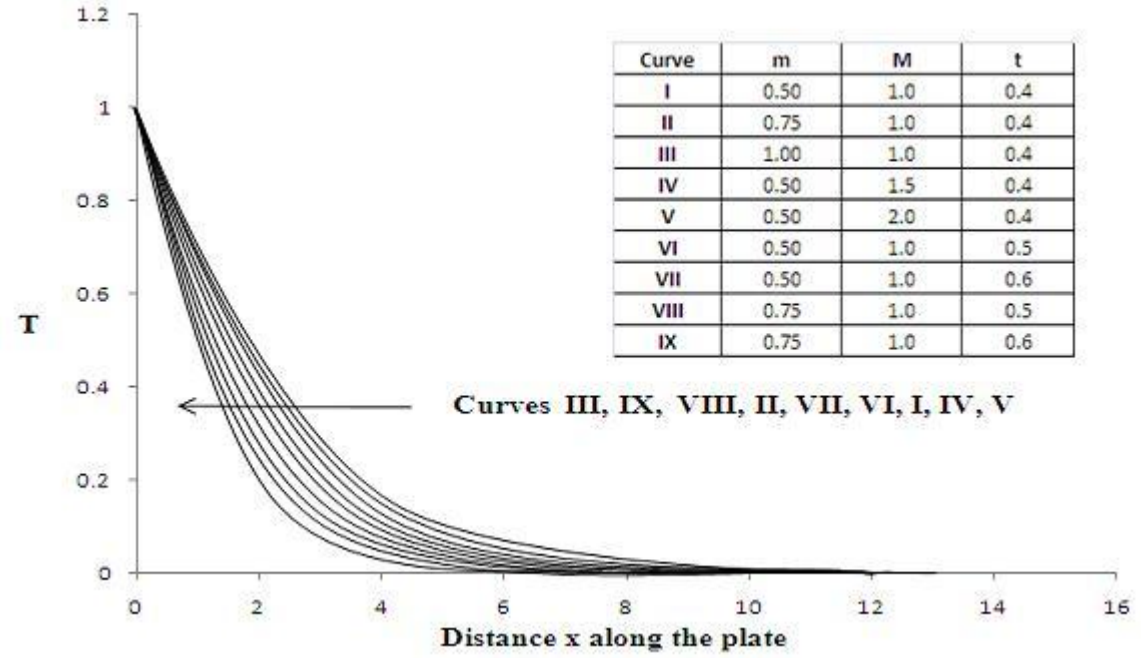

Curve	m	M	t
I	0.50	1.0	0.4
II	0.75	1.0	0.4
III	1.00	1.0	0.4
IV	0.50	1.5	0.4
V	0.50	2.0	0.4
VI	0.50	1.0	0.5
VII	0.50	1.0	0.6
VIII	0.75	1.0	0.5
IX	0.75	1.0	0.6

Figure 46 : Temperature profiles when m, M and t are varied.

Figures 4.5, 4.6, 4.7 and 4.8 show that in the presence of a heat source ($Q > 0$), increase in the Schmidt number Sc causes a decrease in the velocity profiles. Increase in Sc causes an increase in concentration and temperature profiles respectively. Physically increase in concentration implies that when subjected to a heat source, Hydrogen diffuses faster in Air (Pr=0.71) than Water vapour does; and Water vapour diffuses slower in Air than it does in Ammonia. Increase in temperature implies that under similar conditions, a mixture of Air and Hydrogen is warmer than a mixture of Air and Water vapour; and Water vapour is warmer than a mixture of Air and Ammonia. Increase in concentration with increase in Sc shows that Ammonia diffuses faster into Air than it does in Water vapour and Hydrogen respectively. A large value of Sc implies a heavier fluid. Figure 4.8 shows that there is a cross-over of the temperature profiles at along the stretching sheet. A cross-over in the temperature profiles takes place when the effect of stretching on temperature is overcome by the effects of Schmidt number on the temperature in

the thermal boundary layer region. Increase in time t leads to a decrease in the velocity, temperature and concentration profiles of the fluid.

Figures 4.5, 4.6, 4.7 and 4.8 show that in the presence of a heat source ($Q > 0$), increase in Prandtl number Pr causes an increase in the velocity and concentration profiles respectively. Increase in Pr causes a decrease in temperature profiles. Physically this means that when subjected to similar conditions, a mixture of Flue gas (Pr = 0.64) and Hydrogen (Sc = 0.22, at 25^oC temperature and one atmosphere pressure) diffuses faster than does a mixture of Air and Hydrogen; and a mixture of Air and Hydrogen diffuses faster than a mixture of Water and Hydrogen. Under similar conditions, Hydrogen diffuses faster in Flue gas than it does in the Air; and the latter diffuses less faster in Water. Increase in time t causes a decrease in concentration and temperature profiles respectively. Increase in time causes an increase in velocity profiles.

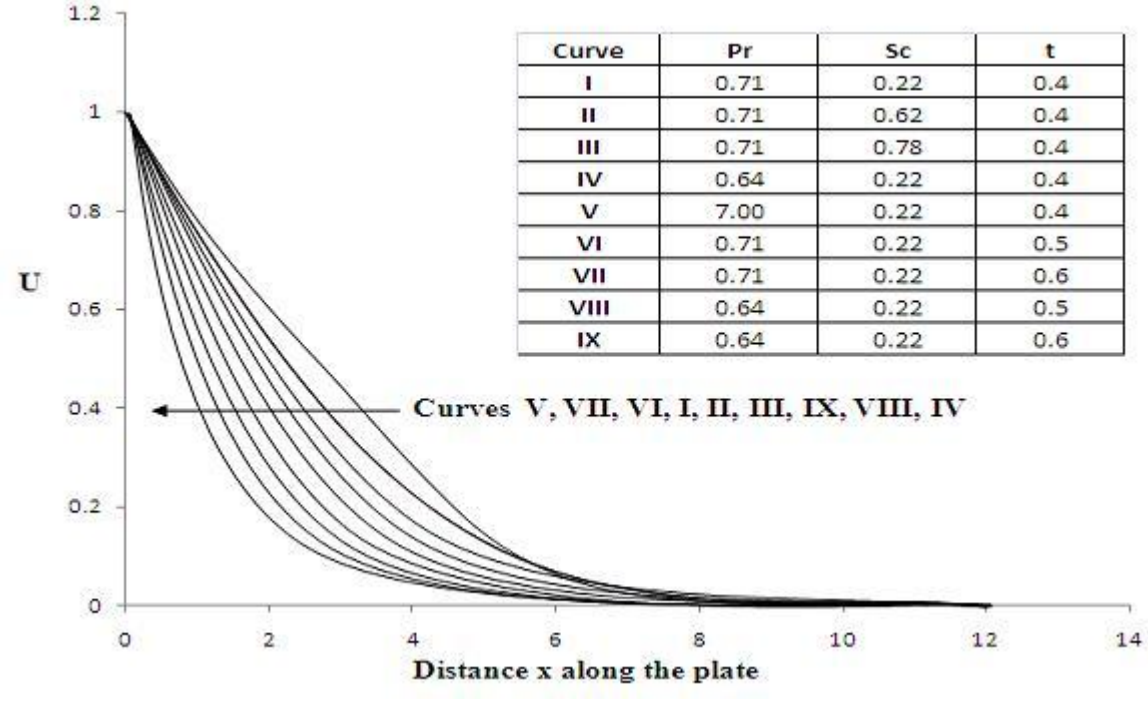

Curve	Pr	Sc	t
I	0.71	0.22	0.4
II	0.71	0.62	0.4
III	0.71	0.78	0.4
IV	0.64	0.22	0.4
V	7.00	0.22	0.4
VI	0.71	0.22	0.5
VII	0.71	0.22	0.6
VIII	0.64	0.22	0.5
IX	0.64	0.22	0.6

Figure 47 : Primary velocity profiles when Pr, Sc and t are varied.

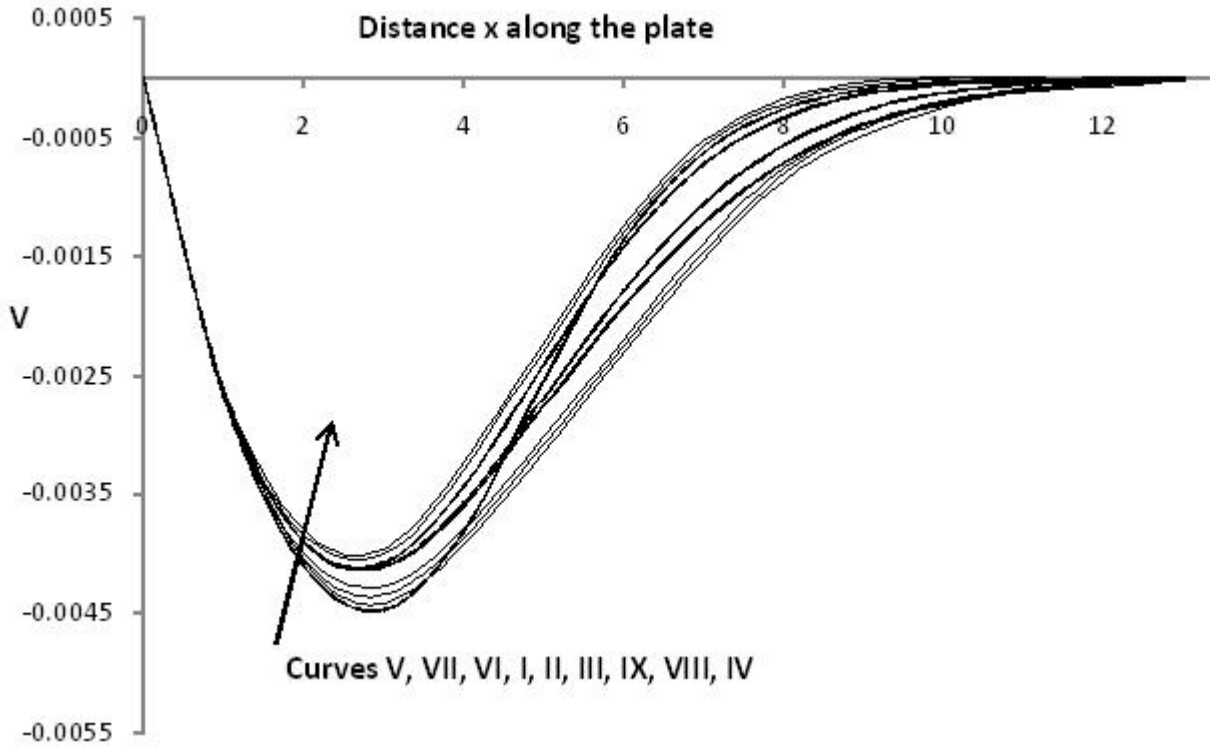

Figure 48 : Secondary velocity profiles when Pr, Sc and t are varied.

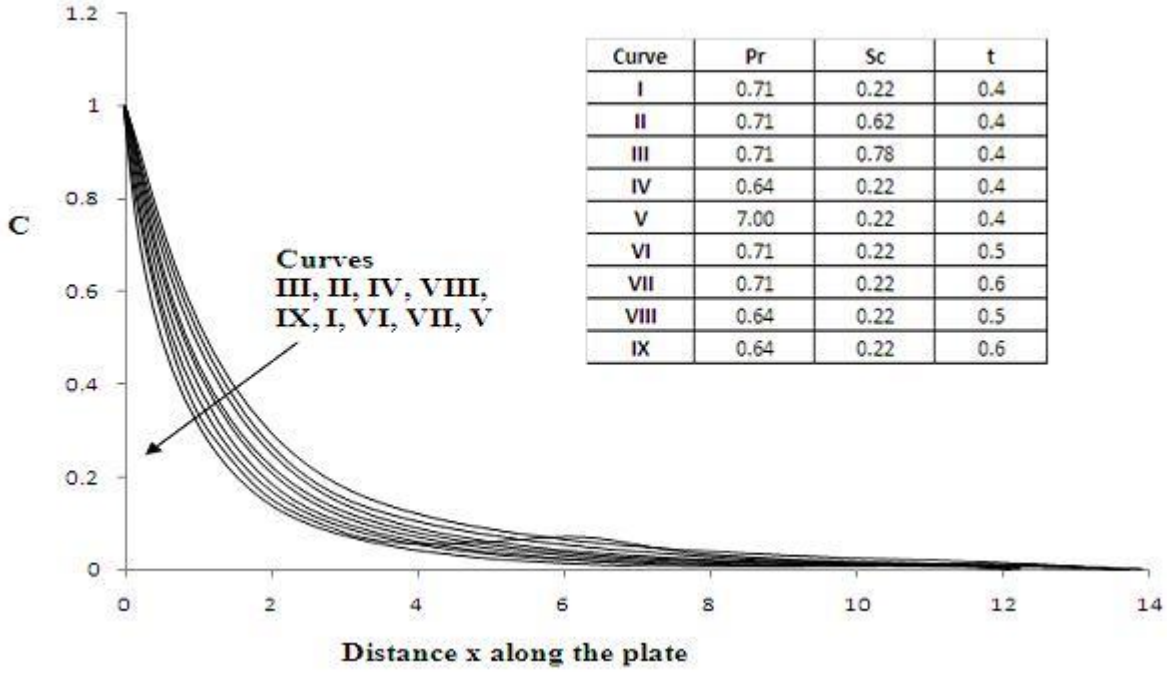

Curve	Pr	Sc	t
I	0.71	0.22	0.4
II	0.71	0.62	0.4
III	0.71	0.78	0.4
IV	0.64	0.22	0.4
V	7.00	0.22	0.4
VI	0.71	0.22	0.5
VII	0.71	0.22	0.6
VIII	0.64	0.22	0.5
IX	0.64	0.22	0.6

Figure 49 : Concentration profiles when Pr, Sc and t are varied.

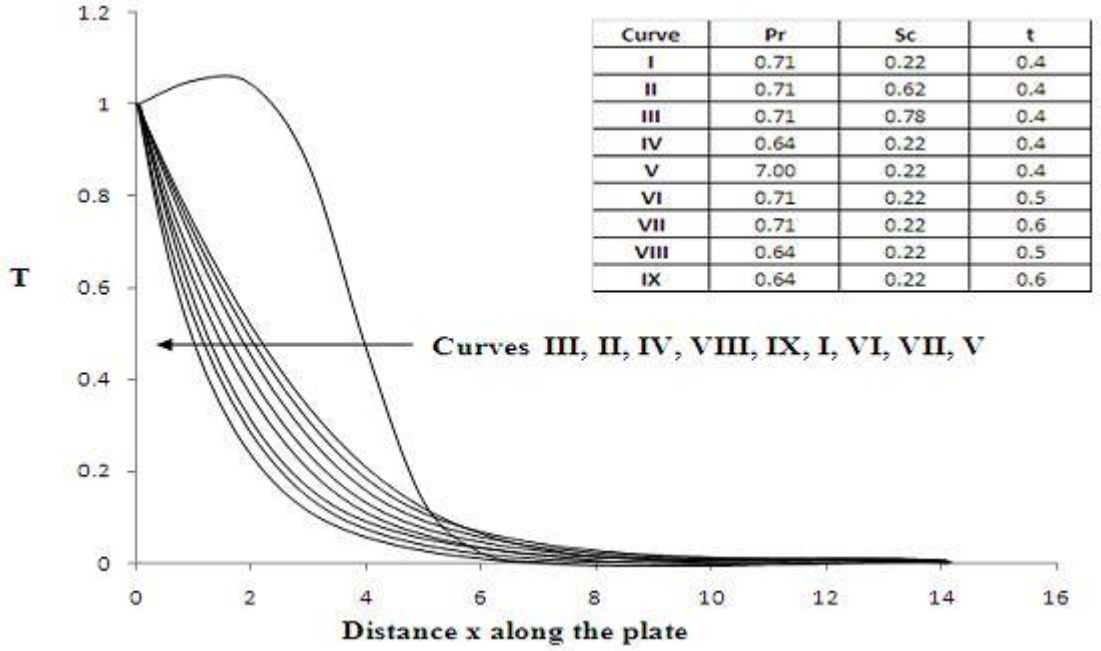

Curve	Pr	Sc	t
I	0.71	0.22	0.4
II	0.71	0.62	0.4
III	0.71	0.78	0.4
IV	0.64	0.22	0.4
V	7.00	0.22	0.4
VI	0.71	0.22	0.5
VII	0.71	0.22	0.6
VIII	0.64	0.22	0.5
IX	0.64	0.22	0.6

Figure 50 : Temperature profiles when Pr, Sc and t are varied.

Figures 4.9, 4.10, 4.11 and 4.12 show that increase in the magnitude of the Heat sink parameter Q leads to a decrease in the magnitude of velocity and temperature profiles respectively. Increase in Q leads to an increase in the concentration profiles. The presence of a heat sink produces a cooling effect that decreases velocity of the convection currents that move upwards next to the surface of the stretching sheet, leading to higher concentration profiles.

Figures 4.9, 4.10, 4.11 and 4.12 show that in the presence of a heat sink, increase in the Eckert number Ec leads to an increase in the magnitude of the velocity and temperature profiles respectively; but to a decrease in the concentration profiles. Increase in Ec means the fluid absorbs more heat energy that is released from the internal viscous forces. This in turn increases the temperature and the velocity of the convection currents due to increased thermal buoyancy forces respectively. Higher velocity profiles imply an increased rate of species transportation away from the boundary layer region, and hence the observed decrease in the concentration profiles.

Figures 4.9, 4.10, 4.11 and 4.12 show that in the presence of a heat sink, increase in the Radiation parameter N leads to a decrease in the magnitude of the velocity and temperature profiles respectively; but to an increase in the concentration profiles. Thus radiation can be used to control the velocity and thermal boundary layers quite effectively. Increase in time t leads to an increase in the magnitude of the velocity, concentration and temperature profiles. This shows that the transient velocity, concentration and temperature increase with time.

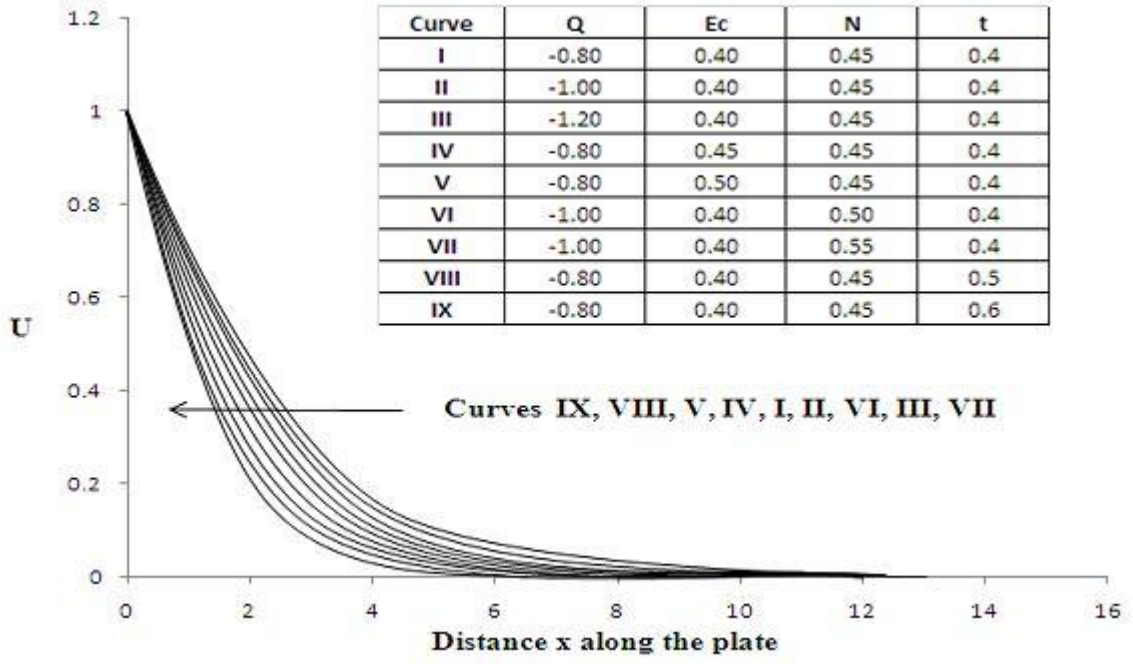

Curve	Q	Ec	N	t
I	-0.80	0.40	0.45	0.4
II	-1.00	0.40	0.45	0.4
III	-1.20	0.40	0.45	0.4
IV	-0.80	0.45	0.45	0.4
V	-0.80	0.50	0.45	0.4
VI	-1.00	0.40	0.50	0.4
VII	-1.00	0.40	0.55	0.4
VIII	-0.80	0.40	0.45	0.5
IX	-0.80	0.40	0.45	0.6

Figure 51 : Primary velocity profiles when Q, Ec, N, and t are varied.

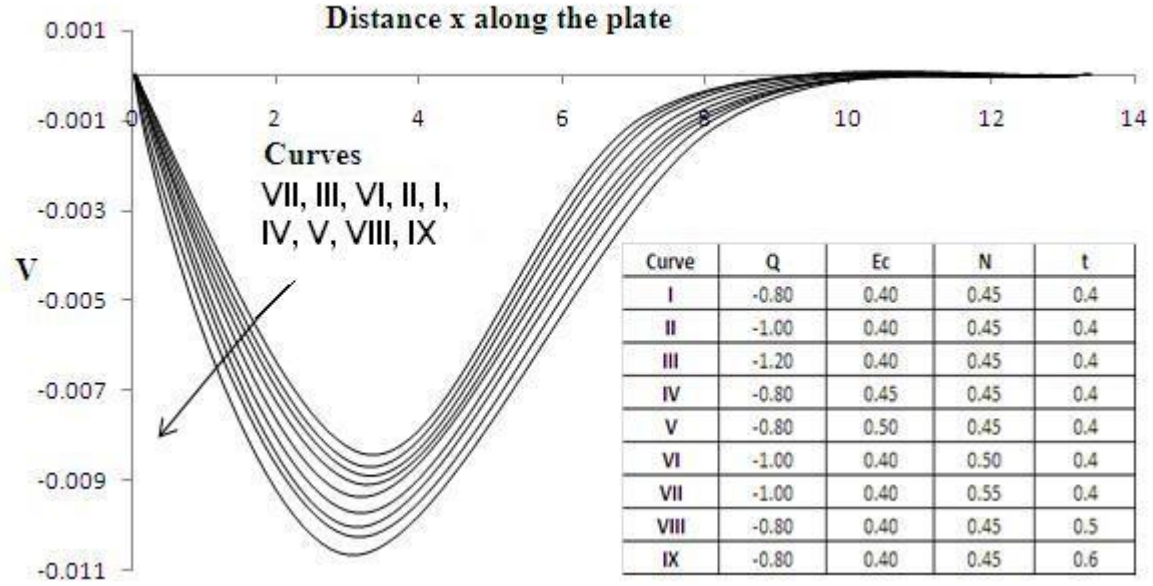

Curve	Q	Ec	N	t
I	-0.80	0.40	0.45	0.4
II	-1.00	0.40	0.45	0.4
III	-1.20	0.40	0.45	0.4
IV	-0.80	0.45	0.45	0.4
V	-0.80	0.50	0.45	0.4
VI	-1.00	0.40	0.50	0.4
VII	-1.00	0.40	0.55	0.4
VIII	-0.80	0.40	0.45	0.5
IX	-0.80	0.40	0.45	0.6

Figure 52 : Secondary velocity profiles when Q, Ec, N, and t are varied.

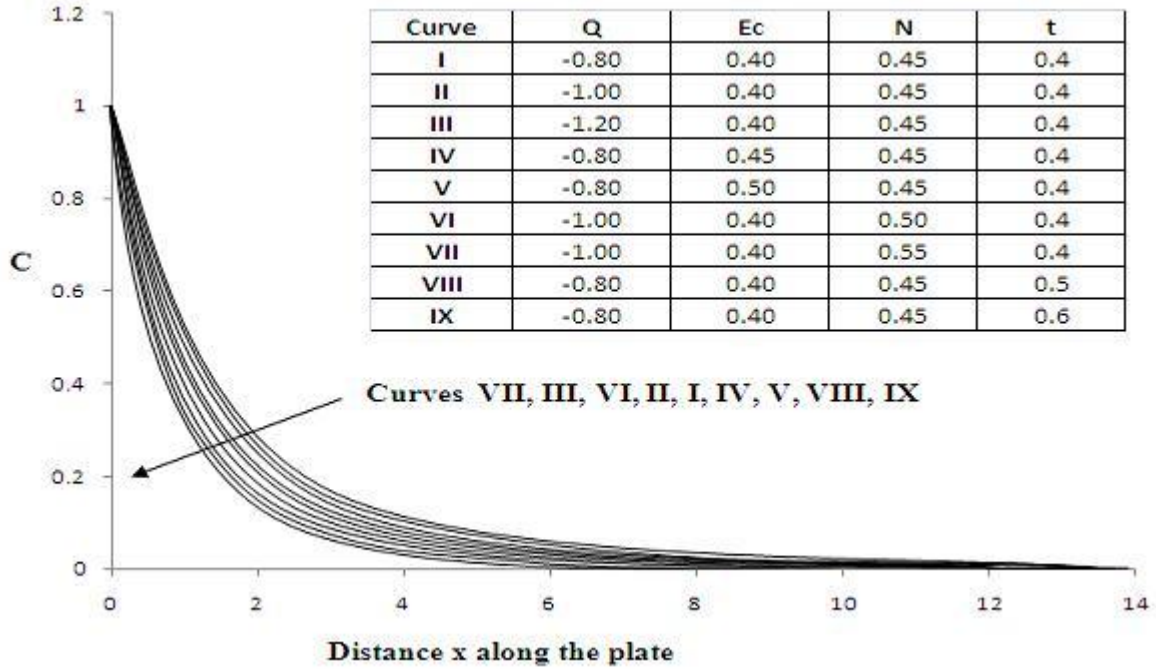

Curve	Q	Ec	N	t
I	-0.80	0.40	0.45	0.4
II	-1.00	0.40	0.45	0.4
III	-1.20	0.40	0.45	0.4
IV	-0.80	0.45	0.45	0.4
V	-0.80	0.50	0.45	0.4
VI	-1.00	0.40	0.50	0.4
VII	-1.00	0.40	0.55	0.4
VIII	-0.80	0.40	0.45	0.5
IX	-0.80	0.40	0.45	0.6

Figure 53 : Concentration profiles when Q, Ec, N, and t are varied.

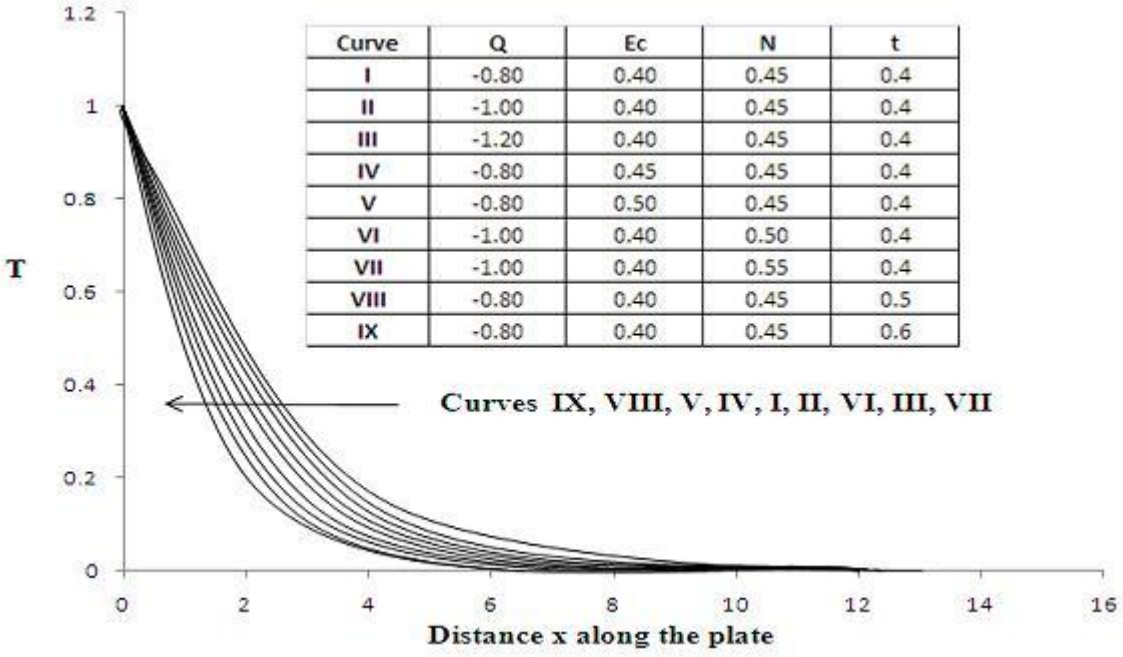

Curve	Q	Ec	N	t
I	-0.80	0.40	0.45	0.4
II	-1.00	0.40	0.45	0.4
III	-1.20	0.40	0.45	0.4
IV	-0.80	0.45	0.45	0.4
V	-0.80	0.50	0.45	0.4
VI	-1.00	0.40	0.50	0.4
VII	-1.00	0.40	0.55	0.4
VIII	-0.80	0.40	0.45	0.5
IX	-0.80	0.40	0.45	0.6

Figure 54 : Temperature profiles when Q, Ec, N, and t are varied.

Figures 4.13, 4.14, 4.15 and 4.16 show that in the presence of a heat sink, increase in the magnitude of the Injection parameter w_o leads to an increase in the velocity and temperature profiles respectively; but to a decrease in the concentration profiles. Injection increases the velocity of the fluid thus increasing the rate at which the species are carried away from the boundary layer region, and hence the observed decrease in the species concentration. Thus velocity, temperature and concentration boundary layers can be controlled by varying the rate of injection. Increase in the Permeability parameter Xi leads to a decrease in the velocity and temperature profiles; but to an increase in the concentration profiles. Increase in the Rotation parameter Ro leads to a decrease in the velocity and temperature profiles; but to an increase in the concentration profiles. Increase in Xi will results in increased resistance to the flow by the porous medium (as the permeability physically becomes less with increasing Xi) which will in turn lead to deceleration of the flow velocity of the fluid; resulting into reduced magnitudes of the primary and the secondary velocities respectively. Increase in the Joule heating parameter R leads to an increase in the velocity and temperature profiles respectively; but to a decrease in the concentration profiles. Increase in Joule heating parameter leads to the heating of the fluid thereby boosting the velocity of the convection currents on the surface of the stretching

sheet.

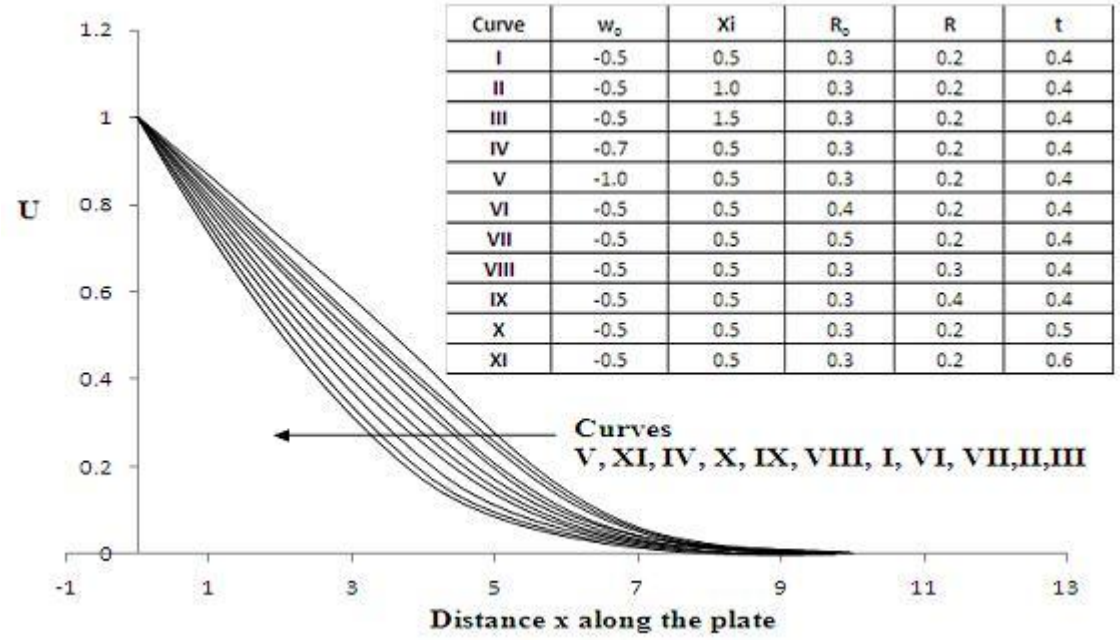

Curve	w_o	Xi	R_o	R	t
I	-0.5	0.5	0.3	0.2	0.4
II	-0.5	1.0	0.3	0.2	0.4
III	-0.5	1.5	0.3	0.2	0.4
IV	-0.7	0.5	0.3	0.2	0.4
V	-1.0	0.5	0.3	0.2	0.4
VI	-0.5	0.5	0.4	0.2	0.4
VII	-0.5	0.5	0.5	0.2	0.4
VIII	-0.5	0.5	0.3	0.3	0.4
IX	-0.5	0.5	0.3	0.4	0.4
X	-0.5	0.5	0.3	0.2	0.5
XI	-0.5	0.5	0.3	0.2	0.6

Figure 55 : Primary velocity profiles when w_o, Xi, Ro, R, and t are varied.

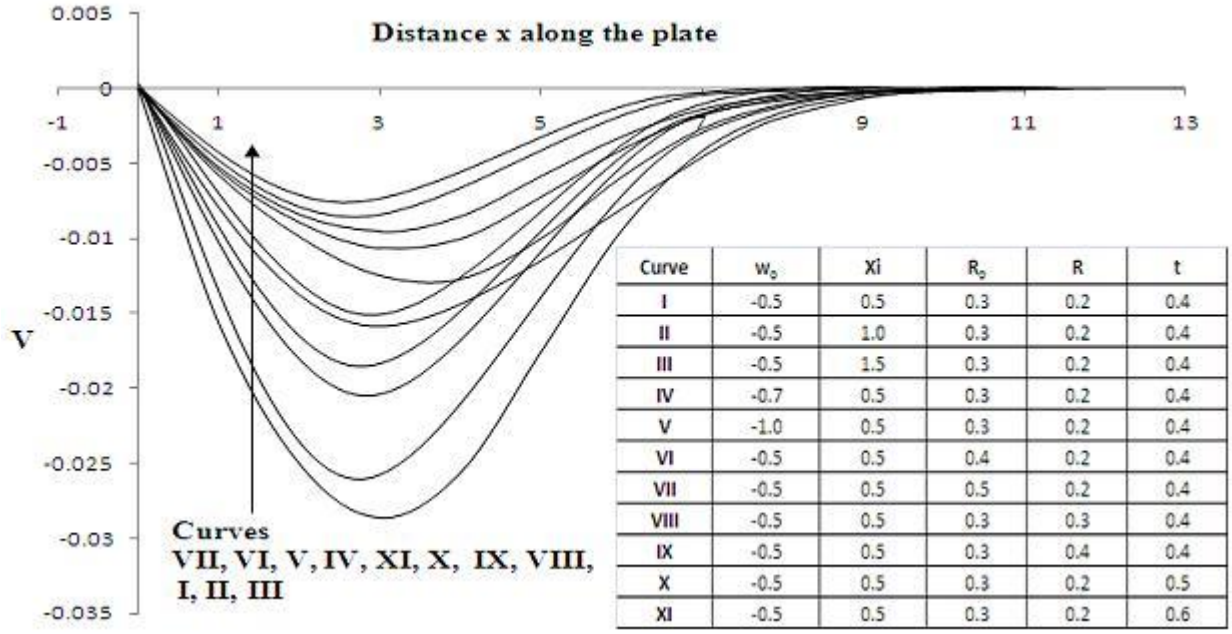

Curve	w_o	Xi	R_o	R	t
I	-0.5	0.5	0.3	0.2	0.4
II	-0.5	1.0	0.3	0.2	0.4
III	-0.5	1.5	0.3	0.2	0.4
IV	-0.7	0.5	0.3	0.2	0.4
V	-1.0	0.5	0.3	0.2	0.4
VI	-0.5	0.5	0.4	0.2	0.4
VII	-0.5	0.5	0.5	0.2	0.4
VIII	-0.5	0.5	0.3	0.3	0.4
IX	-0.5	0.5	0.3	0.4	0.4
X	-0.5	0.5	0.3	0.2	0.5
XI	-0.5	0.5	0.3	0.2	0.6

Figure 56 : Secondary velocity profiles when w_o, Xi, Ro, R, and t are varied.

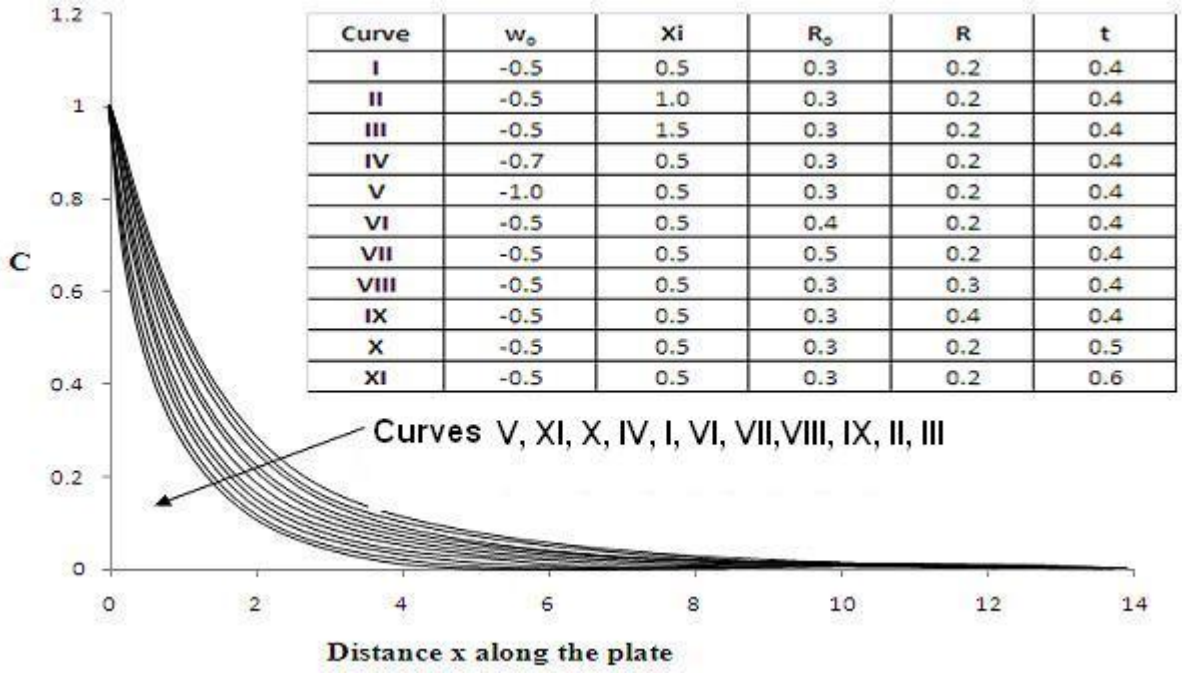

Curve	w_o	Xi	R_o	R	t
I	-0.5	0.5	0.3	0.2	0.4
II	-0.5	1.0	0.3	0.2	0.4
III	-0.5	1.5	0.3	0.2	0.4
IV	-0.7	0.5	0.3	0.2	0.4
V	-1.0	0.5	0.3	0.2	0.4
VI	-0.5	0.5	0.4	0.2	0.4
VII	-0.5	0.5	0.5	0.2	0.4
VIII	-0.5	0.5	0.3	0.3	0.4
IX	-0.5	0.5	0.3	0.4	0.4
X	-0.5	0.5	0.3	0.2	0.5
XI	-0.5	0.5	0.3	0.2	0.6

Figure 57 : Concentration profiles when w_o, Xi, Ro, R, and t are varied.

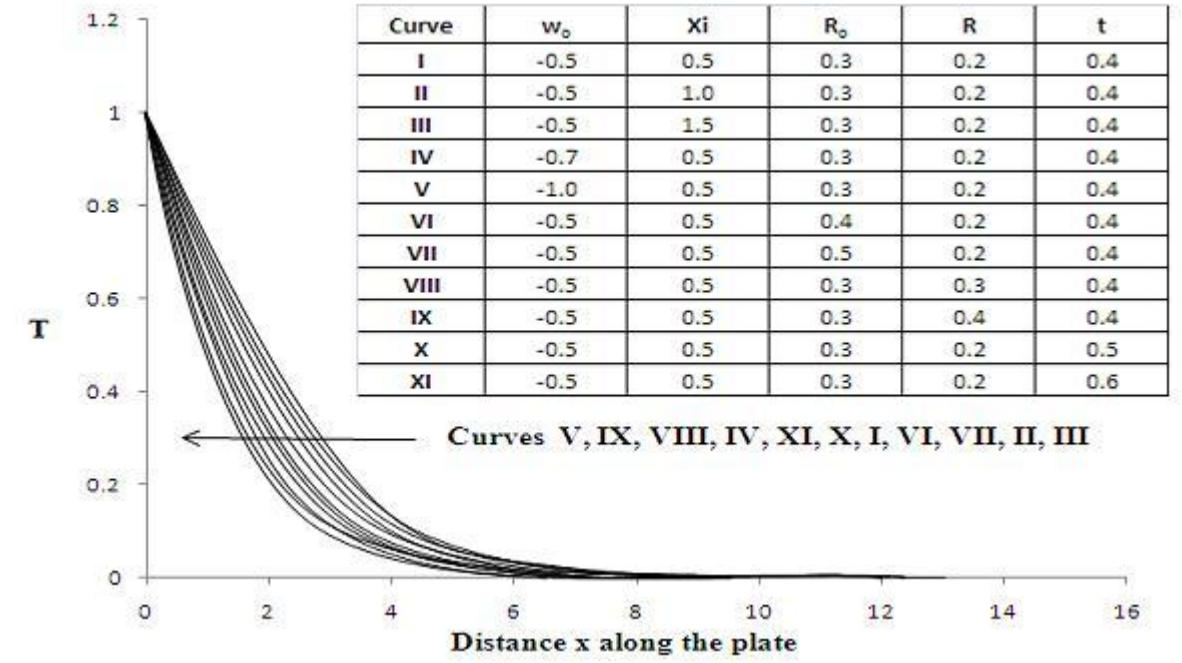

Curve	w_o	Xi	R_o	R	t
I	-0.5	0.5	0.3	0.2	0.4
II	-0.5	1.0	0.3	0.2	0.4
III	-0.5	1.5	0.3	0.2	0.4
IV	-0.7	0.5	0.3	0.2	0.4
V	-1.0	0.5	0.3	0.2	0.4
VI	-0.5	0.5	0.4	0.2	0.4
VII	-0.5	0.5	0.5	0.2	0.4
VIII	-0.5	0.5	0.3	0.3	0.4
IX	-0.5	0.5	0.3	0.4	0.4
X	-0.5	0.5	0.3	0.2	0.5
XI	-0.5	0.5	0.3	0.2	0.6

Figure 58 : Temperature profiles when w_o, Xi, Ro, R, and t are varied.

4.3. Nusselt number, Sherwood, and Local Skin-friction Coefficient

The velocity, temperature and concentration profiles have been analyzed and discussed above. What follows in this section is therefore an investigation of the rate of heat transfer and mass transfer, and shear stress at the surface of the stretching sheet. Thus the quantities of main interest in the problem at hand are the local Nusselt number Nu, the local Sherwood number Sh, and the shearing stresses C_{fx} and C_{fy}: which indicate physically the rate of heat transfer, rate of mass transfer and the wall shear stresses respectively. The method used in calculating these rates has been discussed in Section 3.3 of Chapter 3.

$$\tau_x = -\mu \left(\frac{\partial u}{\partial z}\right)_{z=0} = -\frac{\mu U_\infty}{H} \left(\frac{\partial u'}{\partial z'}\right)_{z'=0} \tag{4.20}$$

$$\tau_y = -\mu \left(\frac{\partial v}{\partial z}\right)_{z=0} = -\frac{\mu U_\infty}{H} \left(\frac{\partial v'}{\partial z'}\right)_{z'=0} \tag{4.21}$$

The local skin friction coefficients are defined as

$$C_{fx} = -\frac{\tau_x}{\frac{1}{2}\rho {U_\infty}^2} = -\frac{2}{Re} \left(\frac{\partial u'}{\partial z'}\right)_{z'=0} \tag{4.22}$$

$$C_{fy} = -\frac{\tau_x}{\frac{1}{2}\rho {U_\infty}^2} = -\frac{2}{Re} \left(\frac{\partial v'}{\partial z'}\right)_{z'=0} \tag{4.23}$$

Equations (4.22) and (4.23) represent the respective local skin friction coefficients due to the primary and secondary velocity profiles. The local surface mass flux is expressed as

$$\begin{aligned} Q_w &= -D_M \left(\frac{\partial C}{\partial z}\right)_{z=0} \\ &= -D_M \frac{(C_W - C_\infty)}{H} \left(\frac{\partial C'}{\partial z'}\right)_{z'=0} \end{aligned} \tag{4.24}$$

At length H units along the stretching sheet, the Sherwood number Sh is expressed as

$$Sh = \frac{Q_w}{C_W - C_\infty} \cdot \frac{H}{D_M} = -\left(\frac{\partial C'}{\partial z'}\right)_{z'=0} \tag{4.25}$$

The local surface heat flux is expressed as $q_w = -k_f \frac{\partial T}{\partial z}$ where k_f is the thermal conductivity of the saturated porous medium. Thus the local Nusselt number Nu may be expressed as

$$\begin{aligned} Nu &= \frac{q_w}{T_W - T_\infty} \cdot \frac{H}{k_f} \\ &= -\left(\frac{\partial T'}{\partial z'}\right)_{z'=0} \end{aligned} \tag{4.26}$$

4.3.1. The Least Squares Approximation Method

The method of the Least Squares Approximations discussed in Section 3.31 of Chapter 3. Shear is used in the computation of the Nusselt number, Sherwood number, and the respective local Skin-friction coefficients. The respective values have been computed at i = 3 and k = 400, that is, x = 0.15 and t = 0.401 respectively. The values of t, z, and U are shown in Table 4.1.

Table 4.1 : Values of t, z and U(z,t) for M = 1, Pr = 0.71, m = 0.5, N = 0.45, Q = 0.8, R = 0.2, Ec = 0.4, Sc = 0.78, Xi = 0.5, Sr = 1, Ro = 0.3, w_o = -0.5, Re = 50, Df = 0.03, Gr_θ = 5, Gr_c = 2.

t	0.399	0.400	0.401	0.402	0.403	0.404
z	0	0.03	0.06	0.09	0.12	0.15
U(z, t)	0.36538	0.42951	0.44124	0.44298	0.44328	0.44340

[Table continued]

t	0.407	0.408	0.409
z	1.75	2.00	2.25
U(z, t)	0.44349	0.44359	0.44368

The matrix for coefficients $a_1, b_1, c_1, d_1, e_1, f_1$ derived from the normal equations is

$$A = \begin{pmatrix} 10 & 1.08 & 3.627 & 0.1836 & 1.461741 & 0.43704 \\ 1.08 & 0.1836 & 0.43704 & 0.03499 & 0.17686 & 0.07442 \\ 3.627 & 0.43704 & 1.46174 & 0.07442 & 0.58913 & 0.17686 \\ 0.1836 & 0.03499 & 0.07442 & 0.00711 & 0.03017 & 0.01419 \\ 1.46174 & 0.17686 & 0.58913 & 0.03017 & 0.23745 & 0.07157 \\ 0.43704 & 0.07442 & 0.17686 & 0.01419 & 0.07157 & 0.03017 \end{pmatrix} \tag{4.27}$$

The resulting column matrix C is given is

$$C = \begin{pmatrix} 3.89653876 \\ 0.478395677 \\ 1.570665488 \\ 0.081410076 \\ 0.633148648 \\ 0.193593544 \end{pmatrix} \tag{4.28}$$

The column matrix of the constants $a_1, b_1, \cdots, f_1$ is given by matrix B shown below.

$$B = \begin{pmatrix} a_1 \\ b_1 \\ c_1 \\ d_1 \\ e_1 \\ f_1 \end{pmatrix} \tag{4.29}$$

The matrix equation $\mathbf{AB=C}$ is solved using Matlab command $B = A\backslash C$ so as to obtain the constants $a_1, b_1, \cdots, f_1$. These constants are used in evaluating the four bivariates for U, V, C and T. Thus

$U(z,t) = 0.7176z + 1.9392t - 2.7097335z^2 - 2.434t^2 + 0.3284zt.$

Similarly the bivariates for $V(z,t)$, $C(z,t)$ and $T(z,t)$ are:

$$V(z,t) = -0.1017z - 0.2544t + 0.2402z^2 + 0.4897t^2 + 0.0523zt.$$

$$C(z,t) = -0.5891z - 0.7827t + 3.7904z^2 + 3.0699t^2 - 1.5768zt.$$

$$T(z,t) = 0.6348z + 0.7132t + 0.5181z^2 + 0.8454t^2 - 1.7645zt.$$

The bivariates for U, V, C and T obtained above are used in obtaining the results in Table 4.2.

Table 4.2: Variation of Coefficients of friction, Sherwood and Nusselt numbers with various parameters.

M	Pr	m	N	Q	R	Ec	t	C_{fx}	C_{fy}	Sh	Nu
1.0	0.71	0.50	0.45	0.8	0.2	0.40	0.4	-0.03396	0.00323	1.21982	0.07100
2.0	0.71	0.50	0.45	0.8	0.2	0.40	0.4	-0.02207	0.00212	1.25290	0.16228
3.0	0.71	0.50	0.45	0.8	0.2	0.40	0.4	-0.01369	0.00206	1.25974	0.26508
1.0	0.89	0.50	0.45	0.8	0.2	0.40	0.4	-0.03398	0.00335	1.19728	0.09954
1.0	0.64	0.50	0.45	0.8	0.2	0.40	0.4	-0.03322	0.00329	1.23594	0.04404
1.0	0.71	1.00	0.45	0.8	0.2	0.40	0.4	-0.03735	0.00258	1.20272	0.03108
1.0	0.71	1.50	0.45	0.8	0.2	0.40	0.4	-0.03887	0.00144	1.19998	0.01416
1.0	0.71	0.50	0.10	0.8	0.2	0.40	0.4	-0.04531	0.00353	1.55106	-1.56942
1.0	0.71	0.50	1.00	0.8	0.2	0.40	0.4	-0.03169	0.00310	1.15656	0.31710
1.0	0.71	0.50	0.45	1.4	0.2	0.40	0.4	-0.03443	0.00316	1.21932	0.04528
1.0	0.71	0.50	0.45	2.0	0.2	0.40	0.4	-0.03490	0.00310	1.21882	0.03022
1.0	0.71	0.50	0.45	0.8	0.5	0.40	0.4	-0.03651	0.00371	1.23336	-0.22190
1.0	0.71	0.50	0.45	0.8	1.5	0.40	0.4	-0.04626	0.00382	1.27518	-1.41616
1.0	0.71	0.50	0.45	0.8	0.2	0.80	0.4	-0.03378	0.00328	1.21288	0.06726
1.0	0.71	0.50	0.45	0.8	0.2	1.00	0.4	-0.03360	0.00340	1.20916	0.06352
1.0	0.71	0.50	0.45	0.8	0.2	0.40	0.6	-0.03459	0.00313	1.21526	0.04784
1.0	0.71	0.50	0.45	0.8	0.2	0.40	0.8	-0.03472	0.00247	1.21262	0.04078

4.3.2. Discussion of the results

From Table 4.2 following observations are noted:

1. When $Q > 0$, increase in the Magnetic parameter M leads to a decrease in the magnitude of the local skin-friction coefficients C_{fx} and C_{fy} due to the primary and the secondary velocity profiles respectively. The decreasing frictional drag is due to increase in the Lorentz force that decreases the primary velocity of the fluid. Decrease in C_{fy} is due to decreasing secondary velocity with increasing M. Increase in M leads to an increase in the Sherwood number Sh and in Nusselt number Nu respectively. Increase in M leads to increase in the concentration gradients hence the observed increase in the value of Sh. Increase in the value of M results into a lower rate of transportation of the species in the concentration boundary layer. Thermal boundary layer thickness decreases with increase in M leading to the observed increase in the Nusselt number.
2. When $Q > 0$ increase in the Prandtl number Pr leads to an increase in the magnitude of C_{fx} and C_{fy} respectively; but to a decrease in Sh and Nu respectively. Increase in Pr leads to higher velocities and hence the observed increase in the values C_{fx} and C_{fy} respectively. Fluids which are good conductors of heat have a relatively small value of Prandtl number. Increase Pr decreases the thickness of thermal boundary layer leading to a higher rate of heat transfer. Decrease in Sherwood number is due to an increased rate of transportation of the species toward the surface of the stretching sheet due to increased velocity of the fluid.
3. When $Q > 0$ increase in the Hall parameter m leads to an increase in the magnitude of C_{fx}, Sh and Nu respectively; but to a decrease in C_{fy}. Increase in m leads to higher primary velocity thereby increasing the shear stressC_{fx}. Decrease in the magnitude of

the secondary velocity profiles lead to a decrease in C_{fy}. Increase in m increases the Joule heating since the conductivity of the fluid decreases, leading to a thicker thermal boundary layer. This leads to a reduced rate of heat transfer.

4. Increase in the Radiation parameter N leads to an increase in the magnitudes of C_{fx}, C_{fy}, and Nu respectively; but to a decrease in Sh. Increase in N leads to an increase in the rate of species transportation. This result qualitatively agrees with expectations, since the effect of radiation is to decrease the rate of energy transport to the fluid, thereby decreasing the temperature of the fluid. Increase in Radiation parameter leads to a thinner thermal boundary layer, leading to an increase in the rate of heat transfer. Increase in N enhances convection currents on the surface of the sheet, leading to increase in C_{fx} and C_{fy} respectively.
5. Increase in the heat source parameter Q leads to an increase in the magnitudes of C_{fx}, C_{fy} respectively; but to a decrease in the Sherwood number Sh and Nusselt number Nu respectively. Increase in Q enhances convection currents on the surface of the sheet, leading to increase in C_{fx} and C_{fy} respectively. Increase in Q leads to a thicker thermal boundary layer, leading to lower temperature gradients leading to a decrease in Nu.
6. Increase in the Joule heating parameter R leads to an increase in C_{fx}, C_{fy}, Sh and Nu respectively. The results qualitatively agree with what is expected since the effect of Joule heating is to decrease the rate of energy transport to the fluid, thereby decreasing the temperature of the fluid. Increase in the velocity of the fluid leads to an increase in the values of C_{fx} and C_{fy}, that in turn lead to a decrease in the species concentration.
7. Increase in the Eckert number Ec leads to an increase in C_{fx}, C_{fy} but to a decrease in Nu and Sh respectively. Increasing the velocity of the fluid leads to an increase in the species concentration. A positive Eckert number implies cooling of the stretching sheet

thereby enhancing convection currents leading to increased velocity and the temperature of the fluid respectively. The resulting thicker thermal boundary layer leads to a reduced rate of heat transfer.

8. Increase in time t leads to a decrease in the magnitude of C_{fx}, C_{fy}, Nu and Sh respectively. This physically means that shear stresses C_{fx} and C_{fy}, Nu and Sh decrease with time. This is expected since the velocity, temperature and concentration of the fluid decrease gradually with time, finally equalizing with their respective freestream values.

4.4. Conclusion

In order to assess the validity of the presented results, the results obtained by the present method are compared with those of Ram (1991). Ram analyzed the effects of Hall current on hydromagnetic free convective flow past an infinite porous plate in a rotating fluid with mass transfer through a porous medium when a magnetic field is imposed in a plane that makes various angles with the normal to the plate. The plate used in Ram's work is not stretching. He also considered ion-slip currents. In order to validate the current results, the boundary conditions one of the plates in Ram's work is changed so as to reflect stretching, magnetic field is imposed at an angle of 90^o to the flow and ion-slip currents are ignored. Both this work and Ram's work have observed that increase in Hall parameter m leads to an increase in the shear stress C_{fx}; but such an increase leads to a decrease in both the shear stress C_{fy} and the rate of heat transfer respectively. This study has observed that increase in Hall parameter leads to an increase in the rate of mass transfer; though Ram did not investigate the effect of m on the rate of mass transfer. It can be seen that the present results agree very well with those previously published by Ram. This has established confidence in the numerical results and observations presented in this chapter.

CHAPTER FIVE

5.0 CONCLUSIONS AND RECOMMENDATIONS

In this chapter conclusions from the results obtained in this work are presented. The recommendations for further future are also discussed.

5.1 Conclusion

The analysis of various parameters on unsteady MHD laminar boundary layer flow of an incompressible, electrically conducting, and viscous Newtonian fluid past a stretching electrically non-conducting sheet embedded in porous media in a rotating system with heat and mass transfer has been carried out. The direction of the applied magnetic field is considered to be normal to the direction of the flow. The effects of free convection currents on the flow have been investigated by varying the values of the local temperature Grashof number Gr_{θ}. The PDE's governing the flow are highly non-linear and coupled, and the equations have been solved by using the finite difference method as outlined in Section 3.21 of Chapter 3. In the FD method the spatial mesh sizes used in the computations are reduced and there is no significant difference in the results obtained. Thus the scheme used in the computations is stable. Chapter 3 and Chapter 4 are each concluded by determining the approximate local rate of heat transfer and mass transfer, and the coefficients of friction due to the primary and the secondary flow fields respectively.

The results obtained in Chapter 3 show that the rates of heat transfer and mass transfer on the stretching sheet embedded in a porous medium in a rotating system is influenced

by the Magnetic field parameter, Soret number, mass Grashof number, thermal Grashof number, Injection parameter, Rotational parameter, Permeability parameter, Dufour number, Reynold's number, Radiation parameter, the Eckert number, Schmidt number and time. For instance the current study has shown that imposing a transverse magnetic field to a flow slows down the velocity of the fluid, decreases the temperature of the fluid, but increases the concentration of the fluid. Increasing the value of the Soret number increases the velocity, concentration and temperature of the fluid. Increasing the Soret number causes a cross-over in the concentration profiles at some distance away from the fixed end of the stretching sheet. However increasing the value of the Dufour number decreases the velocity and temperature of the fluid respectively; but to leads to an increase in the concentration profiles. The results obtained in this study regarding thermal and mass diffusion effects can be applied in the industry, for instance, in the separation of isotopes contained in a mixture of very light molecular-weight gases (for instance, hydrogen and helium) and medium molecular-weight gases (for instance, nitrogen and air). This study has also shown that increasing the thermal Grashof number causes an increase in the velocity profiles; while a decrease in the temperature and concentration profiles is observed. Increasing the value of local mass Grashof number causes an increase in the velocity profiles; but a decrease in the temperature and concentration profiles respectively. Increasing the value of the Schmidt number causes a decrease in the velocity profiles; but an increase in the temperature profiles. The effect of heat source has also been investigated and the results on the same have been discussed. Other important findings of Chapter 3 are:

1. Velocity of the fluid can be controlled by introducing a porous medium in a rotating system.
2. Both thermal and concentration boundary layers thickness decrease with increase in time; but the velocity boundary layer increases with time.
3. The velocity, temperature and concentration of a fluid can be controlled by varying the Reynold's number.
4. Radiation can be used to control the velocity, concentration and thermal boundary layers of flow in porous media quite effectively.
5. Introducing injection/suction can be used to control the boundary layer growth, the shear stresses and rates of heat transfer and mass transfer.
6. Varying time can be used as a means of controlling the velocity, concentration and temperature of a fluid flowing in porous media over a stretching surface.
7. Rotational can be used to control the magnitude of shear stresses and the boundary layer formation over a stretching sheet.
8. Introducing porous media in a flow domain can be used to control the velocity, concentration and temperature of the fluid.

The study of MHD flows with Hall and ion-slip currents has important applications in engineering problems such as MHD generators, Hall accelerators and flight magnetohydrodynamics. Chapter 4 has included the effects of Hall currents to the flow problem encountered in Chapter 3. The problem of heat source/sink is important for it has applications in areas such as effective cooling of electronic equipment, air

circulation in buildings and cooling of combustion engines. Various flow parameters have been investigated by subjecting the flow to a heat source, and then to a heat sink. The parameters investigated in this chapter include the Magnetic field parameter, Hall parameter, Heat source parameter, Prandtl number, Eckert number, Radiation parameter, Injection parameter, Joule heating parameter and time. Chapter 4 has been concluded by investigating the coefficients of shear stress, rate of heat transfer and rate mass transfer. The study in Chapter 4 has shown that increasing the strength of a magnetic field decreases the frictional drag due to velocity profiles, but the same leads to an increase in the rate of heat transfer and the rate mass transfer respectively. Other important findings of Chapter 4 are:

1. Varying the Prandtl number can be used to control the fluid's flow velocity, temperature, concentration, sheer stress, and the rates of heat and mass transfer respectively.
2. The Hall effects can be utilized in controlling the fluid's velocity, concentration, temperature and sheer stress and the rates of heat and mass transfer respectively.
3. Varying the value of the Heat source parameter can be used to control the shear stresses, rate of heat transfer and rate of mass transfer respectively.
4. Varying time can used as a measure of controlling the velocity, concentration and temperature of a fluid. Radiation can be use to control the shear stress, rate of heat transfer and mass transfer on the surface of a stretching sheet.

5.2 Recommendations

This work has considered the unsteady laminar boundary layer MHD flow of an incompressible, viscous, and electrically conducting Newtonian fluid over a stretching sheet in a fluid-saturated porous medium in a rotating system. The Hall current effects have also been taken into consideration. The present work can provide a basis for further research by including the following considerations:

1. Flow over a surface stretching with a non-linear velocity.
2. Flow that involves non-Newtonian fluids.
3. Flow over a contracting surface.
4. Three dimensional flows.
5. Flow of a compressible fluid.
6. Flow subjected to a variable magnetic field.
7. Flow with chemical reaction.
8. Flow with Hall and ion-slip currents.
9. Flow with variable suction/injection.
10. Turbulent flow over a stretching surface.
11. Flow over a stretching surface with variable viscosity and thermal conductivity.
12. Variation of the method of solving the coupled non-linear equations.

CHAPTER 6

PAPERS PUBLISHED AND ACCEPTED FOR PUBLICATION

1. Kinyanjui M., Giterere, K., Theuri, D., "Hydromagnetic Flow Past an Impulsively Started Flat Plate in a Transverse Inhomogeneous Magnetic Field." Submitted to Far East Journal of Applied Mathematics for publication.
2. Giterere, K., Kinyanjui, M., and Uppal, S. M., "MHD Flow in Porous Media over A Stretching Surface in Rotating System with Heat and Mass Transfer," *International Electronic Journal of Pure and Applied Mathematics – IeJPAM, ISSN 1314-0744*, March 2011, to appear.
3. Kinyanjui, M., Giterere, K., and Uppal, S. M., "MHD Flow in Porous Media over A Stretching Surface in Rotating System with Hall Currents, Heat and Mass Transfer," *International Electronic Journal of Pure and Applied Mathematics – IeJPAM, ISSN 1314-0744*, March 2011, to appear.

REFERENCES

Andersson, H. I., (1992). "MHD flow of a visco-elastic fluid past a stretching surface," *Acta Mechanica*, **95**, 227.

Aboeldahab, E. M. and El Aziz, (2005). "Hydrodymagnetic three-dimensional flow over a stretching surface with heat and mass transfer," *Heat and Mass Transfer*, **41**, (8): 734-743.

Aboeldahab, E. M., (2001). "'Convective heat transfer in an electrically conducting fluid at a stretching surface by the presence of radiation," *Canadian Journal of Physics*, **79**: 929.

Aboeldahab, E. M. and Salem, A. M., (2004). "Hall effect on MHD free convection flow of a non-Newtonian power low fluid at a stretching surface," *International Communications in Heat and Mass Transfer*, **31** (3): 343.

Ahmed, N., Kalita, H. and Barua, D. P., (2010). "Unsteady MHD free convective flow past a vertical porous plate immersed in a porous medium with Hall current, thermal diffusion and heat source," *International Journal of Engineering, Science and Technology*, **2**, (6): 59-74.

Antia, M., (1991). "*Numerical Methods for Scientists and Engineers*," Tata McGraw-Hill: New Delhi.

Bhag G. and Huseyin H., (2005). "*Electromagnetic Field Theory Fundamentals*," Cambridge University Press, 2nd ed., 287-314.

Bathaiah, D. and Venkataramana, S., (1986). "Buoyancy Effect on MHD Flow Past a Permeable Bed," *Dcf Science Journal*, **36**, (4, October): 395-408.

Beard, D. and Wallters, K., (1964). "*Elastico-viscous boundary-layer flows, Part I. Two-dimensional flow near a stagnation point*, *Mathematical Proceedings of the Cambridge Philosophical Society*, **60** , 667-674.

Bejan, A., (1984). "*Convective Heat Transfer*," Wiley, New York, 17-21 and 301-303.

Brinkman, H. C., (1947). "A calculation of the viscous force exerted by a flowing fluid on a dense swarm of particle," Applied Sciences Research, **A1**, 27-34.

Burden R. L. and Faires, J. D., (1997). "*Numerical Analysis*," Brooks/Cole Publishing Company, New York, sixth edition.

Chaturvedi, N., (2003). "Finite Difference Study of MHD Stokes Problem for a Vertical Infinite Plate in a Dissipative Heat Generating Fluid with Hall and Ionslip Currents," *Botswana Journal of Technology*, **12**, (2).

Chen, C. K. and Char, C. K., (1988). "Heat transfer on a continuous stretching surface with suction or blowing," *Journal of Mathematical Analysis and Applications*, **135**, 544.

Crane, L. J., (1970). "Flow Past a Stretching Plane," *Journal of Applied Mathematics and Physics (ZAMP)*, **21**, 645.

Danberg, J. E. and Fansler, K. S., (1976). "A nonsimilar moving-wall boundary-layer problem," Quarterly Journal of Mechanics and Applied Mathematics **34**, 305-309.

Dawood, A. S. and Hmood, B. O., (2006). "Steady free convection through Porous medium Enclosing a Rectangular Isothermal body," *Al- Rafidain Engineering*, **14**, (1).

Dutta, B. K., Roy, P. and Gupta, A. S., (1985). "Temperature field in flow over a stretching sheet with uniform heat flux," *International Communications in Heat and Mass Transfer*, **12**: pp.89-94.

Emmanuel Osalusi, (2007). "Effects of Thermal Radiation on MHD and Slip Flow over a Porous Rotating Disk with Variable Properties," *Romanian Journal of Physics*, **52**, (3-4): 217-229.

Erickson, L. E., L. T. Fan and Fox, V. G., (1966). "Heat and mass transfer on a moving continuous flat plate with suction and injection," *Industrial and Engineering Chemistry Fundamentals*, **5**, 19-25.

Forchheimer, P. H., (1901). "Wasserbevegung durch Boden" Z. Ver. Deutsh. Ing., **45**.

Fox, V. G., Erickson, L. E. and Fan, L. T., (1966). "Heat and mass transfer on a moving and continuous flat plate with suction or injection," *Industrial and Engineering Chemistry Fundamentals*, **5**, (9).

Ferdows, M., Koji Kaino and Chien-Hsin Chen, (2010). "Dufour, Soret and Viscous Dissipation Effects on Heat and Mass Transfer in Porous Media with High Porosities," *International Journal of Applied Engineering Research, ISSN 0973-4562*, **5**, (3): 477-484.

Frank, P.I. and David, P. D., (1996). "*Fundamentals of Heat and Mass Transfer*," School of Mechanical Engineering, **4**, 306.

Griffin, J. F. and Thorne, J. L., (1967). "Thermal boundary layer growth on continuous moving belts," *American International Chemical Engineering Journal*, **13**(6),

1210-1211.

Gupta, P. S. and Gupta, A. S., (1977). "Heat and Mass transfer on a stretching sheet with suction or blowing," *Canadian Journal of Chemical Engineering*, **55**, 744.

Hayat, T., Abbas, Z., Javed, T. and Sajid, M., (2009). "Three-dimensional rotating flow induced by a shrinking sheet for suction," *Chaos, Solitons and Fractals*, **39**, 1615–1626.

Herrero, J., Humphrey, J. A. C. and Gilralt F., (1994). "Comparative analysis of coupled flow and heat transfer between co-rotating disks in rotating and fixed cylindrical enclosures," *ASME Journal of Heat Transfer*, **300**), 111-121.

Hinze, J. O., (1959). "*Turbulence: An Introduction to Its Mechanism and Theory*," McGraw-Hill Book Company, Inc.

Hoffman Joe D., (1992). "*Numerical Methods for Engineers and Scientists*," McGraw-Hill, New York.

Incropera, F. P. and DeWitt, D. P., (2002). "*Fundamentals of Heat and Mass Transfer*," fifth ed., John Wiley Sons, New York, 465-531.

Ishak, A., R. Nazar and Pop, I., (2008). "Hydromagnetic flow and heat transfer adjacent to a stretching vertical sheet," *Heat and Mass Transfer*, **44**,(8), 921-927.

Ishak, A. and Nazar, R., (2006). "Unsteady mixed convection boundary layer flow due to a stretching vertical surface," *The Arabian Journal for Science and Engineering*, **31**, (2B).

Jagadeeswara, K., Vijaya, S. and Syam, M., (1987). "MHD Free Convective Flow Past a Hot Vertical Porous Plate," *Defence Science Journal*, **37**, (3): 327-332.

Joseph, D.D., Nield, D. A. and Papanicolaou, G., (1982). "Nonlinear Equation Governing Flow in a Saturated Porous Media," *Water Resources Research*, **18**, 1049-1052.

Kinyanjui, M., Chaturvedi, N. and Uppal, S. M., (1998). "MHD Stokes problem for a vertical infinite plate in a dissipative rotating fluid with Hall current," *Energy conversion and Management*, **39**, 541-548.

Kinyanjui, M., Kwanza, J. K. and Uppal, S.M., (2001). "MHD free convection heat and mass transfer of a heat generating fluid past an impulsively started infinite vertical porous plate with Hall current and radiation absorption," *Energy Conversion and Managemen*t, **42**, 917-931.

Kumari, M. and Nath, G., (2005). "Transient rotating flow over a moving surface with a magnetic field," *International Journal of Heat and Mass Transfer*, **48**, (14): 2878-2885.

Kumari, M., Grosan, T. and Pop I., (2006). "Rotating flow of power law fluids over a rotating surface," *Technische Mechanik*, **26**, 11–19.

Liao, S. J. and Pop, I., (2004). "Explicit analytic solution for similarity boundary layer equations," *International Journal of Heat and Mass Transfer*, **47**, 75-85.

Lighthill, M., (1954). "The response of laminar skin friction and heat transfer to fluctuations in the stream velocity," *Proceedings of the Royal Society A: Mathematical, Physical and Engineering Sciences*, **224**,(1156): 1-23.

Mahapatra, T. R. and Gupta, A. S., (2004). "Stagnation-point flow of a viscoelastic fluid towards a stretching surface," *International Journal of Non-Linear Mechanics*, **39**, 811–820.

Magyari, E. and Keller B., (1999). "Heat and mass transfer in the boundary layers on an exponentially stretching continuous surface," *Journal of Physics. D: Applied Physics*, **32**, 577-586.

Magyari, E. and Keller, B., (2000). "Exact solutions for self-similar boundary-layer flows induced by permeable stretching surfaces", *European Journal of Mechanics. B-Fluids*, **19**, 109-122.

Millsaps, K. and Pohlhausen, K., (1952). "Heat Transfer by Laminar Flow from a Rotating Disk," *Journal of the Aeronautical Sciences*, **19**, 120-126.

Nakayama Akira, (1995). "*PC-Aided numerical heat transfer and convective flow*," CRC Press Inc., 103-105.

Nazar, R., Amin, N. and Pop, I., (2004). "Unsteady boundary layer flow due to a stretching surface in a rotating fluid," *Mechanics Research Communications*, **31**, 121-128.

Palani, G. and Srikanth, U., (2009). "MHD Flow past a Semi-Infinite Vertical Plate with Mass Transfer," **Nonlinear Analysis: Modelling and Control**, **14**, (3): 345–356.

Persson, A., (1998). "How do we Understand the Coriolis Force?", *Bulletin of the American Meteorological Society*, **79**, 1373-1385.

Ram, P.C., (1991). "Hall Effects on Hydromagnetic Convective Flow in a Rotating Fluid Through Porous Medium," *Journal of Engineering Science*, **5**, (1): 43-53.

Raptis A. A. and Perdikis, C. P., (1985). "Oscillatory flow through a porous medium by the presence of free convective flow," *International Journal of Engineering Science*, **23**, 51.

Raptis, A., Tzivanidis, G. and Kafousias, N., (1981). "Free convection and mass transfer flow through a porous medium bounded by an infinite vertical limiting surface constant suction," Lett. Heat Mass Transfer **8**, 417.

Rohsenow, W. M., Hartnett J. P. and Cho, Y. I., (1998). "*Handbook of Heat Transfer*," 3rd ed., McGraw-Hill, New York.

Sakiadis, B.C., (1961a). "Boundary layer behaviour on continuous solid surfaces: I boundary layer equations for two dimensional and axisymmetric flow," *American International Chemical Engineering Journal*, **7**, 26-28.

Sakiadis, B.C., (1961b). "Boundary layer behaviour on continuous solid surfaces: II boundary layer on a continuous flat surface," *American International Chemical Engineering Journal*,**7**, 221–225.

Sam Lawrence, P. and Nageswara Rao, B., (1995). "The non uniqueness of the MHD flow of a visco-elastic fluid past a stretching sheet," *Acta Mechanica*, **112**, 223.

Sattar, A. M. and Maleque, A. K., (2005). "Steady laminar convective flow with variable properties due to a porous rotating disk," *Journal of Heat Transfer*, **127**, 1406-1409.

Shateyi, S., (2008). "Thermal radiation and buoyancy effects on heat and mass transfer over a semi-infinite stretching surface with suction and blowing,", *Journal of Applied Mathematics*, 12.

Singh, A. K., (2003). "Numerical solution of hydromagnetic unsteady free convection flow past an infinite porous plate," *Indian Journal of Pure and Applied Physics*, **41**, 167-70.

Soundalgekar, V. and Patil, V., (1982). "Unsteady mass transfer flow past a porous plate," *Indian Journal of Pure and Applied Mathematics*, **13**, 399.

Sparrow, E. M. and Gregg, J. L., (1960). "Mass Transfer, Flow, and Heat Transfer about a Rotating Disk", *ASME Journal of Heat Transfer*, 294-302.

Stuart, J., (1955). "A solution of the Navier-Stokes and energy equations illustrating the response of skin friction and temperature of an infinite plate thermometer to fluctuations in the stream velocity," *Proceedings of the Royal Society A: Mathematical, Physical and Engineering Sciences*, **231**, 116-130.

Subhas, A. M., Joshi A. and Sonth R. M., (2001). "Heat Transfer in MHD Visco-elastic Fluid Flow over a Stretching Surface," *Journal of Applied Mathematics and Mechanics*, **81**, (10): 691-698.

Tamanna S., Sumon S., Mohammad M. R. and Goutam S., (2009). "Heat Transfer in a Porous Medium in a Porous Medium over a Stretching Surface with Internal Heat Generation and Suction or Injection in the presence of Radiation," *Journal of Mechanical Engineering*, **ME 40**, (1) : 22-28.

Tania, S. K. and Samad, M. A., (2010). "Effects of Radiation, Heat Generation and Viscous Dissipation on MHD Free Convection Flow along a Stretching Sheet," *Research Journal of Applied Sciences, Engineering and Technology*, **2**,(4): 368-377.

Wu, Q., Weinbaum, S. and Amdreopoulos, Y.,(2005). "Stagnation Point Flows in a Porous Medium," *Chemical Engineering Science*, **60**, 123-134.

Yamamoto, K. and Iwamura, N., (1976). "Flow with convective acceleration through a porous medium," *Journal of Engineering Mathematics*, **10**, 41-54.

PROGRAM CODES

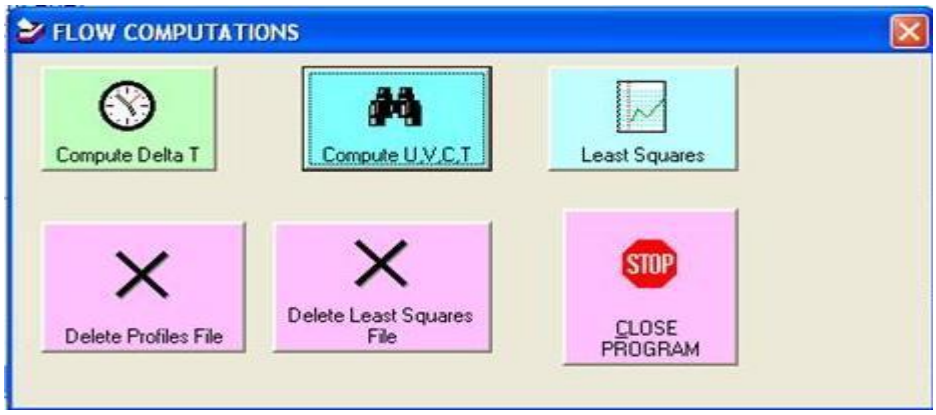

Figure 59 : The GUI for the Program.

CODES FOR CHAPTER THREE

```
Private Sub cmdCompute_Click()
Dim Choice As Integer
Choice = CInt(InputBox("Enter 1 for Steady " & vbCrLf & "2 for Unsteady", "User", 2))
If Choice = 2 Then
   Call ComputeUnsteadyValues
Else
      Call ComputeSteadyValues
End If
MsgBox "AM THROUGH!!!"
End Sub

Private Sub cmdDelete_Click()
On Error GoTo kan
Kill "C:\Documents and Settings\kangethe\Desktop\Numerical experiments\Thesis
Prog\LaxConc.txt"
kan:
Exit Sub
```

```
End Sub

Private Sub cmdEnd_Click()
Dim Response As Integer
Response = CInt(MsgBox("Are you sure you want to close?", vbYesNo + vbCritical))
If Response = vbYes Then
   End
Else
   Exit Sub
End If
End Sub

Private Sub cmdLeastSquares_Click()
Dim U(0 To 43, 0 To 43, 0 To 1501) As Double, V(0 To 43, 0 To 43, 0 To 1501) As
Double, C(0 To 43, 0 To 43, 0 To 1501) As Double, T(0 To 43, 0 To 43, 0 To 1501) As
Double, Sc As Single, Sr As Single, Ma As Single
Dim Re As Single, Df As Single, Ec As Single, Gr_theta As Single, Gr_c As Single, wo
As Single, Ro As Single, Xi As Single, Str As Single
Dim Pr As Single, R As Single, Ni As Single
Dim ITMAX As Double, M As Integer, N As Integer, K As Integer
Dim delX As Double, delZ As Double, delT As Double, I As Integer, J As Integer
Dim ITCOUNT As Integer
Dim FILENUM As Byte
M = 41:   N = 41 'Grid
Re = 3: Sc = 0.6: Sr = 1: Ma = 0.5: Re = 50: Df = 0.03: Ec = 0.5: R = 0.2: Ni = 0.5:
Gr_theta = 5: Gr_c = 2: wo = 0.5: Pr = 0.71: Ro = 0.3: Xi = 0.5: Str = 1     'Constants
Sc = 0.78: Sr = 0.4: Ma = 1: Xi = 1.5: Ro = 0.5: Ni = 0.5: wo = 0.5: Ec = 0.5: Re = 50:
Df = 0.03: R = 0.2: Gr_theta = 5: Gr_c = 10: Pr = 0.71: Str = 1
delT = 0.001
```

```
'*************** the following ensures aspect ratio h=H/L=0.5***************
delX = 0.05
delZ = 0.25
'*********************************************************
ITMAX = 710
FILENUM = FreeFile()
Open "C:\Documents and Settings\kangethe\Desktop\Numerical experiments\Thesis
Prog\LeastSquares.txt" For Append As FILENUM
Rem Initial condition
For I = 0 To M
        For J = 0 To N
                For K = 0 To ITMAX
                U(I, J, 0) = 0: V(I, J, 0) = 0: C(I, J, 0) = 0: T(I, J, 0) = 0
                Next
        Next
Next
 Rem  Boundary conditions
For I = 1 To M
        For K = 1 To ITMAX
          U(I, 0, K) = I * Str * delX: V(I, 0, K) = 0#: C(I, 0, K) = 1: T(I, 0, K) = 1#
'stretching wall
          U(I, N, K) = 0: V(I, N, K) = 0#: C(I, N, K) = 0: T(I, N, K) = 0# 'impermeable
plate
        Next
Next
For J = 0 To N
        For K = 1 To ITMAX
          'inlet variables
          U(0, J, K) = 1#:    V(0, J, K) = 0#:    C(0, J, K) = 1#:    T(0, J, K) = 1#
```

```
        Next
Next
'Solving for velocities

For I = 1 To M - 1
   For J = 1 To N - 1
      For K = 1 To ITMAX - 1
       'calculate u
      U(I, J, K + 1) = (U(I, J, K) - (delT / (2 * delX)) * U(I, J, K) * (-U(I - 1, J, K + 1) +
      U(I, J, K) - U(I -1, J, K)) + (delT * wo / (2 * delZ)) * (-U(I, J - 1, K + 1) + U(I, J, K)
      - U(I, J - 1, K)) + Ro * delT *  (V(I, J, K + 1) + V(I, J, K))   + (delT / (2 * Re * delX
      * delX)) * (U(I + 1, J, K + 1) + U(I - 1, J, K )+  U(I + 1, J, K) - 2 * U(I, J, K) + U(I -
      1, J, K)) + (delT / (2 * Re * delZ * delZ)) * (U(I, J + 1, K + 1) + U(I, J - 1, K + 1) +
      U(I, J + 1, K) - 2 * U(I, J, K) + U(I, J - 1, K)) - (delT * Xi / 2) * U(I, J, K) - (delT *
      Ma / 2) * U(I, J, K) + (delT * Gr_theta / 2) * (T(I, J, K + 1) + T(I, J, K)) + (delT * _
      Gr_c / 2) * (C(I, J, K + 1) + C(I, J, K))) / (1 + U(I, J, K) * delT / (2 * delX) - (wo *
      delT) / (2 *    delZ) + delT / (Re * delX * delX) + delT / (Re * delZ * delZ) + delT *
      Xi / 2 + Ma * delT / 2)

       'calculate v
      V(I, J, K + 1) = (V(I, J, K) - (delT / (2 * delX)) * U(I, J, K) * (-V(I - 1, J, K + 1) +
      V(I, J, K) - V(I - 1,  J, K)) + (delT * wo / (2 * delZ)) * (-V(I, J - 1, K + 1) + _
      V(I, J, K) - V(I, J - 1, K)) - Ro * delT * (U(I,  J, K + 1) + U(I, J, K)) + _
      (delT / (2 * Re * delX * delX)) * (V(I + 1, J, K + 1) + V(I - 1, J, K + 1) + V(I + 1, J,
      K) - 2 * V(I, J, K) + V(I - 1, J, K)) + (delT / (2 * Re * delZ * delZ)) * (V(I, J + 1, K
      + 1) + V(I,   J - 1, K + 1) + V(I, J + 1, K) - 2 * V(I, J, K) + V(I, J - 1, K)) -_
      (delT * Xi / 2) * V(I, J, K) - (delT * Ma / 2) * V(I, J, K)) /_
     (1 + U(I, J, K) * delT / (2 * delX) - (wo * delT) / (2 * delZ) +_
      delT / (Re * delX   * delX) + delT / (Re * delZ * delZ) + _ delT * Xi / 2 +_
```

```
    Ma * delT / 2)
 'Solving for temperatures C
 C(I, J, K + 1) = (C(I, J, K) - (delT / (2 * delX)) * U(I, J, K) * (-C(I - 1, J, K + 1) + C(I, J,
K) + C(I - 1, J, K)) + (delT * wo / (2 * delZ)) * (-C(I, J - 1, K + 1) + C(I, J, K) - _
C(I, J - 1, K)) + ((delT) / (2 * Sc * Re * delX * delX)) * (C(I + 1, J, K + 1) +_
 C(I - 1, J, K + 1) + C(I + 1, J, K) - 2 * C(I, J, K) + C(I - 1, J, K))  _
  + ((delT) / (2 * Sc * Re * delZ * delZ)) * (C(I, J + 1, K + 1) + C(I, J - 1, K + 1) + _
C(I, J + 1, K) - 2 * C(I, J, K) + C(I, J - 1, K)) + ((delT * Sr) / (2 * Re * delX * delX)) *
(T(I + 1, J, K + 1) - 2 * T(I, J, K + 1) + T(I - 1, J, K + 1) + T(I + 1, J, K) - 2 * T(I, J, K) +
T(I - 1, J, K)) + ((delT * Sr) / (2 * Re * delZ * delZ)) * (T(I, J + 1, K + 1) - 2 * T(I, J, K
+ 1) + T(I, J - 1, K + 1) + T(I, J + 1, K) - 2 * T(I, J, K) + T(I, J - 1, K))) / _
(1 + U(I, J, K) * delT / (2 * delX) - (wo * delT) / (2 * delZ) + delT / (Re * Sc * delX *
delX) + delT / (Re * Sc * delZ * delZ))

  'Solving for temperatures T
 T(I, J, K + 1) = (T(I, J, K) - (delT / (2 * delX)) * U(I, J, K) * (-T(I - 1, J, K + 1) + T(I, J,
K) - T(I - 1, J, K)) + (delT * wo / (2 * delZ)) * (-T(I, J - 1, K + 1) + T(I, J, K) - T(I, J - 1,
K)) + ((Df * delT) / (2 * Re * delX * delX)) * (C(I + 1, J, K + 1) - 2 * C(I, J, K + 1) +
C(I - 1, J, K + 1) + C(I + 1, J, K) - 2 * C(I, J, K) + C(I - 1, J, K)) _
        + ((Df * delT) / (2 * Re * delZ * delZ)) * (C(I, J + 1, K + 1) - 2 * C(I, J, K + 1) +
C(I, J - 1, K + 1) + C(I, J + 1, K) - 2 * C(I, J, K) + C(I, J - 1, K)) + (delT / (2 * Pr * Re *
delX * delX)) * (T(I + 1, J, K + 1) + T(I - 1, J, K + 1) + T(I + 1, J, K) - 2 * T(I, J, K) +
T(I - 1, J, K)) + (delT / (2 * Pr * Re * delZ * delZ)) * (T(I, J + 1, K + 1) + T(I, J - 1, K +
1) + T(I, J + 1, K) - 2 * T(I, J, K) + T(I, J - 1, K)) + (delT * R * Re / 4) * (U(I, J, K) ^ 2 _
        + V(I, J, K) ^ 2) - ((4 * delT) / (3 * Ni * Pr * Re * 2 * delZ * delZ)) * (T(I, J + 1, K
+ 1) + T(I, J - 1, K + 1) + T(I, J + 1, K) - 2 * T(I, J, K) + T(I, J - 1, K)) + (Ec * delT / (Re
* 4 * delX * delX)) * (U(I, J, K + 1) - U(I - 1, J, K + 1) + U(I, J, K) - U(I - 1, J, K)) ^ 2 +
(Ec * delT / (Re * 4 * delZ * delZ)) * (V(I, J, K + 1) - V(I, J - 1, K + 1) + V(I, J, K) -
V(I, J - 1, K)) ^ 2) / (1 + U(I, J, K) * delT / (2 * delX) - (wo * delT) / (2 * delZ) + delT /
```

```
(Re * Pr * delX * delX) + delT / (Re * Pr * delZ * delZ) - 4 * delT / (3 * Ni * Pr * Re *
delZ * delZ))
Next
Next
Next
I = 3  'position along the plate
Print #FILENUM, U(I, 1, 401); U(I, 2, 402); U(I, 3, 403); U(I, 4, 404); U(I, 5, 405);_
U(I, 6, 406); U(I, 7, 407); U(I, 8, 408); U(I, 9, 409)
Print #FILENUM, V(I, 1, 401); V(I, 2, 402); V(I, 3, 403); V(I, 4, 404); V(I, 5, 405);_
V(I, 6, 406); V(I, 7, 407); V(I, 8, 408); V(I, 9, 409)
Print #FILENUM, C(I, 1, 401); C(I, 2, 402); C(I, 3, 403); C(I, 4, 404); C(I, 5, 405); _
C(I, 6, 406); C(I, 7, 407); C(I, 8, 408); C(I, 9, 409)
Print #FILENUM, T(I, 1, 401); T(I, 2, 402); T(I, 3, 403); T(I, 4, 404); T(I, 5, 405);_
T(I, 6, 406); T(I, 7, 407); T(I, 8, 408); T(I, 9, 409)
Close #FILENUM
MsgBox "AM THROUGH!!!"
End Sub
```

CODES FOR CHAPTER FOUR

```
REM**********CODE FOR GENERAL DECLARATIONS SECTION
const M = 41
Const N = 41
Dim Re As Single, Df As Single, Ec As Single, Gr_theta As Single, Gr_c As Single, wo
As Single, Ro As Single, Xi As Single, Str As Single
Dim Pr As Single, R As Single, Ni As Single, Q As Single, mi As Single
Dim ITMAX As Double, K As Integer
```

```
Dim U(0 To 43, 0 To 43, 0 To 1501) As Double, V(0 To 43, 0 To 43, 0 To 1501) As
Double, C(0 To 43, 0 To 43, 0 To 1501) As Double, T(0 To 43, 0 To 43, 0 To 1501) As
Double, Sc As Single, Sr As Single, Ma As Single
Dim delZ As Double, delX As Double, delT As Double, I As Integer, J As Integer
Dim ITCOUNT As Integer
Dim UTep As Single, CTep As Single, VTep As Single, TTep As Single, UTepCon As
Single  'temporary storage
Dim FILENUM As Byte

'REM c  is the stretching parameter

Public Sub MainBody()
'M = 41:   N = 41 'Grid
'Sc = 0.6: Sr = 1: Ma = 0.5: Re = 3: Df = 0.03: Ec = 0.5: R = 0.2: Ni = 0.5: Gr_theta = 5:
Gr_c = 2: wo = 0.5: Pr = 0.71: Ro = 0.3: Xi = 2.5: Str = 1     'Constants
Sr = 1: Pr = 0.71: mi = 0.5: Ma = 1#: Sc = 0.62: Q = 0.8: Xi = 0.5: Ro = 0.3: Ni = 0.5:
wo = -0.5: Ec = 0.5: Re = 50: Df = 0.03: R = 0.2: Gr_theta = 5: Gr_c = 2: Str = 1

delT = 0.001
delX = 0.05
delZ = 0.25

REM ************************************************************
ITMAX = 900
FILENUM = FreeFile()
Open "E:\PhD Thesis\Thesis Prog Chap 3\Laxconc.txt" For Append As FILENUM
Rem Initial conditions
For I = 0 To M
For J = 0 To N
```

```
        U(I, J, 0) = 0: V(I, J, 0) = 0: C(I, J, 0) = 1: T(I, J, 0) = 1
Next
Next
 Rem  Boundary conditions

For I = 1 To M
    For K = 1 To ITMAX

       U(I, 0, K) = I * Str * delX: V(I, 0, K) = 0#: C(I, 0, K) = 1: T(I, 0, K) = 1#
       'permeable hot stretching wall
      U(I, N, K) = 0: V(I, N, K) = 0#:  C(I, N, K) = 0: T(I, N, K) = 0# 'impermeable plate
   Next
Next
For J = 0 To N
      For K = 1 To ITMAX
            'inlet variables
           U(0, J, K) = 1#
           V(0, J, K) = 0#
           C(0, J, K) = 1#
           T(0, J, K) = 1#
      Next
Next
'Considering radiation
'Solving for velocities

For I = 1 To M - 1
   For J = 1 To N - 1
      For K = 1 To ITMAX - 1
       'calculate U
```

```
U(I, J, K + 1) = (U(I, J, K) - (delT / (2 * delX)) * U(I, J, K) * (-U(I - 1, J, K + 1) +
U(I, J, K) - U(I - 1, J, K)) + (delT * wo / (2 * delZ)) * (-U(I, J - 1, K + 1) _
 + U(I, J, K)   - U(I, J - 1, K)) + Ro * delT * (V(I, J, K + 1) + V(I, J, K)) _
 + (delT / (2 * Re * delX * delX)) * (U(I + 1, J, K + 1) + U(I - 1, J, K + 1) +_
 U(I + 1, J, K) - 2 * U(I, J, K) + U(I - 1, J, K)) + _
  (delT / (2 * Re * delZ * delZ)) * (U(I, J + 1, K + 1) + U(I, J - 1, K + 1) + _
  U(I, J + 1, K) - 2 * U(I, J, K) + U(I, J - 1, K))  - (delT * Xi / 2) * U(I, J, K)_
 - (delT * Ma / 2) * U(I, J, K) + (Ma / (2 + 2 * mi ^ 2)) * delT *_
 (mi * V(I, J, K + 1) + mi * V(I, J, K) - U(I, J, K)) + (delT * Gr_theta / 2) *_
   (T(I, J, K + 1) + T(I, J, K)) + (delT * Gr_c / 2) * (C(I, J, K + 1) + C(I, J, K))) / (1 +
  U(I, J, K) * delT / (2 * delX) + ((wo) * delT) / (2 * delZ) + delT / (Re * delX *
   delX) + delT / (Re * delZ * delZ) + delT * Xi / 2 + Ma * delT / 2 + (Ma * delT) / _
    (2 + 2 * mi ^ 2))
        '  calculate V
      V(I, J, K + 1) = (V(I, J, K) - (delT / (2 * delX)) * U(I, J, K) * (-V(I - 1, J, K + 1)
      + V(I, J, K) - V(I - 1, J, K)) + (delT * (wo) / (2 * delZ)) * (-V(I, J - 1, K + 1) +
      V(I, J, K) - V(I, J - 1, K)) - Ro * delT * (U(I, J, K + 1) + U(I, J, K)) _
            + (delT / (2 * Re * delX * delX)) * (V(I + 1, J, K + 1) + V(I - 1, J, K + 1) +
      V(I + 1, J, K) - 2 * V(I, J, K) + V(I - 1, J, K)) + (delT / (2 * Re * delZ * delZ)) *
      (V(I, J + 1, K + 1) + V(I, J - 1, K + 1) + V(I, J + 1, K) - 2 * V(I, J, K) + V(I, J - 1,
      K)) - (delT * Xi / 2) * V(I, J, K) - (delT * Ma / 2) * V(I, J, K) + (delT * Ma / (2 +
      2 * mi ^ 2)) * (V(I, J, K) + mi * (U(I, J, K + 1) + U(I, J, K)))) / (1 + U(I, J, K) *
      delT / (2 * delX) + ((wo) * delT) / (2 * delZ) + delT / (Re * delX * delX) + delT
      / (Re * delZ * delZ) + delT * Xi / 2 + Ma * delT / _
      2 - Ma * delT / (2 + 2 * mi ^ 2))
  '   calculate W
   ' W(I, J, K + 1) = (W(I, J, K) - (delT / (2 * delX)) * U(I, J, K) * (-W(I - 1, J, K + 1) +
W(I, J, K) - W(I - 1, J, K)) - (delT / (2 * delZ)) * W(I, J, K) * (-W(I, J - 1, K + 1) + W(I,
J, K) - W(I, J - 1, K))  + (delT / (2 * Re * delX * delX)) * (W(I + 1, J, K + 1) + W(I - 1,
```

```
J, K + 1) + W(I + 1, J, K) - 2 * W(I, J, K) + W(I - 1, J, K)) + (delT / (2 * Re * delZ *
delZ)) * (W(I, J + 1, K + 1) + W(I, J - 1, K + 1) + W(I, J + 1, K) - 2 * W(I, J, K) + W(I, J
- 1, K))  - (delT * Xi / 2) * W(I, J, K)) / (1 + U(I, J, K) * delT / (2 * delX) + ((W(I, J, K))
* delT) / (2 * delZ) + delT / (Re * delX * delX) + delT / (Re * delZ * delZ) + _
delT * Xi / 2)
 'calculate W
 ' W(I, J, K + 1) = (U(I - 1, J, K + 1) - U(I, J, K + 1)) * delZ / delX + W(I - 1, J, K + 1)

 'Solving for temperatures C
 C(I, J, K + 1) = (C(I, J, K) - (delT / (2 * delX)) * U(I, J, K) * (-C(I - 1, J, K + 1) + C(I, J,
K) + C(I - 1, J, K)) + (delT * (wo) / (2 * delZ)) * (-C(I, J - 1, K + 1) + C(I, J, K) - C(I, J -
1, K))  + ((delT) / (2 * Sc * Re * delX * delX)) * (C(I + 1, J, K + 1) + C(I - 1, J, K + 1) +
C(I + 1, J, K) - 2 * C(I, J, K) + C(I - 1, J, K)) + ((delT) / (2 * Sc * Re * delZ * delZ)) *
(C(I, J + 1, K + 1) + C(I, J - 1, K + 1) + C(I, J + 1, K) - 2 * C(I, J, K) + C(I, J - 1, K)) +
((delT * Sr) / (2 * Re * delX * delX)) * (T(I + 1, J, K + 1) - 2 * T(I, J, K + 1) + T(I - 1, J,
K + 1) + T(I + 1, J, K) - 2 * T(I, J, K) + T(I - 1, J, K)) + ((delT * Sr) / (2 * Re * delZ *
delZ)) * (T(I, J + 1, K + 1) - 2 * T(I, J, K + 1) + T(I, J - 1, K + 1) + T(I, J + 1, K) - 2 *
T(I, J, K) + T(I, J - 1, K))) / (1 + U(I, J, K) * delT / (2 * delX) - (wo * delT) / (2 * delZ)
+ delT / (Re * Sc * delX * delX) + delT / (Re * Sc * delZ * delZ))

 'Solving for temperatures T
Private Sub cmdLeastSquares_Click()

Dim U(0 To 43, 0 To 43, 0 To 1501) As Double, V(0 To 43, 0 To 43, 0 To 1501) As
Double, C(0 To 43, 0 To 43, 0 To 1501) As Double, T(0 To 43, 0 To 43, 0 To 1501) As
Double, Sc As Single, Sr As Single, Ma As Single
Dim Re As Single, Df As Single, Ec As Single, Gr_theta As Single, Gr_c As Single, wo
As Single, Ro As Single, Xi As Single, Str As Single
Dim Pr As Single, R As Single, Ni As Single, Q As Single
```

```
Dim ITMAX As Double, M As Integer, N As Integer, K As Integer, mi As Integer
Dim delX As Double, delZ As Double, delT As Double, I As Integer, J As Integer
Dim ITCOUNT As Integer
Dim FILENUM As Byte
M = 41:   N = 41 'Grid

Ma = 1#: Pr = 0.71: mi = 0.5: Ni = 0.45: Q = 1: R = 0.2: Ec = 1: Sc = 0.78: Xi = 0.5: Sr
= 1: Ro = 0.3: wo = -0.5: Re = 50: Df = 0.03: Gr_theta = 5: Gr_c = 2: Str = 1
delT = 0.001
'*************** the following ensures aspect ratio h=H/L=0.5***************
delX = 0.05
delZ = 0.25
'************************************************************
ITMAX = 900
FILENUM = FreeFile()
Open "E:\PhD Thesis\Thesis Prog Chap 3\LeastSquares.txt" For Append As FILENUM
Rem Initial condition
For I = 0 To M
For J = 0 To N
      U(I, J, 0) = 0: V(I, J, 0) = 0: C(I, J, 0) = 1: T(I, J, 0) = 1
Next
Next
 Rem  Boundary conditions
For I = 1 To M
For K = 1 To ITMAX
  U(I, 0, K) = I * Str * delX: V(I, 0, K) = 0#: C(I, 0, K) = 1: T(I, 0, K) = 1#
'permeable  hot stretching wall
  U(I, N, K) = 0: V(I, N, K) = 0#:  C(I, N, K) = 0: T(I, N, K) = 0# 'impermeable plate
Next
```

```
Next
For J = 0 To N
For K = 1 To ITMAX
    'inlet variables
   U(0, J, K) = 1#
   V(0, J, K) = 0#
   C(0, J, K) = 1#
   T(0, J, K) = 1#
Next
Next
'*****************************Solving for velocities
For I = 1 To M - 1
  For J = 1 To N - 1
    For K = 1 To ITMAX - 1
'*****************************calculate U
U(I, J, K + 1) = (U(I, J, K) - (delT / (2 * delX)) * U(I, J, K) * (-U(I - 1, J, K + 1) + U(I, J,
K) - U(I - 1, J, K)) + (delT * wo / (2 * delZ)) * (-U(I, J - 1, K + 1) + U(I, J, K) - U(I, J -
1, K)) + Ro * delT * (V(I, J, K + 1) + V(I, J, K)) _
       + (delT / (2 * Re * delX * delX)) * (U(I + 1, J, K + 1) + U(I - 1, J, K + 1) + U(I + 1,
J, K) - 2 * U(I, J, K) + U(I - 1, J, K)) + (delT / (2 * Re * delZ * delZ)) * (U(I, J + 1, K +
1) + U(I, J - 1, K + 1) + U(I, J + 1, K) - 2 * U(I, J, K) + U(I, J - 1, K)) _
       - (delT * Xi / 2) * U(I, J, K) - (delT * Ma / 2) * U(I, J, K) + (Ma / (2 + 2 * mi ^ 2))
* delT * (mi * V(I, J, K + 1) + mi * V(I, J, K) - U(I, J, K)) + (delT * Gr_theta / 2) * (T(I,
J, K + 1) + T(I, J, K)) + (delT * Gr_c / 2) * (C(I, J, K + 1) + C(I, J, K))) / (1 + U(I, J, K)
* delT / (2 * delX) + ((wo) * delT) / (2 * delZ) + delT / (Re * delX * delX) + delT / (Re
* delZ * delZ) + delT * Xi / 2 + Ma * delT / 2 + (Ma * delT) / (2 + 2 * mi ^ 2))
'UTep = U(I, J, K + 1)
  '  calculate V
```

```
V(I, J, K + 1) = (V(I, J, K) - (delT / (2 * delX)) * U(I, J, K) * (-V(I - 1, J, K + 1) + V(I, J, K) - V(I - 1, J, K)) + (delT * (wo) / (2 * delZ)) * (-V(I, J - 1, K + 1) + V(I, J, K) - V(I, J - 1, K)) - Ro * delT * (U(I, J, K + 1) + U(I, J, K)) _
    + (delT / (2 * Re * delX * delX)) * (V(I + 1, J, K + 1) + V(I - 1, J, K + 1) + V(I + 1, J, K) - 2 * V(I, J, K) + V(I - 1, J, K)) + (delT / (2 * Re * delZ * delZ)) * (V(I, J + 1, K + 1) + V(I, J - 1, K + 1) + V(I, J + 1, K) - 2 * V(I, J, K) + V(I, J - 1, K)) - (delT * Xi / 2) * V(I, J, K) - (delT * Ma / 2) * V(I, J, K) + (delT * Ma / (2 + 2 * mi ^ 2)) * (V(I, J, K) + mi * (U(I, J, K + 1) + U(I, J, K)))) / (1 + U(I, J, K) * delT / (2 * delX) + ((wo) * delT) / (2 * delZ) + delT / (Re * delX * delX) + delT / (Re * delZ * delZ) + delT * Xi / 2 + Ma * delT / 2 - Ma * delT / (2 + 2 * mi ^ 2))

'**************************Solving for temperatures C
C(I, J, K + 1) = (C(I, J, K) - (delT / (2 * delX)) * U(I, J, K) * (-C(I - 1, J, K + 1) + C(I, J, K) + C(I - 1, J, K)) + (delT * (wo) / (2 * delZ)) * (-C(I, J - 1, K + 1) + C(I, J, K) - C(I, J - 1, K)) _
    + ((delT) / (2 * Sc * Re * delX * delX)) * (C(I + 1, J, K + 1) + C(I - 1, J, K + 1) + C(I + 1, J, K) - 2 * C(I, J, K) + C(I - 1, J, K)) + ((delT) / (2 * Sc * Re * delZ * delZ)) * (C(I, J + 1, K + 1) + C(I, J - 1, K + 1) + C(I, J + 1, K) - 2 * C(I, J, K) + C(I, J - 1, K)) + ((delT * Sr) / (2 * Re * delX * delX)) * (T(I + 1, J, K + 1) - 2 * T(I, J, K + 1) + T(I - 1, J, K + 1) + T(I + 1, J, K) - 2 * T(I, J, K) + T(I - 1, J, K)) + ((delT * Sr) / (2 * Re * delZ * delZ)) * (T(I, J + 1, K + 1) - 2 * T(I, J, K + 1) + T(I, J - 1, K + 1) + T(I, J + 1, K) - 2 * T(I, J, K) + T(I, J - 1, K))) / (1 + U(I, J, K) * delT / (2 * delX) - (wo * delT) / (2 * delZ) + delT / (Re * Sc * delX * delX) + delT / (Re * Sc * delZ * delZ))
'**************************Solving for temperatures T
T(I, J, K + 1) = (T(I, J, K) + (Q * delT / 2) * T(I, J, K) - (delT / (2 * delX)) * U(I, J, K) * (-T(I - 1, J, K + 1) + T(I, J, K) - T(I - 1, J, K)) + ((delT * (wo)) / (2 * delZ)) * (-T(I, J - 1, K + 1) + T(I, J, K) - T(I, J - 1, K)) _
    + ((Df * delT) / (2 * Re * delX * delX)) * (C(I + 1, J, K + 1) - 2 * C(I, J, K + 1) + C(I - 1, J, K + 1) + C(I + 1, J, K) - 2 * C(I, J, K) + C(I - 1, J, K)) + ((Df * delT) / (2 * Re
```

```
* delZ * delZ)) * (C(I, J + 1, K + 1) - 2 * C(I, J, K + 1) + C(I, J - 1, K + 1) + C(I, J + 1,
K) - 2 * C(I, J, K) + C(I, J - 1, K)) + (delT / (2 * Pr * Re * delX * delX)) * (T(I + 1, J, K
+ 1) + T(I - 1, J, K + 1) + T(I + 1, J, K) - 2 * T(I, J, K) + T(I - 1, J, K)) + (delT / (2 * Pr *
Re * delZ * delZ)) * (T(I, J + 1, K + 1) + T(I, J - 1, K + 1) + T(I, J + 1, K) - 2 * T(I, J,
K) + T(I, J - 1, K)) + (delT * R * Re / 4) * (U(I, J, K) ^ 2 _
        + V(I, J, K) ^ 2) - ((4 * delT) / (3 * Ni * Pr * Re * 2 * delZ * delZ)) * (T(I, J + 1, K
+ 1) + T(I, J - 1, K + 1) + T(I, J + 1, K) - 2 * T(I, J, K) + T(I, J - 1, K)) + (Ec * delT / (Re
* 4 * delX * delX)) * (U(I, J, K + 1) - U(I - 1, J, K + 1) + U(I, J, K) - U(I - 1, J, K)) ^ 2 +
(Ec * delT / (Re * 4 * delZ * delZ)) * (V(I, J, K + 1) - V(I, J - 1, K + 1) + V(I, J, K) -
V(I, J - 1, K)) ^ 2) / (1 + U(I, J, K) * delT / (2 * delX) - ((wo) * delT) / (2 * delZ) + delT
/ (Re * Pr * delX * delX) + delT / (Re * Pr * delZ * delZ) - Q * delT / 2 - 4 * delT / (3 *
Ni * Pr * Re * delZ * delZ))
Next
Next
Next
 I = 3
 Print #FILENUM, U(I, 1, 401); U(I, 2, 402); U(I, 3, 403); U(I, 4, 404); U(I, 5, 405);
U(I, 6, 406); U(I, 7, 407); U(I, 8, 408); U(I, 9, 409)
Print #FILENUM, V(I, 1, 401); V(I, 2, 802); V(I, 3, 403); V(I, 4, 404); V(I, 5, 405); V(I,
6, 406); V(I, 7, 407); V(I, 8, 408); V(I, 9, 409)
 Print #FILENUM, C(I, 1, 401); C(I, 2, 402); C(I, 3, 403); C(I, 4, 404); C(I, 5, 405); C(I,
6, 406); C(I, 7, 407); C(I, 8, 408); C(I, 9, 409)
Print #FILENUM, T(I, 1, 401); T(I, 2, 402); T(I, 3, 403); T(I, 4, 404); T(I, 5, 405); T(I,
6, 406); T(I, 7, 407); T(I, 8, 408); T(I, 9, 409)
Close #FILENUM
MsgBox "AM THROUGH!!!"

End Sub
```

```
Private Sub Command1_Click()
On Error GoTo kan
Kill "E:\PhD Thesis\Thesis Prog Chap 3\LeastSquares.txt"
kan:
Exit Sub

End Sub

Private Sub cmdCompute_Click()
   Call ComputeUnsteadyValues
End If
MsgBox "AM THROUGH!!!"
End Sub

Private Sub cmdDelete_Click()
On Error GoTo kan
Kill "E:\PhD Thesis\Thesis Prog Chap 3\LaxConc.txt"
kan:
Exit Sub
End Sub
```